AN ABSTRACT OF THE DISSERTATION OF

Eric R. Moore for the degree of Doctor of Philosophy in Microbiology presented on December 12, 2019.

Title: Impacts of Microbial Chemical Interactions on Marine Plankton Physiology

Abstract approved:

_____

Kimberly H. Halsey

The bioavailability of chemical compounds in the marine environment fundamentally influences the growth and physiology of microorganisms. Organic and inorganic chemicals that are produced by some marine plankton can be consumed by other plankton for energy production, growth, or to initiate essential physiological processes. Cultures of the diatom *Thalassiosira pseudonana,* a model phytoplankton species, and *Pelagibacter ubique*, the most abundant heterotrophic bacteria in the ocean, were used to study how microbial chemical interactions influence the physiology of these two groups of co-occurring marine plankton that have substantial roles in the carbon cycle. Specifically, the production and consumption of volatile organic compounds (VOCs) were studied in monocultures and co-cultures of these plankton. In co-culture, *Pelagibacter* benefited from a wide variety of VOCs produced by *T. pseudonana,* and heterotrophic consumption of VOCs taxed carbon fixation in the diatom by promoting the loss of diffusible VOCs from the primary producer. In this interaction, VOCs were shown to be a large fraction (ca. 20%) of fixed carbon that is transferred to heterotrophic bacteria, suggesting that VOC cycling

by phytoplankton and bacteria is a significant component of the global carbon cycle. Acetone and isoprene, VOCs with important roles in atmospheric processes, were two of the VOCs utilized by *Pelagibacter* in co-culture. *Pelagibacter* metabolized acetone and isoprene at rates sufficient to explain discrepancies in measured fluxes of these compounds between the ocean and atmosphere, demonstrating that heterotrophic bacteria have significant control over the emission of VOCs from the ocean. While working with these cultures, *T. pseudonana* was shown to initiate the essential sexual reproduction phase of the diatom life cycle in the presence of ammonium. This chemical, released by other plankton to maintain elemental homeostasis, is a cue that initiates cell size restoration and introduces genetic diversity in centric diatom populations. The experiments and results herein give new information about how the chemical environment controls physiology in plankton, and that changes in physiology can further modify the chemical environment. These processes and feedbacks establish a complex network of microbe-mediated chemical interactions that have important implications for global biogeochemical processes.

Impacts of Microbial Chemical Interactions on Marine Plankton Physiology

by
Eric R. Moore

A DISSERTATION

submitted to

Oregon State University

in partial fulfillment of
the requirements for the
degree of

Doctor of Philosophy

Presented December 12, 2019
Commencement June 2020

Doctor of Philosophy dissertation of Eric R. Moore presented on December 12, 2019

APPROVED:

Major Professor, representing Microbiology

Head of the Department of Microbiology

Dean of the Graduate School

I understand that my dissertation will become part of the permanent collection of Oregon State University libraries. My signature below authorizes release of my dissertation to any reader upon request.

Eric R. Moore, Author

ACKNOWLEDGEMENTS

My journey as a graduate student at Oregon State University would not have been possible without the help and support of the many amazing people I had the fortune to encounter in my time here. First and foremost, I'd like to thank my mentor, Kim, who welcomed me into her lab and provided me with so many opportunities, helped me to grow as a person and scientist, and believed in me every step of the way. I'd also like to thank Steve, my co-advisor who I probably should have met with more often, but who always gave me useful guidance and unique perspectives. Many colleagues helped to make this research possible, and I am incredibly grateful to Brianna Bullington, Jordan Coelho, Alec Weaver, Cleo Davie-Martin, Alex Weissberg, Jeff Chang, Yuan Jiang, and Ed Davis for their valuable expertise and input. Of course, I need to thank the many other past and present members of the Halsey and Giovannoni labs, Bryce, Michelle, James, Kelsey, Lindsay, Chris, Luis, Stephen, Quinn, Sarah, Chih Ping, Jimmy, Nerissa, Bethan, Duncan and many more for making the lab such a warm, friendly and helpful place that I was (almost) always excited to go to every day. Finally, I would like to thank my mom, dad, brother and grandparents, and all of the amazing friends I've made along the way, Brandon, Andrea, Garrett, Jordy, Nicole, Hanna, and so many others. Your endless love, support and friendship helped to make the last five years the most amazing time of my life, I couldn't have done it without you.

CONTRIBUTION OF AUTHORS

Brianna Bullington, Alec Weaver, and Dr. Cleo Davie-Martin assisted with experiments and data collection. Dr. Cleo Davie-Martin, Dr. Alexandra Weissberg, Dr. Yuan Jiang, Dr. Jeff Chang and Dr. Ed. Davis assisted with data analysis. Dr. Kimberly Halsey and Dr. Stephen Giovannoni assisted with experimental design, data interpretation, and writing of manuscripts.

TABLE OF CONTENTS

TABLE OF CONTENTS (Continued)

Page

LIST OF FIGURES

LIST OF FIGURES (Continued)

LIST OF TABLES

Literature Review

Microorganisms are dependent on a broad range of different chemicals in their environment for a wide variety of fundamental biological processes. Other organisms produce many of the organic and inorganic compounds available in the environment, and their production is controlled by many factors (Azam and Malfatti, 2007; Falkowski *et al.*, 2008; Fuhrman *et al.*, 2015). Microbial communities and activities are shaped by complex networks of interactions that are mediated by direct and indirect chemical exchange among organisms (Fuhrman *et al.*, 2015; Ponomarova and Patil, 2015). Such chemical interactions allow microorganisms to acquire energy, synthesize fundamental biological building blocks needed for growth, directly interact with other cells and organisms in the environment, or stimulate behaviors and physiological responses that are important for microbial life cycles. Among the wide variety of biologically important chemicals, volatile organic compounds (VOCs) are a class of chemicals that are of increasing interest in marine microbial systems because these chemicals have important implications in primary production, microbial food webs, chemical signaling, and cell physiology (Fink, 2007; Bitas *et al.*, 2013; Schmidt *et al.*, 2015; Halsey *et al.*, 2017).

Volatile organic compounds are low molecular weight organic chemicals that have high vapor pressures and low boiling temperatures, allowing them to vaporize easily. These chemicals fall into a variety of broad classes based on their chemical components and structures, including hydrocarbons, oxygenated volatiles and halogenated volatiles. Hydrocarbons are linear or branching chains of carbon and hydrogen that are typically very reduced and non-polar, such as octane or isoprene, and consequentially tend to be hydrophobic. Oxygenated volatile compounds contain varying

numbers of oxygen atoms, forming compounds such as organic acids, ketones, esters and aldehydes. Other VOCs can contain additional elements, such as halogens (Cl, Br, I), sulfur, nitrogen or phosphorous, and their chemical composition dictates their solubility in water, volatility and reactivity. VOCs are broadly recognized as solvents that are used frequently in industrial applications. As a result, VOCs have large anthropogenic emission sources (Friedrich and Obermeier, 1999). Nevertheless, biogenic sources of VOCs in the terrestrial and marine environments are substantial and of great interest because of their contributions to the global carbon cycle, multiple hypothesized and proven ecological functions, and roles in atmospheric processes (Folkins and Chatfield, 2000; Bitas *et al.*, 2013; Audrain *et al.*, 2015; Brooks and Thornton, 2018; Zuo, 2019).

VOCs are of significant interest because they are important in atmospheric chemistry. Many VOCs regulate the oxidative capacity of the atmosphere by reacting with oxidative free radicals in the atmosphere, leading to the production or destruction of ozone (Moore *et al.*, 1996; Müller and Brasseur, 1999; Folkins and Chatfield, 2000; Liakakou *et al.*, 2007). Oxidation of compounds like isoprene or dimethylsulfide may also lead to the formation secondary organic aerosols, which can directly influence light scattering or form cloud condensation nuclei, leading to cloud formation and further effects on weather, climate, and the solar radiation budget (Yoch, 2002; Brooks and Thornton, 2018). As a result, VOC emissions are significant regulators of atmospheric chemistry and climate, but the contributions of marine biological systems remain unclear.

Terrestrial plants are a large source of VOC emissions worldwide, with around 760 Tg C emitted each year (Sindelarova *et al.*, 2014). In contrast, VOC emissions from the ocean are not well understood, but the ocean is thought to be an important source of

VOCs over marine regions (Guenther *et al.*, 1995). Some VOCs have relatively short lifetimes in the atmosphere, thus terrestrial VOC sources do not contribute significantly to the VOC pool over remote marine regions (Kesselmeier and Staudt, 1999; Lewis *et al.*, 2005; Booge *et al.*, 2017). Therefore, marine sources are needed to explain the presence of VOCs in ocean regions, and microorganisms are likely important contributors to the marine VOC pool. A few studies on VOC production by phytoplankton and other organisms have been carried out in the laboratory and field, yet many questions remain about the quantity and diversity of VOCs produced by plankton in the ocean, the biological roles VOCs serve, what variables influence VOC production by plankton, and the impacts biologically derived VOCs have on atmospheric processes (Sinha *et al.*, 2007; Spracklen *et al.*, 2008; Arnold *et al.*, 2009; Zuo, 2019). This review discusses VOCs in the context of the marine carbon cycle, and focuses on the influences phototrophic and heterotrophic plankton have on the production and degradation of volatiles in the ocean.

VOCs abundance in the ocean

The marine carbon cycle begins with photoautotrophic organisms, including phytoplankton, macroalgae and marine plants. These organisms take up inorganic carbon in the form of carbon dioxide, and use photosynthesis to reduce CO_2 to organic carbon. Fixed organic carbon has multiple fates, where it may be respired by the cell back to CO_2 for ATP production, used by the organism for growth and biomass production, or released as dissolved organic carbon (DOC) (Myklestad, 2000; Thornton, 2014). DOC is

released directly by healthy phytoplankton, at a rate of up to 30% of total carbon fixation, or through other mechanisms leading to cell death, such as sloppy feeding and viral lysis (Myklestad, 2000). Once released, DOC becomes a pool of public goods that can be utilized by other organisms. About 50% of the carbon fixed by phytoplankton is eventually re-mineralized to carbon dioxide by heterotrophic bacteria (Azam and Malfatti, 2007), thus highlighting the significance of the DOC pool in the movement of carbon from primary producers to heterotrophic bacteria. VOCs are a hidden component of the DOC pool, but the contribution of VOCs to DOC is not known because measurements of DOC rely on combustion based methods that are unable to accurately quantify volatile compounds (Bisutti *et al.*, 2004). As a result, bulk measurements of VOCs in the marine environment are rare (Hauser *et al.*, 2013) and could be a significant pool of carbon that is unaccounted for in the marine carbon budget.

Three studies have attempted to quantify bulk VOC concentrations in seawater. Volatile compounds that can diffuse between liquid and gas media are also known as exchangeable DOC (EDOC). EDOC can be quantified by allowing volatile compounds in seawater to vaporize and equilibrate with the headspace of a sealed vessel and a pure water trap; a process dependent on Henry's Law (Dachs *et al.*, 2005; Ruiz-Halpern *et al.*, 2010). In the northeast Atlantic ocean, the concentrations of total EDOC were measured to be 30 ± 6 μmol C L^{-1}, representing 30-40% of the total DOC pool in those samples (Dachs *et al.*, 2005). Another study quantified EDOC in an arctic fjord over the course of a year, with concentrations ranging from below the detection limit to 133 μmol C L^{-1} (Ruiz-Halpern *et al.*, 2010). In that study, EDOC concentrations were also about 30% of total DOC throughout the year, but were as high as 50% of total DOC during winter

when the fjord was ice covered, which may have limited VOCs emission to the atmosphere (Ruiz-Halpern *et al.*, 2010). The authors also measured EDOC flux between the fjord and atmosphere and found that the flux ranged from -22 (water served as a VOC sink) to +2 (water served as a VOC source) mmol C $m^{2\ -1}$ d^{-1}, suggesting that the biology of the fjord was partially responsible for this variability. These two studies were the first to attempt to quantify bulk VOCs in the ocean; however, their methods did not account for variability in partitioning among different chemicals (Hauser *et al.*, 2013). Using a similar approach, (Hauser *et al.*, 2013) attempted to improve EDOC measurements in estuarine water by capturing volatile and semi volatile components of EDOC separately. Using sorbent tubes to capture volatiles, and water traps to capture semi-volatile compounds, bulk VOCs were more accurately quantified by better approximating the Henry's law constants for each VOC class, which vary significantly (Hauser *et al.*, 2013). Volatile and semi-volatile components of EDOC were measured to be 131-560 ng C L^{-1} (0.011 – 0.047 μmol C L^{-1}) and 58-2450 ng C L^{-1} (0.0048-0.204 μmol C L^{-1}) respectively (Hauser *et al.*, 2013). Notably, these values are significantly lower than those reported in the other studies, but no comparisons to total DOC concentrations were made in this study.

Despite a lack of bulk measurements, it appears that the pool of VOCs present in the surface ocean represents a sizeable portion of the total dissolved organic carbon (Dachs *et al.*, 2005; Ruiz-Halpern *et al.*, 2010; Hauser *et al.*, 2013). Most studies have focused on quantifying a handful of individual VOCs with known roles in atmospheric chemistry and microbial food webs (Williams *et al.*, 2004; Sinha *et al.*, 2007; Beale *et al.*, 2013; Dixon *et al.*, 2013; Yang *et al.*, 2014). These compounds of interest include

acetone, acetaldehyde, isoprene, methanol, and DMS. Generally, these compounds have concentrations in seawater in the pico- to nanomolar range, but the net flux of these compounds between the ocean and atmosphere can vary substantially.

Acetone concentrations range from 2 to 24 nM across ocean provinces (Williams *et al.*, 2004; Marandino *et al.*, 2005; Beale *et al.*, 2013). The ocean has been observed to sometimes serve as a sink for acetone, but has more often served as a source to the atmosphere. Flux rates were dependent on location and conditions, but ranged from -7 to +8.5 $\mu M\ m^2\ d^{-1}$, where negative rates indicate a net flux from atmosphere to ocean (Williams *et al.*, 2004; Sinha *et al.*, 2007; Beale *et al.*, 2013). Extrapolating localized measurements gave global marine acetone fluxes ranging from -48.0 to 3.1 $Tg\ yr^{-1}$ (Marandino *et al.*, 2005; Beale *et al.*, 2013), with the ocean acting as a sink more often at temperate latitudes than in the tropics, where emission to the atmosphere is dominant (Beale *et al.*, 2013).

Isoprene, which is the most abundant non-methane volatile in the atmosphere, has a massive terrestrial source, primarily from plants, on the order of 500 $Tg\ C\ yr^{-1}$ (Hackenberg *et al.*, 2017). By comparison, the ocean has a much smaller, but uncertain, contribution to the global isoprene budget. The the ocean is estimated to be an isoprene source of 0.1 to 11.6 $Tg\ C\ yr^{-1}$ (Sinha *et al.*, 2007; Hackenberg *et al.*, 2017), and isoprene concentrations in seawater in one study ranged from 0.7 - 900 pM (Alvarez, Daniel A. Exton, *et al.*, 2009; Hackenberg *et al.*, 2017). Despite low emission rates relative to terrestrial regions, the short lifetime of isoprene in the atmosphere means that marine sources are the primary source of isoprene to the atmosphere over remote parts of the ocean, and important in atmospheric oxidative regulation and the formation of secondary

organic aerosols in these regions (Andreae and Crutzen, 1997; Liakakou *et al.*, 2007; Booge *et al.*, 2017).

Dimethyl sulfide is an important aerosol-forming VOC that is emitted from the ocean and has been studied extensively. DMS is a product of DMSP degradation in marine biological systems and released to the atmosphere where it participates in the formation of secondary aerosols (Yoch, 2002). Sulfate aerosols formed from DMS can directly scatter light, or form cloud condensation nuclei, leading to cloud formation and increased planetary albedo (Yoch, 2002). Thus, the ocean source of DMS may have significant impacts on cloud formation and climate. DMS exists at 1.7 nM in seawater (Williams *et al.*, 2004), and is released from the ocean at a rate of 2.5 – 167 nmol m^{-2} d^{-1} (Williams *et al.*, 2004; Sinha *et al.*, 2007).

Acetonitrile is a VOC often associated with the burning of terrestrial biomass (de Gouw, 2003). Acetonitrile has a long lifetime in the atmosphere, but concentrations in the atmosphere over the ocean are very low, suggesting the ocean is a major sink, estimated to be -11 Tg N yr^{-1} (Bange and Williams, 2000; de Gouw, 2003). Few studies have examined acetonitrile concentrations or flux in the marine environment, but one study measured acetonitrile concentrations of 6.2 nM in seawater, and a net flux to the atmosphere of 1.6 μmol m^{-2} d^{-1} along a transect in the tropical Atlantic ocean, a result that contradicts the proposed ocean sink hypothesis for acetonitrile (Williams *et al.*, 2004).

Acetaldehyde is another well-studied VOCs in the marine environment. Seawater concentrations in the temperate North Atlantic have been measured to be 3 – 37nM (Beale *et al.*, 2013, 2015). Two reports on ocean-atmosphere flux found flux rates of -9 to

+4 μmol m^{-2} d^{-1} (Beale *et al.*, 2013) and 0.58 μmol m^{-2} d^{-1} (Sinha *et al.*, 2007), indicating that the ocean can act as a source or sink for acetaldehyde, depending on location and conditions.

Methanol is the most abundant oxygenated VOC in the atmosphere (Read *et al.*, 2012), and the ocean is generally a net sink for atmospheric methanol, with air to sea fluxes of -0.7 μmol m^{-2} d^{-1} (Sinha *et al.*, 2007) and -33.7 m^{-2} d^{-1} (Williams *et al.*, 2004). Methanol fluxes of -29 to +19 μmol m^{-2} d^{-1} were also reported in the field, where the sea was a sink in temperate regions of the North Atlantic and a source in the North Atlantic gyre (Beale *et al.*, 2013). Similarly, methanol concentrations were lower in temperate regions than in the gyre, with a range of 48 – 361 nM (Beale *et al.*, 2013), or around 118 nM in the tropical Atlantic (Williams *et al.*, 2004).

Halogenated volatile compounds are highly reactive VOCs with marine, terrestrial and anthropogenic sources. Seawater is supersaturated with certain halogenated VOCs, such as $CHBr_3$, CH_2Br_2 and CHI_3 due to their production by marine algae (Paul and Pohnert, 2011). Methyl chloride (CH_3Cl) is the most abundant halogenated VOC, with a concentration of 75-110 pM in seawater, and net flux from sea to air of 0.38 – 0.64 Tg C, or 0.46 Tg Cl yr^{-1} (Khalil *et al.*, 1999; Paul and Pohnert, 2011). Halogenated compounds, especially those containing bromine, are destructive to ozone in the atmosphere, thus these compounds have significant influence on the oxidative capacity of the atmosphere and the protective ozone layer (Anbar *et al.*, 1996).

Despite a small collection of specific VOCs, including the ones discussed here, that have been described to occur in the environment, their source terms (production rates and the organisms involved) are not known. Furthermore, the production rates,

concentrations and flux of other specific VOCs and the bulk VOC pool are not known. Many physical variables can influence the behavior of VOCs in the ocean, including temperature, wind speed, and the concentration gradient between the atmosphere and water (O'Dowd and de Leeuw, 2007; Spracklen *et al.*, 2008), but biological activities have also been hypothesized to substantially contribute to the VOC sources and sinks in the sea (Kesselmeier and Staudt, 1999; Fall and Copley, 2000; Sinha *et al.*, 2007; Halsey *et al.*, 2017). VOCs may be produced and consumed by marine microorganisms, and evidence exists for both (Colomb *et al.*, 2008b; Alvarez, Daniel A Exton, *et al.*, 2009; Dixon *et al.*, 2014; Halsey *et al.*, 2017; Zuo, 2019); however, similar to the VOC source terms, the biological contributions to VOC production and degradation are not yet well understood. VOCs may serve many roles in microbial ecosystems, including signaling, stress responses, energy sources, or in antagonistic interactions (Jüttner *et al.*, 2010; Bitas *et al.*, 2013; Zuo, 2019). These multiple roles for VOCs make their dynamics complex and dependent on many variables, where variation in community structure, microbial physiology, or the physical and chemical environments can influence the release or uptake of specific chemicals (Srikanta Dani *et al.*, 2017; Ye *et al.*, 2018a; Zuo, 2019). These factors also may also influence the microbial community structure and the interactions that occur between organisms, further influencing VOC dynamics.

Chemical mediation of microbial Interactions

In addition to providing carbon and energy sources, phytoplankton may also serve as a source of vitamins, nutrients or other exudates (Amin *et al.*, 2012; Goecke *et al.*,

2013; Durham *et al.*, 2019). In turn, bacteria are able to utilize the provisions of phytoplankton for growth and energy, and are able to produce and release their own collection of nutrients, vitamins, or other exudates that can be beneficial or antagonistic to other bacteria or phytoplankton (Mayali and Doucette, 2002; Amin *et al.*, 2012; Sañudo-Wilhelmy *et al.*, 2014; Bryndan P. Durham *et al.*, 2015). Thus, when considering entire microbial communities made up of hundreds of different taxa, a complicated network of microbial interactions is formed. A lot of research has attempted to understand microbial interactions by using co-cultures at varying degrees of complexity. Studies employing co-cultures bridge the gap between pure, axenic cultures and whole community studies by simulating some of the complexities of the actual environment, leading to a more complete understanding of the whole ecosystem.

One common thread in many of the co-culture studies done to date is that phytoplankton-bacterial interactions can be very specific. Particular interactions or associations between microbes are dependent on many factors, including species or strain differences, nutrient or other chemical conditions, and growth status of the organisms involved. A major basis for phytoplankton-bacterial interactions is that phytoplankton are a carbon source for bacteria, and the carbon that is available for bacteria is dependent on the type of phytoplankton present. Dissolved organic carbon production varies among different phytoplankton species and physiological status (Myklestad, 2000; Colomb *et al.*, 2008a; Barofsky *et al.*, 2009; Longnecker *et al.*, 2015).

The availability of compounds produced by individual species is important in selecting for and recruitment of particular organisms that flourish on certain types of exudates. Evidence for this is seen in the field where particular bacterial groups are

typically found together in blooms of certain types of phytoplankton (Grossart *et al.*, 2005; Rooney-Varga *et al.*, 2005; Goecke *et al.*, 2013). Phytoplankton species and physiological status selected for unique bacterial communities that varied over algal growth phase; where bacteria like *Roseobacter* were dominant in the free living fraction, while *Flavobacteria* and *Sphingobacteria* dominated the algae- attached fraction, particularly during algal stationary phase (Grossart *et al.*, 2005). Distinct bacterial communities were present in cultures of different, non-axenic diatoms, and the addition of particular bacterial strains had negative effects on some phytoplankton species and positive effects on another. This may have been the result of unique metabolic profiles produced by the specific combination organisms involved that promote positive or negative interactions (Koedooder *et al.*, 2019). The sensitivity of such interactions to a particular organism or environmental condition emphasize the complexity of phytoplankton-bacteria interactions in nature, where many physical or chemical factors, and diverse community structures can independently or synergistically influence interaction dynamics between organisms.

Numerous papers have reported bacterial growth enhancement when in co-culture with phytoplankton, but the interaction can breakdown once conditions change. In co-cultures of the oligotrophic bacterium SAR11 strain HTCC7211 with several strains of the abundant cyanobacteria *Prochlorococcus*, SAR11 growth improved as a result of the carbon substrates that the cyanobacteria provided, but the benefit provided to SAR11 depended on the strain and growth status of *Prochlorococcus* in the co-culture (Becker *et al.*, 2019). In some cases, the interaction with *Prochlorococcus* became detrimental to SAR11, such as in co-culture with a particular strain of the cyanobacteria that did not

meet the sulfur requirements of SAR11, forcing competition for reduced sulfur, or when *Prochlorococcus* entered stationary phase and began producing compounds that favored the growth of other copiotrophic bacteria (Becker *et al.*, 2019). *Roseobacter* synthesized the phyto-hormone indole-3-acetic acid when provided tryptophan by the cocolithophore *Emiliana huxlei,* which promoted growth of the phytoplankton. This interaction established a positive feedback loop where *E. huxlei* stimulated *Roseobacter* growth and production of the hormone, further stimulating *E. huxlei* activity (Segev *et al.*, 2016). However, this mutualistic interaction became antagonistic once *E. huxlei* growth ceased, causing *Roseobacter* to over produce indole-3-acetic acid which became toxic to *E. huxlei* (Segev *et al.*, 2016).

Similarly, changes in the phytoplankton population alter bacterial interactions with phototrophs and force changes in bacterial physiology. Responses and interactions with other organisms are often cryptic and sometimes difficult to observe. Transcriptomics is commonly used to examine cryptic interactions by measuring the gene expression underlying many physiological mechanisms. In a co-culture of *Roseobacter* and the dinoflagellate *Alexandrium*, the phytoplankton community was altered by the addition of the diatom *Thalassiosira,* which quickly became the dominant phytoplankton in the culture (Landa *et al.*, 2017). The *Roseobacter* transcriptome changed substantially in response to the altered phytoplankton community, and included shifts in expression of genes involved in quorum sensing, and the metabolism and transport of particular substrates associated with each phytoplankton species, but *Roseobacter* growth was not affected (Landa *et al.*, 2017). Similarly, co-cultures of *Alteromonas* and *Prochlorococcus* showed no differences in the growth of the cyanobacteria in co-culture (Biller *et al.*,

2016; Becker *et al.*, 2019). Nevertheless, gene expression patterns in *Prochlorococcus* changed due to the presence of *Alteromonas* in the co-culture, and suggested a mutualistic interaction was occurring where *Prochlorococcus* supplied organic carbon to *Alteromonas*, in return for detoxification of reactive oxygen species (Biller *et al.*, 2016). In a diatom-*Roseobacter* co-culture, the diatom produced dihydroxypropane-1-sulfonate (DHPS). Genes involved in the transport and metabolism of DHPS were up-regulated in *Roseobacter* when compared to the mono-culture (Durham *et al.*, 2015). Similar genes were identified in other bacteria, including SAR11 and SAR116, suggesting that a variety of taxa were able to actively acquire and metabolize this diatom-produced compound. In return, *Roseobacter* supported growth of the diatom by providing vitamin B12 in the co-cultures (Bryndan P Durham *et al.*, 2015). In many of the examples discussed so far, an exchange of growth promoting compounds occurs. In some cases, the interaction is very specific to a certain taxa due to the unique metabolic capabilities of the organisms involved or dependent on other conditions. Any single change in community composition, growth phase, nutrient availability, or other perturbations may alter the metabolic production of organisms, thus influencing interaction dynamics.

Phytoplankton-bacterial interactions can be antagonistic. In the dilute, often resource limited marine environment, competition for resources is fierce, so plankton have evolved mechanisms to outcompete or inhibit other species directly (Nan *et al.*, 2004; Prince *et al.*, 2008; Boyd *et al.*, 2012; Fuhrman *et al.*, 2015). In one unique example, a parasitic interaction between phytoplankton and SAR11 (and likely other methylovorous bacteria) occurs in phosphorous limited environments, like the mid-ocean gyres. In this interaction, arsenate, an analogue to phosphate, has a high concentration

relative to phosphate, causing the phytoplankton to accidentally take up toxic arsenate. To detoxify the arsenate, the phytoplankton methylates then releases the methylated arsenic species into the environment. Methylovorous bacteria metabolize methylated arsenic and release toxic inorganic arsenate, perpetuating a cycle where carbon and energy is siphoned from the phytoplankton in a parasitic way (Giovannoni *et al.*, 2019). Another study co-cultured *Croceibacter atlanticus*, a Flavobacterium, with a variety of different diatom species. Bacteria growing on diatom cell surfaces inhibited diatom cell division, and resulted in benefits for the bacterium including increased surface area and greater access to more organic substrates (Van Tol *et al.*, 2016).

Volatile organic compounds are likely important in phytoplankton-bacterial interactions. VOCs have not been studied much in the context of marine microbiology, but are thought to have roles as info chemicals, in stress responses and as carbon substrates for plankton. A variety of organisms, particularly phytoplankton, produce VOCs, but their involvement in interactions needs to be examined. In terrestrial environments, VOCs mediate interactions between soil bacterial communities, soil fungi and plants, where certain VOCs may have inhibitory effects on competing bacteria and fungi or act as info chemicals (Bitas *et al.*, 2013; Schmidt *et al.*, 2015). In the ocean, similar examples are discussed, but there remains a general lack of understanding of the biological roles of VOCs in the marine environment. The next section of this review discusses the production and consumption of VOCs by plankton, examples of VOCs that may serve in roles or interactions, and the impact these biologically important VOCs have on the broader ecosystem and carbon cycle.

VOC Production by phytoplankton and other aquatic organisms

All organisms produce VOCs in some capacity, but phytoplankton are a primary source for many VOCs in the ocean. Algal VOC production rates under particular conditions are rarely quantified and few studies have tested the effects of variable conditions on VOC production in algae. Light intensity, nutrient limitation, and community composition, among other factors, may influence VOC production by altering algal physiology and carbon allocation pathways (Thornton, 2014; Halsey and Jones, 2015). Thus, these variables are likely important factors when considering the impacts of VOC production or consumption by plankton and the roles they serve in the ecosystem.

Diatoms are a unique group of phytoplankton that often dominate plankton communities, particularly in temperate and coastal environments, and are major contributors to primary production (Uitz *et al.*, 2010). The abundance and dominance of diatoms means they have a large impact on their environment, and this is likely true for their role in producing VOCs. Diatoms produce a variety of different halomethanes, such as CH_2Br_2, $CHBr_2Cl$, CH_2I_2, CH_2ICl, CH_3Cl and CH_3Br (Moore *et al.*, 1996; Mtolera *et al.*, 1996; Colomb *et al.*, 2008a; Paul and Pohnert, 2011). Production of these compounds was light and growth dependent, and only occurred when haloperoxidases were present (Moore *et al.*, 1996). Halomethanes were produced more at higher light intensities, suggesting that haloperoxidases may be involved in the quenching of reactive oxygen species (Moore *et al.*, 1996). Methyl chloride production was associated with diatoms; however, production continued following cell death, and may have been a result of degradation of diatom exudate by bacteria or abiotic processes (Tait and Moore, 1995). A

more recent study also found evidence of halogenated VOC production, particularly methyl bromide, as well as isoprene (C_5H_8); however, the effects of particular environmental conditions on VOC production were not tested (Colomb *et al.*, 2008a).

Isoprene emission by diatoms has been documented in several studies (Mckay *et al.*, 1996; Halsey *et al.*, 2017), and is estimated to have a global source of 4.8 Tg C y^{-1} (Srikanta Dani *et al.*, 2017). Other experiments examined the relationship between photosynthesis and isoprene production in a selection of diatom species. Under increasing light levels, isoprene emission and non-photochemical quenching (NPQ) were negatively correlated in low light adapted diatoms, suggesting NPQ was the primary pathway involved in dissipating excess light energy at higher light levels. The two genera tested, *Chatocerous* and *Phaeodactulum,* showed distinct responses to light and isoprene production, and increasing CO_2 availability reduced isoprene emissions (Srikanta Dani *et al.*, 2017). This example emphasizes how isoprene production is rooted in primary production, and is dependent on species-specific responses to changing environmental conditions. In addition to isoprene, the diatom *Skeletonema costatum* produced other hydrocarbons, including ethane, ethane, propane and n-hexane, with isoprene and n-hexane being produced more during active growth than in stationary phase (Mckay *et al.*, 1996). Experiments on various diatom species identified the production of various ketones, terpenoids, aldehydes, alcohols, and pyrazines (Cotsaris *et al.*, 1995; Colomb *et al.*, 2008a; Halsey *et al.*, 2017). Notably, diatoms are only a minor source of DMS compared to other phytoplankton groups, and isoprene may be produced in favor of DMS or the precursor DMSP (Keller, 1989; Dani and Loreto, 2017).

Cyanobacteria are photosynthetic bacteria that live in freshwater and marine environments. Freshwater cyanobacteria are often implicated as the source of malodor in drinking water, and a variety of VOCs have been identified that effect water quality (Milovanović *et al.*, 2015). VOC profiles of three different freshwater cyanobacteria species identified an abundance of medium length hydrocarbons, and the compound 2-methylisoborneol was also prevalent (Milovanović *et al.*, 2015). Isoprene was produced by the abundant cyanobacteria *Prochlorococcus*, as well as three diverse eukaryotic algae: *Pelagomonas calceolare*, *Micromonas pusilla*, and *Emiliana huxlei* (Shaw *et al.*, 2003). Isoprene production rates ranged from $1x10^{-21}$ to $4x10^{-19}$ mol $cell^{-1}$ d^{-1} and was dependent on species, cell size, light intensity, temperature, and viral infection (Shaw *et al.*, 2003). Similar to diatoms, cyanobacteria were only minor producers of DMS while dinoflagellates and prymnesiophytes are larger contributors (Keller, 1989).

In addition to phytoplankton, heterotrophic bacteria are also producers of VOCs. Over 1000 different VOCs produced by bacteria have been characterized, many of which are involved in cell to cell interactions (Audrain *et al.*, 2015). Heterotrophic bacteria catabolize DMSP produced by phytoplankton and emit copious amounts of the climate active volatile DMS (Yoch, 2002; Sun *et al.*, 2016). In soil environments, gram positive bacteria are common producers of isoprene (Fall and Copley, 2000), while in marine environments, *Vibrio sp*. produced acetone while growing in cultures, especially when supplemented with leucine (Nemecek-Marshall *et al.*, 1995). The full diversity of organisms and their associated volatile exudates have only just begun to be characterized in a handful of organisms and focus is typically on only a few VOCs of interest.

Furthermore, the environmental variables that control VOC production, and the roles VOCs perform for plankton are not well understood.

Factors controlling microbial VOC production

In phytoplankton, abiotic factors modify physiology, and many studies have characterized the influence of light, nutrients, temperature and other variables on the growth and productivity of plankton (Bucciarelli and Sunda, 2003; Marchetti and Cassar, 2009; Sunda and Huntsman, 2011; Fouilland *et al.*, 2014; Halsey and Jones, 2015; Fisher and Halsey, 2016; Arandia-Gorostidi *et al.*, 2017; Xu *et al.*, 2017; Ye *et al.*, 2018). Just as VOC production can vary at the species level, VOC production is sensitive to small changes in the environment. In cultures of the green alga *Dunaliella tertiolecta* and diatom *Thalassiosira pseudonana*, the production of acetone, acetaldehyde, isoprene and methanol were strongly dependent on light intensity, with higher production rates observed at high light levels (Halsey *et al.*, 2017). Further, isoprene production was also dependent on light intensity in two diatoms, *Chatocerous* and *Phaeodactulum*, but isoprene production peaked at different light intensities for each organism (Srikanta Dani *et al.*, 2017). Similarly, the production of halogenated volatile compounds by *Eucheuma denticulatum* and a variety of diatoms was enhanced by cells growing under high light intensity (Moore *et al.*, 1996; Mtolera *et al.*, 1996). Light intensity also explained isoprene production rates across a diverse set of algae, which included *Prochlorococcus, Pelagomonas, Micromonas*, and *Emiliana* species (Shaw *et al.*, 2003). In the same study, temperature and cell size were also correlated to isoprene production, while isoprene

production decreased during phage infection, and grazing by zooplankton had no impact on production (Shaw *et al.*, 2003).

Few studies have examined the influence of nutrient availability on VOC production in phytoplankton, but two examples highlight the substantial impact that nutrient limitation, starvation, or chemical form of nitrogen or phosphorous may affect VOC production. VOC emission rates were higher under nitrogen limitation, and VOC profiles changed when different nitrogen sources were utilized by the cyanobacterium *Microcystis flos-aquae* (Xu *et al.*, 2017). In a similar study, VOCs produced by *Microcystis aeruginosa* varied depending on the phosphorous source available to the culture, and bulk VOC production was greater under phosphorous limitation and starvation (Ye *et al.*, 2018b).

In the field, discerning biotic and abiotic ecological variables driving a particular VOC emission profile are more complicated to understand than those testing pure cultures in the laboratory. A mesocosm experiment was performed in the Baltic Sea to examine the influence CO_2 concentrations had on the production of volatile compounds from seawater. Under the highest CO_2 concentrations, DMS emission was lower, possibly as a result of effects on the bacterial community responsible for degrading DMSP to DMS, and no changes in the production of halogenated VOCs was observed (Webb *et al.*, 2016). In a eutrophic lake, VOC emissions varied over the course of the year as the plankton community changed seasonally and heterotrophic activity degraded phytoplankton produced VOCs (Jüttner, 1984). In the ocean, an apparent trade-off exists in isoprene and DMS emission across latitudes, where isoprene emissions are highest in the tropics and DMS emission is highest at the poles (Dani and Loreto, 2017). It is

possible this trend is driven by variability in phytoplankton communities at different latitudes; however, diatoms from polar climates also produce less isoprene in culture than their tropical counterparts (Bonsang *et al.*, 2010; Exton *et al.*, 2013). While variation in VOC production at the species level may be a driver, additional factors not associated with community composition, such as temperature, may be important in this tradeoff. Ultimately, VOC production in phytoplankton depends on many environmental variables, such as light and nutrient availability, temperature, community composition, or latitude, many of which are co-variables. Unraveling the factors associated with particular VOC emission behaviors is challenging, but understanding more about the roles VOCs serve phytoplankton may help to elucidate these responses.

VOC roles in microbial ecosystems

VOCs are ubiquitous in the environment and serve a wide variety of functions for the organisms that produce them. The diffusivity of VOCs makes them effective signaling molecules and they can be released by cells in response to stress stimuli to signal or retaliate against adjacent individuals (Zuo, 2019). In response to grazing by copepods, the diatom *Cocconeis scutellum* releases polyunsaturated aldehydes upon cellular wounding, that inhibited reproduction in copepods (Jüttner *et al.*, 2010). Similarly, polyunsaturated aldehydes were differentially produced in a selection of closely related phytoplankton species, and these compounds inhibited copepod egg development and hatching (Pohnert *et al.*, 2002). In terrestrial plants, releases of VOCs such as ethylene are able to signal adjacent plants and activate grazer defense

mechanisms (Kesselmeier and Staudt, 1999). The cyanobacteria *Microcystis flos-aquae* released VOCs, including limonene and eucalyptol, under nitrogen limitation that inhibited the green alga *Chlorella*, a potential competitor (Xu *et al.*, 2017). Additionally, some brominated VOCs produced by phytoplankton interfere with bacterial quorum sensing and attachment mechanisms, preventing colonization by potentially inhibitory or competitive bacteria (Paul and Pohnert, 2011). This array of examples shows that plants and phytoplankton use VOCs to defend against grazers and competing organisms.

Communication within a community of organisms via volatile info-chemicals facilitates the coordination of community scale activities, such as the sexual reproduction phase of the diatom life cycle. Diatoms must periodically reproduce sexually in order to restore their cell size, and chemical signaling may allow for synchronization of the life cycle and onset of the sexual phase to facilitate successful fertilization in a dilute environment. The pheromones fucoserratene and ectocarpene are volatile terpenoids produced by diatoms and brown algae that facilitate gamete cell recognition and increase the likelihood of successful fertilization, while other VOCs initiate other parts of the diatom sexual phase (Sato *et al.*, 2011; Stonik and Stonik, 2015). Two unidentified pheromones were involved in the sexual reproduction of the diatom *Pseudostaurosira trainorii*. One pheromone induced sexual development in the opposite mating type, while another helped direct spermatozoa towards oogonia for fertilization (Sato *et al.*, 2011). Although the authors did not identify the specific pheromones involved, they may be similar to other terpenoid pheromones shown to be produced by sexually reproducing brown algae (Stonik and Stonik, 2015).

VOCs serve important roles in plant stress responses to excess light, temperature and reactive oxygen species, and may function in similar ways in phytoplankton. Elevated isoprene emissions in plants exposed to high light and temperatures has been documented for some time and is hypothesized to provide resistance to reactive oxygen species (Sharkey and Yeh, 2001). This hypothesis is supported in an experiment that treated the leaves of isoprene producing plants with fosmidomycin, an inhibitor of the non-mevalonate isoprenoid synthesis pathway in the chloroplast, and exposing them to high light and temperature. Leaves where isoprene synthesis was inhibited recovered from the stressor less than untreated leaves, but inhibited leaves exposed to exogenous isoprene (including non-isoprene producing plants) showed improved recovery, highlighting the importance of isoprene in the photo-oxidative stress response of plants (Sharkey *et al.*, 2001). VOCs such as isoprene are hypothesized to have similar roles in dealing with oxidative stress in phytoplankton. In a variety of phytoplankton species, isoprene and monoterpene production increased when cultures were shifted from low to high light, and from low to high temperatures (Meskhidze *et al.*, 2015). Halogenated VOCs are also likely to be involved in the dissipation of reactive oxygen species. Phytoplankton possess different types of haloperoxidase enzymes that destroy reactive peroxides (Moore *et al.*, 1996). Haloperoxidase activity likely leads to the formation of halogenated volatile compounds, thus these VOCs may be byproducts that are released as a result of oxidative stress (Paul and Pohnert, 2011). Other VOCs may be produced as a result of degradation of other cellular components, such as fatty acids, pigments and other isoprenoids or other metabolic intermediates (Palmer and Shaw, 2005; Santos *et al.*, 2016), though in many cases, these mechanisms are not well understood (Booge *et al.*,

2017). In the marine environment, phytoplankton acclimated to certain conditions must be able to respond rapidly to changing conditions. Cells acclimated to low light would contain high concentrations of chlorophyll and other pigments. If suddenly exposed to high light, the cell would be oversaturated and need a way to rapidly dissipate the excess energy. Rapid degradation of photo-pigments would prevent damage by reducing light harvesting while also evolving isoprene, which may act as an electron sink to reduce oxidative stress.

Biological VOC sinks (heterotrophic consumption)

VOCs also serve as carbon substrates for marine heterotrophic bacteria that have evolved mechanisms to acquire and metabolize VOCs. Some studies hypothesize that degradation of VOCs by heterotrophic bacteria may account for large discrepancies in sea to atmosphere fluxes of VOCs, but few examples of VOC catabolism exist in aquatic environments. Field work comparing estimated versus measured flux of isoprene from the ocean show a 70% overestimation of modeled fluxes compared to measured values, and including a bacterial VOC consumption rate improved the performance of the model (Palmer and Shaw, 2005; Booge *et al.*, 2017). In a study examining bacterial communities, a variety of bacterial taxa were identified in isoprene-enriched estuarine water, particularly the Actinobacteria *Mycobacterium*, and *Rhodococcus*, Bacteriodetes and some alpha- and beta-proteobacteria (Alvarez, Daniel A Exton, *et al.*, 2009). In these communities, isoprene production and consumption rates were coupled, but low concentrations suggested that isoprene was more likely an energy supplement rather than

a sole carbon source for these taxa (Alvarez, Daniel A Exton, *et al.*, 2009). In estuarine sediments enriched with ^{13}C labeled isoprene, DNA stable isotope probing also identified the Actinobacteria *Mycobacterium*, *Rhodococcus*, *Gordonia*, and *Microbacterium*, and suggested promiscuous enzyme activities may enable isoprene metabolism in cells lacking specific isoprene degradation pathways (Johnston *et al.*, 2017). Similar taxa metabolize isoprene in terrestrial soils, in particular, *Rhodococcus* (El Khawand *et al.*, 2016; McGenity *et al.*, 2018). A *Rhodococcus* strain isolated from marine sediments was characterized for its ability to use isoprene as a growth substrate, and encoded an operon containing an isoprene monooxygensae gene (van Hylckama Vlieg *et al.*, 2000), though poly-aromatic dioxygenases can also degrade isoprene (McGenity *et al.*, 2018). Some of the taxa capable of degrading isoprene can also metabolize other VOCs. A *Rhodococcus* strain isolated from wastewater utilized a nitrile hydratase and amidase enzymes to metabolize acetonitrile (Acharya and Desai, 1999), and this pathway was implicated in acetonitrile degradation by *Natronocella acetinitrilica* in an alkaline lake (Sorokin *et al.*, 2007).

Metabolism of oxygenated volatile compounds by bacteria is supported by bulk measurements and flux rates of these compounds in the ocean. Methanol degradation was highest in the oligotrophic gyres where bacterial production measured by ^{14}C-leucine incorporation was low, and oxidation rates were positively correlated with the abundance of SAR11 bacteria (Sargeant *et al.*, 2018). Work by the same group compared the oxidation rates of acetone, acetaldehyde and methanol in coastal waters of the UK over the course of a year. Microbial oxidation rates of methanol and acetaldehyde were 1-11 nM h^{-1} and 5-31 nM h^{-1} respectively, and heterotrophic metabolism was the primary sink

for these compounds in seawater (Beale *et al.*, 2015). Microbial oxidation rates of acetone measured over the course of a year were much lower than acetaldehyde or methanol at 1-380 pmol h^{-1} and only explained a fraction of the total losses in seawater, but acetone oxidation was higher in the winter when more preferred substrates, such as acetaldehyde, are less abundant (Dixon *et al.*, 2014; Beale *et al.*, 2015). In the surface of the Sargasso sea where cell concentrations average $5.7x10^8$ cells mL^{-1} (Morris *et al.*, 2002), microbial oxidation of methanol and formaldehyde were around 228 pmol L^{-1} h^{-1} (Sun *et al.*, 2011). Culturing work with a selection of microbes isolated from the ocean has also demonstrated VOC utilization. The oligotrophic bacteria SAR11, abundant throughout the ocean, particularly in oligotrophic regions, utilizes acetaldehyde, methanol, formaldehyde, and dimethyl sulfide (Sun *et al.*, 2011, 2016; Halsey *et al.*, 2017). HTCC2181 (β-proteobacteria), an organism isolated from the mesopelagic is an obligate methanol oxidizing bacterium, raising questions about the source of methanol in the marine environment (Halsey *et al.*, 2012).

While some marine bacteria have been shown to metabolize a variety of oxygenated VOCs, less is known about the mechanisms and biochemical pathways involved, but we can look to a few examples from other environments to start to understand the pathways that might be used by marine bacteria. *Gordonia*, a genus common in soil, is capable of acetone degradation, which occurs as a part of a pathway used in the metabolism of propane (Kotani *et al.*, 2007). In the described pathway, propane is the starting substrate, then subsequently converted to 2-propanol, acetone, and methyl acetate before ending in the formation of acetic acid and methanol, and the enzymes in this biochemical pathway were also capable of reactions with ketones other than acetone (Kotani *et al.*, 2007). This

is in contrast to other pathways for acetone degradation, which show a conversion of acetone to acetol, rather than methyl acetate (Kotani *et al.*, 2007). In *Corynebacterium*, acetone is converted to acetol, methylglyoxal then pyruvate (Taylor *et al.*, 1980), or may also result in the formation of acetaldehyde and a C1 compound (Levine and Krampitz, 1952). Despite differences in the proposed biochemical pathways, an acetone monooxygenase is implicated in the first conversion of acetone, and may be key in the microbial breakdown of acetone. Understanding VOC metabolic pathways, such as those for acetone, aids in the search for other microorganisms that have important roles in VOC cycling. Thus, identifying the organisms involved will lead to a better understanding of the biologically driven movement of VOCs within the ocean and other environments.

Summary

VOCs have multiple important roles in microbial food webs, physiological stress responses, and cell-to-cell interactions. In the atmosphere, VOCs are involved in ozone formation and degradation, secondary aerosol formation, and atmospheric oxidative regulation (Moore *et al.*, 1996; Müller and Brasseur, 1999; Folkins and Chatfield, 2000; Brooks and Thornton, 2018). These chemical interactions have the potential to regulate weather and climate, thus the processes regulating VOC sea-air flux are of significant interest. In the context of the global carbon cycle, the volatile fraction of the total carbon budget is not well defined, but the ocean is thought to have a significant role in the global cycling of VOCs, serving as either a source or sink depending on the compound and environment. While physical factors are important in VOC cycle regulation, biological

processes are often implicated in the production or degradation of VOCs, but only a small number of examples have begun to answer the questions surrounding contributions of biology, in particular, microorganisms, in the marine VOC cycle. Important questions remain to be answered: What is the bulk mass of volatile compounds in the ocean and how does it compare to the total DOC pool? How much VOC do primary producers or other microbes produce? What fraction of primary production is funneled to the formation of VOCs? What organisms are important in producing or degrading certain compounds? What are the functions of the VOCs and biochemical pathways involved? What is the significance of plankton in regulating the movement of VOCs between the ocean and atmosphere? Studies attempting to answer these questions are necessary to understand the connections between marine plankton, VOCs and the greater carbon cycle.

The work presented in this thesis attempts to answer some of these outstanding questions by using cultures of diatoms and SAR11, two important plankton groups that have large roles in the marine carbon cycle. In one of the chapters ahead, these cultures are used as model organisms to understand the movement of VOCs among plankton, their importance as sources of carbon and energy for heterotrophs, and the fraction of primary production composed of VOCs. In another chapter, I characterized the metabolism of two important VOCs, acetone and isoprene, by the most abundant bacteria in the ocean, *Pelagibacter ubique* (SAR11), and provide clarity on the role of this organism in the cycling of these two climate relevant compounds. Finally, the last chapter of this thesis presents a serendipitous discovery that resulted from the culturing approaches used in the first chapter. In this chapter, the life cycle of the model centric diatom *Thalassiosira*

pseudonana is characterized. While the original study did not focus on VOCs, ammonia, a volatile signaling molecule, was determined to be an important regulator of the diatom life cycle.

Acharya, A. and Desai, A.J. (1999) Acetonitrile-hydrolysing enzymes in Rhodococcus erythropolis A10. *World J Microbiol Biotechnol* **15**: 111–113.

Alvarez, L.A., Exton, Daniel A, Timmis, K.N., Suggett, D.J., and Mcgenity, T.J. (2009) Characterization of marine isoprene-degrading communities. *Environ Microbiol* **11**: 3280–3291.

Alvarez, L.A., Exton, Daniel A., Timmis, K.N., Suggett, D.J., and McGenity, T.J. (2009) Characterization of marine isoprene-degrading communities. *Environ Microbiol* **11**: 3280–3291.

Amin, S.A., Parker, M.S., and Armbrust, E. V. (2012) Interactions between Diatoms and Bacteria. *Microbiol Mol Biol Rev* **76**: 667–684.

Anbar, A.D., Yung, Y.L., and Chavez, F.P. (1996) Methyl bromide: Ocean sources, ocean sinks, and climate sensitivity. *Global Biogeochem Cycles* **10**: 175–190.

Andreae, M.O. and Crutzen, P.J. (1997) Atmospheric aerosols: Biogeochemical sources and role in atmospheric chemistry. *Science (80-)* **276**: 1052–1058.

Arandia-Gorostidi, N., Weber, P.K., Alonso-Sáez, L., Anxelu, X., Morán, G., and Mayali, X. (2017) Elevated temperature increases carbon and nitrogen fluxes between phytoplankton and heterotrophic bacteria through physical attachment. *ISME J* **11**: 641–650.

Arnold, S.R., Spracklen, D. V, Williams, J., Yassaa, N., Sciare, J., Bonsang, B., et al. (2009) Evaluation of the global oceanic isoprene source and its impacts on marine organic carbon aerosol. *Atmos Chem Phys* **9**: 1253–1262.

Audrain, B., Farag, M.A., Ryu, C.-M., and Ghigo, J.-M. (2015) Role of bacterial volatile compounds in bacterial biology. *FEMS Microbiol Rev* **39**: 222–233.

Azam, F. and Malfatti, F. (2007) Microbial structuring of marine ecosystems. *Nat Rev Microbiol* **5**: 782–791.

Bange, H.W. and Williams, J. (2000) New Directions: Acetonitrile in atmospheric and biogeochemical cycles. *Atmos Environ* **34**: 4959–4960.

Barofsky, A., Vidoudez, C., and Pohnert, G. (2009) Metabolic profiling reveals growth stage variability in diatom exudates. *Limnol Oceanogr Methods* **7**: 382–390.

Beale, R., Dixon, J.L., Arnold, S.R., Liss, P.S., and Nightingale, P.D. (2013) Methanol, acetaldehyde, and acetone in the surface waters of the Atlantic Ocean. *J Geophys Res Ocean* **118**: 5412–5425.

Beale, R., Dixon, J.L., Smyth, T.J., and Nightingale, P.D. (2015) Annual study of oxygenated volatile organic compounds in UK shelf waters. *Mar Chem* **171**: 96–106.

Becker, J.W., Hogle, S.L., Rosendo, K., and Chisholm, S.W. (2019) Co-culture and biogeography of Prochlorococcus and SAR11. *ISME J*.

Biller, S.J., Coe, A., and Chisholm, S.W. (2016) Torn apart and reunited: Impact of a heterotroph on the transcriptome of Prochlorococcus. *ISME J* **10**: 2831–2843.

Bisutti, I., Hilke, I., and Raessler, M. (2004) Determination of total organic carbon – an overview of current methods. *Trends Anal Chem* **23**: 716–726.

Bitas, V., Kim, H.-S., Bennett, J.W., and Kang, S. (2013) Sniffing on Microbes: Diverse Roles of Microbial Volatile Organic Compounds in Plant Health. */ 835 MPMI* **26**:.

Bonsang, B., Gros, V., Peeken, I., Yassaa, N., Bluhm, K., Zoellner, E., et al. (2010) Isoprene emission from phytoplankton monocultures: The relationship with chlorophyll-a, cell volume and carbon content. *Environ Chem* **7**: 554–563.

Booge, D., Schlundt, C., Bracher, A., Endres, S., and Zäncker, B. (2017) Marine isoprene production and consumption in the mixed layer of the surface ocean – A field study over 2 oceanic regions. *Biogeosciences Discuss* 1–28.

Boyd, P.W., Strzepek, R., Chiswell, S., Chang, H., DeBruyn, J.M., Ellwood, M., et al. (2012) Microbial control of diatom bloom dynamics in the open ocean. *Geophys Res Lett* **39**: 2–7.

Brooks, S.D. and Thornton, D.C.O. (2018) Marine Aerosols and Clouds. *Ann Rev Mar Sci* **10**: 289–313.

Bucciarelli, E. and Sunda, W.G. (2003) Influence of CO2, nitrate, phosphate, and silicate limitation on intracellular dimethylsulfoniopropionate in batch cultures of the coastal diatom Thalassiosira pseudonana. *Limnol Oceanogr* **48**: 2256–2265.

Colomb, A., Yassaa, N., Williams, J., Peeken, I., and Lochte, K. (2008a) Screening volatile organic compounds (VOCs) emissions from five marine phytoplankton species by head space gas chromatography/mass spectrometry (HS-GC/MS). *J Environ Monit* **10**: 325–330.

Colomb, A., Yassaa, N., Williams, J., Peeken, I., and Lochte, K. (2008b) Screening volatile organic compounds (VOCs) emissions from five marine phytoplankton species by head space gas chromatography/mass spectrometry (HS-GC/MS). *J Environ Monit* **10**: 325–330.

Cotsaris, E., Bruchet, A., Mallevialle, J., and Bursill, D.B. (1995) The identification of odorous metabolites produced from algal monocultures. *Water Sci Technol* **31**: 251–258.

Dachs, J., Calleja, M.L., Duarte, C.M., del Vento, S., Turpin, B., Polidori, A., et al. (2005) High atmosphere-ocean exchange of organic carbon in the NE subtropical Atlantic. *Geophys Res Lett* **32**: L21807.

Dani, K.G.S. and Loreto, F. (2017) Trade-Off Between Dimethyl Sulfide and Isoprene Emissions from Marine Phytoplankton. *Trends Plant Sci* **22**: 361–372.

Dixon, J.L., Beale, R., and Nightingale, P.D. (2013) Production of methanol, acetaldehyde, and acetone in the Atlantic Ocean. *Geophys Res Lett* **40**: 4700–4705.

Dixon, J.L., Beale, R., Sargeant, S.L., Tarran, G.A., and Nightingale, P.D. (2014) Microbial acetone oxidation in coastal seawater. *Front Microbiol* **5**: 1–9.

Durham, B.P., Boysen, A.K., Carlson, L.T., Groussman, R.D., Heal, K.R., Cain, K.R., et al. (2019) Sulfonate-based networks between eukaryotic phytoplankton and heterotrophic bacteria in the surface ocean. *Nat Microbiol* 1.

Durham, Bryndan P., Sharma, S., Luo, H., Smith, C.B., Amin, S.A., Bender, S.J., et al. (2015) Cryptic carbon and sulfur cycling between surface ocean plankton. *Proc Natl Acad Sci* **112**: 453–457.

Durham, Bryndan P, Sharma, S., Luo, H., Smith, C.B., Amin, S.A., Bender, S.J., et al. (2015) Cryptic carbon and sulfur cycling between surface ocean plankton. *PNAS* **112**: 453–457.

Exton, D.A., Suggett, D.J., McGenity, T.J., and Steinke, M. (2013) Chlorophyll-normalized isoprene production in laboratory cultures of marine microalgae and implications for global models. *Limnol Oceanogr* **58**: 1301–1311.

Falkowski, P.G., Fenchel, T., and Delong, E.F. (2008) The microbial engines that drive earth's biogeochemical cycles. *Science (80-)* **320**: 1034–1039.

Fall, R. and Copley, S.D. (2000) Bacterial sources and sinks of isoprene, a reactive

atmospheric hydrocarbon. *Environ Microbiol* **2**: 123–130.
Fink, P. (2007) Ecological functions of volatile organic compounds in aquatic systems. *Mar Freshw Behav Physiol* **40**: 155–168.
Fisher, N.L. and Halsey, K.H. (2016) Mechanisms that increase the growth efficiency of diatoms in low light. *Photosynth Res* **129**: 183–197.
Folkins, I. and Chatfield, R. (2000) Impact of acetone on ozone production and OH in the upper troposphere at high NOx. *J Geophys Res Atmos* **105**: 11585–11599.
Fouilland, E., Tolosa, I., Bonnet, D., Bouvier, C., Bouvier, T., Bouvy, M., et al. (2014) Bacterial carbon dependence on freshly produced phytoplankton exudates under different nutrient availability and grazing pressure conditions in coastal marine waters. *FEMS Microbiol Ecol* **87**: 757–769.
Friedrich, R. and Obermeier, A. (1999) Anthropogenic Emissions of Volatile Organic Compounds. In, *Reactive Hydrocarbons in the Atmosphere*. Elsevier, pp. 1–39.
Fuhrman, J.A., Cram, J.A., and Needham, D.M. (2015) Marine microbial community dynamics and their ecological interpretation. *Nat Publ Gr* **13**: 133–146.
Giovannoni, S.J., Halsey, K.H., Saw, J., Muslin, O., Suffridge, C.P., Sun, J., et al. (2019) A Parasitic Arsenic Cycle That Shuttles Energy from Phytoplankton to Heterotrophic Bacterioplankton. *MBio* **10**:.
Goecke, F., Thiel, V., Wiese, J., Labes, A., and Imhoff, J.F. (2013) Algae as an important environment for bacteria - phylogenetic relationships among new bacterial species isolated from algae. *Phycologia* **52**: 14–24.
de Gouw, J.A. (2003) Emission sources and ocean uptake of acetonitrile (CH_3CN) in the atmosphere. *J Geophys Res* **108**: 4329.
Grossart, H.P., Levold, F., Allgaier, M., Simon, M., and Brinkhoff, T. (2005) Marine diatom species harbour distinct bacterial communities. *Environ Microbiol* **7**: 860–873.
Guenther, A., Nicholas, C., Fall, R., Klinger, L., Mckay, W.A., and Scholes, B. (1995) A global model of natural volatile organic compound emissions. *J Geophys Res* **100**: 8873–8892.
Hackenberg, S.C., Andrews, S.J., Airs, R., Arnold, S.R., Bouman, H.A., Brewin, R.J.W., et al. (2017) Potential controls of isoprene in the surface ocean. *Global Biogeochem Cycles* **31**: 644–662.
Halsey, K.H., Carter, A.E., and Giovannoni, S.J. (2012) Synergistic metabolism of a broad range of C1 compounds in the marine methylotrophic bacterium HTCC2181. *Environ Microbiol* **14**: 630–640.
Halsey, K.H., Giovannoni, S.J., Graus, M., Zhao, Y., Landry, Z., Thrash, J.C., et al. (2017) Biological cycling of volatile organic carbon by phytoplankton and bacterioplankton. *Limnol Oceanogr*.
Halsey, K.H. and Jones, B.M. (2015) Phytoplankton strategies for photosynthetic energy allocation. *Annu Rev Mar Sci* **7**: 265–297.
Hauser, E.J., Dickhut, R.M., Falconer, R., and Wozniak, A.S. (2013) Improved method for quantifying the air-sea flux of volatile and semi-volatile organic carbon. *Limnol Oceanogr Methods* **11**: 287–297.
van Hylckama Vlieg, J.E.T., Leemhuis, H., Jeffrey, H., Spelberg, L., and Janssen, D.B. (2000) Characterization of the Gene Cluster Involved in Isoprene Metabolism in Rhodococcus sp . Strain AD45. *J Bacteriol* **187**: 1956–1963.

Johnston, A., Crombie, A.T., El Khawand, M., Sims, L., Whited, G.M., McGenity, T.J., and Colin Murrell, J. (2017) Identification and characterisation of isoprene-degrading bacteria in an estuarine environment. *Environ Microbiol* **19**: 3526–3537.

Jüttner, F. (1984) Dynamics of the volatile organic substances associated with cyanobacteria and algae in a eutrophic shallow lake. *Appl Environ Microbiol* **47**: 814–820.

Jüttner, F., Messina, P., Patalano, C., and Zupo, V. (2010) Odour compounds of the diatom Cocconeis scutellum: Effects on benthic herbivores living on Posidonia oceanic. *Mar Ecol Prog Ser* **400**: 63–73.

Keller, M.D. (1989) Dimethyl Sulfide Production and Marine Phytoplankton: The Importance of Species Composition and Cell Size. *Biol Oceanogr* **6**: 375–382.

Kesselmeier, J. and Staudt, M. (1999) Biogenic Volatile Organic Compounds (VOC): An Overview on Emission, Physiology and Ecology. *J Atmos Chem* **33**: 23–88.

Khalil, M.A.K., Moore, R.M., Harper, D.B., Lobert, J.M., Erickson, D.J., Koropalov, V., et al. (1999) Natural emissions of chlorine-containing gases: Reactive Chlorine Emissions Inventory. *J Geophys Res* **104**: 8333–8346.

El Khawand, M., Crombie, A.T., Johnston, A., Vavlline, D. V., McAuliffe, J.C., Latone, J.A., et al. (2016) Isolation of isoprene degrading bacteria from soils, development of *isoA* gene probes and identification of the active isoprene-degrading soil community using DNA-stable isotope probing. *Environ Microbiol* **18**: 2743–2753.

Koedooder, C., Stock, W., Willems, A., Mangelinckx, S., De Troch, M., Vyverman, W., and Sabbe, K. (2019) Diatom-Bacteria Interactions Modulate the Composition and Productivity of Benthic Diatom Biofilms. *Front Microbiol* **10**: 1255.

Kotani, T., Yurimoto, H., Kato, N., and Sakai, Y. (2007) Novel acetone metabolism in a propane-utilizing bacterium, Gordonia sp. strain TY-5. *J Bacteriol* **189**: 886–893.

Landa, M., Burns, A.S., Roth, S.J., and Moran, M.A. (2017) Bacterial transcriptome remodeling during sequential co-culture with a marine dinoflagellate and diatom. *ISME J* 1–14.

Levine, S. and Krampitz, L.O. (1952) The oxidation of acetone by a soil diphtheroid.

Lewis, A.C., Hopkins, J.R., Carpenter, L.J., Stanton, J., Read, K.A., and Pilling, M.J. (2005) Sources and sinks of acetone, methanol, and acetaldehyde in North Atlantic marine air. *Atmos Chem Phys* **5**: 1963–1974.

Liakakou, E., Vrekoussis, M., Bonsang, B., Donousis, C., Kanakidou, M., and Mihalopoulos, N. (2007) Isoprene above the Eastern Mediterranean: Seasonal variation and contribution to the oxidation capacity of the atmosphere. *Atmos Environ* **41**: 1002–1010.

Longnecker, K., Kido Soule, M.C., and Kujawinski, E.B. (2015) Dissolved organic matter produced by Thalassiosira pseudonana. *Mar Chem* **168**: 114–123.

Marandino, C.A., De Bruyn, W.J., Miller, S.D., Prather, M.J., and Saltzman, E.S. (2005) Oceanic uptake and the global atmospheric acetone budget. *Geophys Res Lett* **32**: 2–5.

Marchetti, A. and Cassar, N. (2009) Diatom elemental and morphological changes in response to iron limitation: A brief review with potential paleoceanographic applications. *Geobiology* **7**: 419–431.

Mayali, X. and Doucette, G.J. (2002) Microbial community interactions and population dynamics of an algicidal bacterium active against Karenia brevis (Dinophyceae).

Harmful Algae **1**: 277–293.
McGenity, T.J., Crombie, A.T., and Murrell, J.C. (2018) Microbial cycling of isoprene, the most abundantly produced biological volatile organic compound on Earth. *ISME J* **12**: 931–941.
Mckay, W.A., Turner, M.F., Jones, B.M.R., and Halliwell, C.M. (1996) Emissions of hydrocarbons from marine phytoplankton - some results from controlled laboratory experiments. *Atmos Environ* **30**: 2583–2593.
Meskhidze, N., Sabolis, A., Reed, R., and Kamykowski, D. (2015) Quantifying environmental stress-induced emissions of algal isoprene and monoterpenes using laboratory measurements. *Biogeosciences* **12**: 637–651.
Milovanović, I., Mišan, A., Simeunović, J., Kovač, D., Jambrec, D., and Mandić, A. (2015) Determination of Volatile Organic Compounds in Selected Strains of Cyanobacteria. *J Chem* **2015**: 1–6.
Moore, R.M., Webb, M., Tokarczyk, R., and Wever, R. (1996) Bromoperoxidase and iodoperoxidase enzymes and production of halogenated methanes in marine diatom cultures. *J Geophys Res* **101**: 899–919.
Morris, R.M., Rappé, M.S., Connon, S.A., Vergin, K.L., Siebold, W.A., Carlson, C.A., and Giovannoni, S.J. (2002) SAR11 clade dominates ocean surface bacterioplankton communities. *Nature* **420**: 806–810.
Mtolera, M.S.P., Collén, J., Pedersén, M., Ekdahl, A., Abrahamsson, K., and Semesi, A.K. (1996) Stress-induced production of volatile halogenated organic compounds in Eucheuma denticulatum (Rhodophyta) caused by elevated pH and high light intensities. *Eur J Phycol* **31**: 89–95.
Müller, J.F. and Brasseur, G. (1999) Sources of upper tropospheric HOx: A three-dimensional study. *J Geophys Res Atmos* **104**: 1705–1715.
Myklestad, S.M. (2000) Dissolved Organic Carbon from Phytoplankton. *Handb Environ Chem* **5**: 111–148.
Nan, C., Zhang, H., and Zhao, G. (2004) Allelopathic interactions between the macroalga Ulva pertusa and eight microalgal species. *J Sea Res* **52**: 259–268.
Nemecek-Marshall, M., Wojciechowski, C., Kuzma, J., Silver, G.M., and Fall, R. (1995) Marine Vibrio species produce the volatile organic compound acetone. *Appl Environ Microbiol* **61**: 44–47.
O'Dowd, C.D. and de Leeuw, G. (2007) Marine aerosol production: a review of the current knowledge. *Philos Trans R Soc A* **365**: 1753–1774.
Palmer, P.I. and Shaw, S.L. (2005) Quantifying global marine isoprene fluxes using MODIS chlorophyll observations. *Geophys Res Lett* **32**:.
Paul, C. and Pohnert, G. (2011) Production and role of volatile halogenated compounds from marine algae. *Nat Prod Rep* **28**: 186–195.
Pohnert, G., Lumineau, O., Cueff, A., Adolph, S., Cordevant, C., Lange, M., and Poulet, S. (2002) Are volatile unsaturated aldehydes from diatoms the main line of chemical defence against copepods? *Mar Ecol Prog Ser* **245**: 33–45.
Ponomarova, O. and Patil, K.R. (2015) Metabolic interactions in microbial communities: untangling the Gordian knot. *Curr Opin Microbiol* **27**: 37–44.
Prince, E.K., Myers, T.L., and Kubanek, J. (2008) Effects of harmful algal blooms on competitors: Allelopathic mechanisms of the red tide dinoflagellate Karenia brevis. *Limnol Oceanogr* **53**: 531–541.

Read, K.A., Carpenter, L.J., Arnold, S.R., Beale, R., Nightingale, P.D., Hopkins, J.R., et al. (2012) Multiannual Observations of Acetone, Methanol, and Acetaldehyde in Remote Tropical Atlantic Air: Implications for Atmospheric OVOC Budgets and Oxidative Capacity.

Rooney-Varga, J.N., Giewat, M.W., Savin, M.C., Sood, S., Legresley, M., and Martin, J.L. (2005) Links between Phytoplankton and Bacterial Community Dynamics in a Coastal Marine Environment. *Microb Ecol* **49**: 163–175.

Ruiz-Halpern, S., Sejr, M.K., Duarte, C.M., Krause-Jensen, D., Dalsgaard, T., Dachs, J., and Rysgaard, S. (2010) Air-water exchange and vertical profiles of organic carbon in a subarctic fjord. *Limnol Oceanogr* **55**: 1733–1740.

Santos, A.B., Viera, K.R., Nogara, G.P., Wagner, R., Jacob-Lopes, E., and Zepka, L.Q. (2016) Biogeneration of Volatile Organic Compounds by Microalgae: Occurrence, Behavior, Ecological Implications and Industrial Applications. In, *Volatile Organic Compounds: Occurrence, Behavior and Ecological Implications*., pp. 1–24.

Sañudo-Wilhelmy, S.A., Gómez-Consarnau, L., Suffridge, C., and Webb, E.A. (2014) The Role of B Vitamins in Marine Biogeochemistry. *Ann Rev Mar Sci* **6**: 339–367.

Sargeant, S.L., Murrell, J.C., Nightingale, P.D., and Dixon, J.L. (2018) Basin-scale variability of microbial methanol uptake in the Atlantic Ocean. *Biogeosciences* **15**: 5155–5167.

Sato, S., Beakes, G., Idei, M., Nagumo, T., and Mann, D.G. (2011) Novel Sex Cells and Evidence for Sex Pheromones in Diatoms. *PLoS One* **6**: e26923.

Schmidt, R., Cordovez, V., De Boer, W., Raaijmakers, J., and Garbeva, P. (2015) Volatile affairs in microbial interactions. *ISME J* **9**: 2329–2335.

Segev, E., Wyche, T.P., Kim, K.H., Petersen, J., Ellebrandt, C., Vlamakis, H., et al. (2016) Dynamic metabolic exchange governs a marine algal-bacterial interaction. *Elife* **5**: 1–28.

Sharkey, T.D., Chen, X., and Yeh, S. (2001) Isoprene Increases Thermotolerance of Fosmidomycin-Fed Leaves 1.

Sharkey, T.D. and Yeh, S. (2001) Isoprene emission from plants. *Annu Rev Plant Physiol Plant Mol Biol* **52**: 407–436.

Shaw, S.L., Chisholm, S.W., and Prinn, R.G. (2003) Isoprene production by Prochlorococcus, a marine cyanobacterium, and other phytoplankton. *Mar Chem* **80**: 227–245.

Sindelarova, K., Granier, C., Bouarar, I., Guenther, A., Tilmes, S., Stavrakou, T., et al. (2014) Global data set of biogenic VOC emissions calculated by the MEGAN model over the last 30 years. *Atmos Chem Phys* **14**: 9317–9341.

Sinha, V., Williams, J., Meyerhöfer, M., Riebesell, U., Paulino, A.I., and Larsen, A. (2007) Air-sea fluxes of methanol, acetone, acetaldehyde, isoprene and DMS from a Norwegian fjord following a phytoplankton bloom in a mesocosm experiment.

Sorokin, D.Y., van Pett, S., Tourova, T.P., Takaichi, S., and Muyzer, G. (2007) Acetonitrile degradation under haloalkaline conditions by Natronocella acetinitrilica gen. nov., sp. nov. *Microbiology* **153**: 1157–1164.

Spracklen, D. V., Arnold, S.R., Sciare, J., Carslaw, K.S., and Pio, C. (2008) Globally significant oceanic source of organic carbon aerosol. *Geophys Res Lett* **35**:.

Srikanta Dani, K.G., Silva Benavides, A.M., Michelozzi, M., Peluso, G., Torzillo, G., and Loreto, F. (2017) Relationship between isoprene emission and photosynthesis in

diatoms, and its implications for global marine isoprene estimates. *Mar Chem* **189**: 17–24.

Stonik, V. and Stonik, I. (2015) Low-Molecular-Weight Metabolites from Diatoms: Structures, Biological Roles and Biosynthesis. *Mar Drugs* **13**: 3672–3709.

Sun, J., Steindler, L., Thrash, J.C., Halsey, K.H., Smith, D.P., Carter, A.E., et al. (2011) One Carbon Metabolism in SAR11 Pelagic Marine Bacteria. *PLoS One* **6**: e23973.

Sun, J., Todd, J.D., Thrash, J.C., Qian, Y., Qian, M.C., Temperton, B., et al. (2016) The abundant marine bacterium Pelagibacter simultaneously catabolizes dimethylsulfoniopropionate to the gases dimethyl sulfide and methanethiol. *Nat Microbiol* **1**: 16065.

Sunda, W.G. and Huntsman, S.A. (2011) Interactive effects of light and temperature on iron limitation in a diatom: Implications for marine productivity and carbon cycling. *Limnol Oceanogr* **56**: 1475–1488.

Tait, V.K. and Moore, R.M. (1995) Methyl chloride (CH3Cl) production in phytoplankton cultures. *Limnol Oceanogr* **40**: 189–195.

Taylor, D.G., Trudgill, P.W., Cripps, R.E., and Harris, P.R. (1980) The Microbial Metabolism of Acetone. *J Gen Microbiol* **118**: 159–170.

Thornton, D.C.O. (2014) Dissolved organic matter (DOM) release by phytoplankton in the contemporary and future ocean. *Eur J Phycol* **49**: 20–46.

Van Tol, H.M., Amin, S.A., and Armbrust, V. (2016) Ubiquitous marine bacterium inhibits diatom cell division. *ISME J* **11**: 31–42.

Uitz, J., Claustre, H., Gentili, B., and Stramski, D. (2010) Phytoplankton class-specific primary production in the world's oceans: Seasonal and interannual variability from satellite observations. *Global Biogeochem Cycles* **24**: n/a-n/a.

Webb, A.L., Leedham-Elvidge, E., Hughes, C., Hopkins, F.E., Malin, G., Bach, L.T., et al. (2016) Effect of ocean acidification and elevated f CO2 on trace gas production by a Baltic Sea summer phytoplankton community. *Biogeosciences* **13**: 4595–4613.

Williams, J., Holzinger, R., Gros, V., Xu, X., Atlas, E., and Wallace, D.W.R. (2004) Measurements of organic species in air and seawater from the tropical Atlantic. *Geophys Res Lett* **31**: 1–5.

Xu, Q., Yang, L., Yang, W., Bai, Y., Hou, P., Zhao, J., et al. (2017) Volatile organic compounds released from Microcystis flos-aquae under nitrogen sources and their toxic effects on Chlorella vulgaris. *Ecotoxicol Environ Saf* **135**: 191–200.

Yang, M., Beale, R., Liss, P., Johnson, M., Blomquist, B., and Nightingale, P. (2014) Air-sea fluxes of oxygenated volatile organic compounds across the Atlantic Ocean. *Atmos Chem Phys* **14**: 7499–7517.

Ye, C., Yang, Y., Xu, Q., Ying, B., Zhang, M., Gao, B., et al. (2018a) Volatile organic compound emissions from Microcystis aeruginosa under different phosphorus sources and concentrations. *Phycol Res* **66**: 15–22.

Ye, C., Yang, Y., Xu, Q., Ying, B., Zhang, M., Gao, B., et al. (2018b) Volatile organic compound emissions from *Microcystis aeruginosa* under different phosphorus sources and concentrations. *Phycol Res* **66**: 15–22.

Yoch, D.C. (2002) Dimethylsulfoniopropionate: Its sources, role in the marine food web, and biological degradation to dimethylsulfide. *Appl Environ Microbiol* **68**: 5804–5815.

Zuo, Z. (2019) Why Algae Release Volatile Organic Compounds—The Emission and

Roles. *Front Microbiol* **10**: 491.

Pelagibacter metabolism of diatom-derived volatile organic compounds imposes an energetic tax on photosynthetic carbon fixation

Eric R. Moore, Cleo L. Davie-Martin, Stephen J. Giovannoni, Kimberly H. Halsey

Published in *Environmental Microbiology*
Nov. 2019

Abstract

Volatile organic compounds (VOCs) produced by phytoplankton are molecules with high vapor pressures that can diffuse across cell membranes into the environment, where they become public goods. VOCs likely comprise a significant component of the marine dissolved organic carbon (DOC) pool utilized by microorganisms, but are often overlooked as growth substrates because their diffusivity imposes analytical challenges. The roles of VOCs in the growth of the photoautotrophic diatom *Thalassiosira pseudonana* and heterotrophic bacterium *Pelagibacter sp.* HTCC1062 (SAR11) were examined using co-cultures and proton-transfer-reaction time-of-flight mass spectrometry (PTR-TOF/MS). VOCs at 82 m/z values were produced in the cultures, and the concentrations of 9 of these m/z values changed in co-culture relative to the diatom mono-culture. Several of the m/z values were putatively identified and their metabolism by HTCC1062 was confirmed by measuring ATP production. Diatom carbon fixation rates in co-culture with HTCC1062 were 20.3% higher than the diatom mono-culture. Removal of VOCs from the *T. pseudonana* mono-culture using a hydrocarbon trap caused a similar increase in carbon fixation (18.1%). These results show that a wide range of VOCs are cycled in the environment and the flux of VOCs from phytoplankton to bacterioplankton imposes a large and unexpected tax on phytoplankton photosynthesis.

Introduction

Photosynthetic diatoms and the heterotrophic bacteria *Pelagibacter* (SAR11) are both highly abundant in the surface ocean and make major contributions to biological carbon cycling. Microphytoplankton, a pigment-based classification primarily composed of diatoms, are estimated to carry out about 32 % of net primary production in the ocean (Uitz *et al.*, 2010). *Pelagibacter* are estimated to oxidize 6 to 37% of marine gross primary production (White *et al.*, 2018). The flow of carbon between these two groups of organisms is therefore a potentially significant component of the marine carbon cycle.

Diatoms produce and release a wide variety of organic compounds that can vary depending on the species, growth status, and nutrient environment (Barofsky *et al.*, 2009). Low molecular weight and volatile organic carbon compounds (VOCs) have been associated with active growth (Colomb *et al.*, 2008a; Buchan *et al.*, 2014), while more complex organic molecules are synthesized during senescence (Buchan *et al.*, 2014). Production rates of both volatile and non-volatile organic compounds are dependent on light intensity (Halsey *et al.*, 2017), nutrient availability (Bromke *et al.*, 2013) and specific interactions with other microorganisms (Paul *et al.*, 2012; Longnecker *et al.*, 2015; Schmidt *et al.*, 2015). VOCs are estimated to comprise 30-40% of the dissolved organic carbon (DOC) pool that is the basis of the microbial food web (Dachs *et al.*, 2005; Ruiz-Halpern *et al.*, 2010; Hauser *et al.*, 2013).

VOCs have a variety of roles in phytoplankton metabolism and ecology. VOCs can be important in signaling or grazing defense (Fink, 2007), support specific synergistic or antagonistic interactions with other microorganisms (Amin *et al.*, 2015; Van Tol *et al.*,

2016), provide protection from oxidative stress (Dani and Loreto, 2017), or are metabolic waste that may include products from overflow primary production (Schmidt *et al.*, 2015; Srikanta Dani *et al.*, 2017). In our study, we explore the possibility that some VOCs are intermediates or byproducts of metabolism that are uncontrollably lost from cells. Their low molecular weight, high vapor pressure, and, in many cases, hydrophobic properties, enable VOCs to diffuse across cell membranes (Bjørrisen, 1988; Shaw *et al.*, 2003; Halsey *et al.*, 2017). Uncontrollable losses of membrane-permeable organic compounds, including VOCs, could be promoted by heterotrophic removal of these compounds from the environment, and the loss of carbon by this mechanism is potentially taxing to primary producers (Bjørrisen, 1988).

Pelagibacter (*Pelagibacterales*) are ubiquitous, free-living heterotrophic bacterioplankton that have been shown to metabolize many low molecular weight, labile organic compounds, including VOCs (Giovannoni, 2017). As a result of genomic streamlining, *Pelagibacter* have specific carbon and nutrient requirements (Tripp *et al.*, 2008; Carini *et al.*, 2012), and have evolved to transport and metabolize a variety of phytoplankton-derived low molecular weight carbon compounds, including VOCs, using a limited genetic repertoire (Giovannoni *et al.*, 2005). For example, *Pelagibacter* metabolize a variety of methylated and volatile compounds, including methanol, dimethylsulfide (DMS), formaldehyde, acetaldehyde, methylamine, and methylated arsenic species (Sun *et al.*, 2011, 2016; Halsey *et al.*, 2017; S. Giovannoni *et al.*, 2019).

The full diversity and quantity of VOCs produced by phytoplankton are unknown, but the multiple roles of these compounds in ecology and atmospheric chemistry makes understanding their sources and sinks an important goal in marine microbial ecology.

Microbial food web research often relies on the high-temperature catalytic oxidation method to determine the DOC pool available for heterotrophic consumption. However, this method systematically underestimates the volatile components in DOC (Bisutti *et al.*, 2004); therefore, quantitative measurements of bulk VOCs in the ocean or in culture are rare (Hauser *et al.*, 2013). Attention has primarily been given to a handful of compounds, such as dimethyl sulfide (DMS), methanol, and acetone, that are known to be biologically cycled and have impacts on the atmosphere and climate (Sinha *et al.*, 2007; Beale *et al.*, 2013; Dixon *et al.*, 2013).

To understand the dynamics and impacts of VOC exchange in marine microbial food webs, the growth and physiology of the diatom *Thalassiosira pseudonana* (CCMP 1335) and free-living heterotrophic bacterium *Pelagibacter ubique* (HTCC1062) were studied in mono-culture and co-culture. *Pelagibacter* strain HTCC1062 (ecotype 1a.1) used in these experiments was originally isolated from Oregon coastal waters and is common in temperate and polar regions where diatoms, including *T. pseudonana,* contribute significantly to primary production at some times of the year. Proton-transfer-reaction time-of-flight mass spectrometry (PTR-TOF/MS) was used to detect VOCs that changed in concentration in the co-culture relative to the diatom mono-culture, revealing a wide range of VOCs that are substrates for *Pelagibacter* metabolism. Diatom carbon fixation rates increased both in the presence of the heterotroph and when VOCs were removed from the co-culture with a hydrocarbon trap. These results indicate that VOCs are an important conduit of carbon transfer between diatoms and *Pelagibacter* cells, and that the expense of VOC loss from phytoplankton cells imposes a significant tax on the energetics of photosynthetic carbon fixation.

Experimental procedures

Culture growth

Axenic stock and experimental cultures of *Thalassiosira pseudonana* CCMP 1335 and *Pelagibacter ubique* HTCC1062 were maintained in f/2 +Si artificial seawater medium (Guillard and Ryther, 1962) with the following modifications to support growth of HTCC1062: 0.939 mM KCl, 0.802 mM NO_3^-, 1.0 mM NH_4Cl, 0.05 mM glycine, 0.01 mM methionine, 0.078 mM pyruvate, 0.84 μM pantothenate, 0.985 μM 4-amino-5-hydroxymethyl-2-methylpyrimidine (HMP), 0.3 μM thiamine, 0.002 μM biotin, 0.117 μM $FeCl_3$ * $6H_2O$, 0.009 μM $MnCl_2$ 4H2O, 0.0008 μM $ZnSO_4$ $7H_2O$, 0.0005 μM $CoCl_2$* $6H_2O$, 0.0003 μM Na_2MoO_4 2H2O, 0.001 μM Na_2SeO_3, and 0.001 μM $NiCl_2$ * $6H_2O$ (Carini *et al.*, 2012, 2014) . Following autoclaving, the growth medium was bubbled with 0.1μm filter-sterilized carbon dioxide and air for 8 hours and 16 hours respectively prior to use. Cultures were grown in 250 ml to 500 ml polycarbonate flasks or bottles at 16^oC, under 25 μmol photons m^{-2} s^{-1} on a 12-hour light-dark cycle, with gentle shaking at 60 rpm. Starting concentrations were $2x10^3$ cells mL^{-1} for *T. pseudonana* or $2x10^5$ cells mL^{-1} for HTCC1062 to allow both organisms to reach stationary phase at approximately the same time when in co-culture. For all co-cultures, both organisms were added to the medium at the same time, with the exception of the experiment where HTCC1062 was grown in co-culture without pyruvate, glycine or methionine additions. In this case, exponentially growing cultures of *T. pseudonana* was allowed to grow for 72 h prior to

inoculation of HTCC1062. Cell densities of *T. pseudonana* were monitored with a Coulter counter (Beckman Coulter; Brea, CA, USA) while HTCC1062 cells were stained with Sybr Green I and counted using a Guava Technologies flow cytometer (Millipore; Billerica, MA, USA)). All experiments and measurements were conducted while the cells were in exponential growth phase and approximately 3 to 6 hours into the daylight portion of the light cycle.

For VOC removal experiments, 50 mL *T. pseudonana* mono-cultures were grown at 18^{o}C and 25 μmol photons m^{-2} s^{-1} on a 12-hour light-dark cycle. These cultures were grown in a closed system that re-circulated headspace air at 15-20 mL min^{-1} using a peristaltic pump. The headspace was circulated through a Supelpure HC hydrocarbon trap (Millipore-Sigma; St. Louis, MO, USA) that removed VOCs in a loop that flowed back directly into the growth medium. Headspace air in the control cultures was re-circulated in the same manner, except the carbon trap was omitted, thereby ensuring concentrations of CO_2, O_2, and physical turbulence from bubbling did not vary between treatments. Growth media was pre-treated by recirculating headspace air in this system for one week prior to the addition of cells, and continued to run as the cultures grew. *T. pseudonana* growth was monitored daily and harvested for carbon fixation and chlorophyll measurements after growth for about one week.

Carbon fixation measurements

4 μCi of ^{14}C labeled sodium bicarbonate was added to 9mL sub-samples of *T. pseudonana* mono- or co-cultures that were collected during mid to late exponential

phase of growth. Working in the near-dark, samples were split into two aliquots and incubated at 25 μmol photons m^{-2} s^{-1}, or in the dark, for 20 min before terminating carbon uptake by adding 500 μL 1N HCl. Prior to incubation, 50 μL of the ^{14}C-spiked sample was combined with 50 μL phenethylamine and 900 μL additional growth medium for total activity measurements. After samples were allowed to vent for 24 h, 1 mL aliquots were combined with 5 mL EcoScint liquid scintillation cocktail then measured using a scintillation counter (Beckman-Coulter; Brea, CA, USA). pH measurements of each culture were also taken as a proxy for CO_2 concentrations, with no significant differences measured between culture pairs (mean difference = 0.03, p=0.67, paired t-test; n=6). Cell enumerations by Guava flow cytometry indicated no bacterial contamination. One mono- and co-culture pair, or +/- VOC trap culture pair, was assayed at a time. These experiments were repeated several times, on different days, at the same point in the light cycle, using independent pairs of cultures. For each iteration, the treatment condition ("co-culture" or "VOC removed") was compared directly to the associated *T. pseudonana* mono-culture measured at the same time.

Photophysiology

Chlorophyll-a was extracted from cells by collecting 5-10 mL of culture onto glass fiber filters, which were then immersed in 5 mL 90% acetone, and stored at -20^{o} C for 24 hours. Absorbance from 400 to 800 nm of both extracted chlorophyll and whole filtered cells (total absorbance) was measured with a spectrophotometer (Shimadzu; Kyoto, Japan). Chlorophyll concentration was calculated according to the methods of

(Ritchie, 2006). Total cellular absorbance from 400 to 800 nm was measured immediately after filtration and calculated according to (Mitchell and Kieper, 1988). Samples for pigment analysis by HPLC were collected by the same filtration method, sealed in foil and flash frozen in liquid nitrogen and stored at -80 ^{o} C until analysis by the Oregon State University HPLC facility using a modified version of the high-performance liquid chromatography (HPLC) method of Wright *et al.*, 1991 as described by Bidigare *et al.*, 2005. Filters were extracted in 100% acetone for 24 h, at 4°C. Extracts were processed in reverse-phase on a 250 mm C18 column using a Waters separations module and photodiode detector array. *Empower* chromatography software was used for integration and pigment quantification. The instrument was calibrated using chlorophyll-a from *Anacystis nidulans* (Millipore-Sigma; St. Louis, MO, USA) and mixed pigment standards were obtained from DHI (Hørsholm, Denmark). F_v/F_m, a measurement of photosynthetic efficiency, was performed by diluting 100 µL of culture into 3.5 mL of fresh growth medium, then acclimated under dim blue light at 5 µmol photons m^{-2} s^{-1} for 5 minutes followed by an additional minute under complete darkness. Cellular fluorescence was then measured using a custom built fast repetition-rate fluorometer (Kolber *et al.*, 1998).

ATP assays

200 mL HTCC1062 cultures were harvested by centrifugation in late exponential growth phase. Cell pellets were washed and re-suspended three times in modified f/2 +Si medium lacking glycine, methionine and pyruvate to remove residual growth substrates.

Washed cells were re-suspended to 15 mL in the same f/2 medium and incubated in the dark at 16^{o}C overnight. Starved cells were enumerated by flow cytometry, and then split into a minimum of three replicate 500 µL cultures in 2mL sterile cryovials for each condition being tested. Individual VOCs (1 µM each), pyruvate (1 µM, positive control) or water (negative control) were added to the cultures, sealed tightly and incubated in the dark for 4 hours. Cellular ATP was measured by adding 20 µL cell suspension to 90 µL Promega Bac-Titer Glo reagent (Promega; Madison, WI, USA). Luminescence was measured using a luminometer (Tecan; Männedorf, Switzerland), set to 10 ms settle time and 1000 ms integration time, following mixing the sample for 5 seconds and incubating for 4 minutes at room temperature. Luminescence signal was compared to an ATP standard curve to calculate cellular ATP concentrations.

PTR-TOF/MS

PTR-TOF/MS (Ionicon Analytik; Innsbruck, Austria) was utilized to measure VOCs in *T. pseudonana* mono- and co-cultures. Four replicate mono- and co-cultures were grown in vented flasks for about 2 weeks, then destructively sampled 4-6 hours into the daylight portion of the light cycle while both species were in exponential growth phase. *T. pseudonana* cell densities in mono and co-cultures were equalized across replicate cultures by addition of fresh growth medium, which was identical to the medium used as the "blank" control [Table 1]. 100 mL of culture was added to a VOC stripping chamber maintained at 16^{o}C and 25 µmol photons m^{-2} s^{-1}, and bubbled through a glass frit in the bottom of the chamber with breathing grade air at 50 mL min^{-1} for 5

min to strip VOCs from the growth medium, and repeated for each replicate. This apparatus is described in Halsey *et al.*, 2017. Each culture, and a blank fresh growth medium control, was measured independently using the same stripping chamber to reduce any effects due to variation in chamber construction or bubble production. VOCs stripped from the culture into the headspace were measured directly by the PTR-TOF/MS via soft/non-fragmenting ionization with H_3O^+. A mass spectrum ranging from 30-240 a.m.u was acquired at 5 s intervals over the course of 5 min. Each peak in the mass spectrum represents a compound of its molar mass + 1.008 (from the hydrogen ion). Because the first 2.5 min of the measurement was used to expel headspace from the chamber, only the last 2.5 min of data containing VOCs displaced from the culture medium was used in the analysis.

PTR-TOF/MS data was processed using the program *PTR-Viewer* (version 3.2.8.0) (Ionicon Analytik, Innsbruck, Austria). Files were mass calibrated to three chemicals known to be present within each mass spectrum (m/z 29.998, 203.943, and 330.848). Initially, a mass binning approach was used to bin data at intervals of 0.5 mass units, bounded at 0.25 and 0.75 mass units (e.g. the m/z 59 bin ranged from 58.75-60.25). The precision of PTR ToF/ MS allows for detection of small variations in mass, and as a result, some 0.5 mass unit bins contained multiple peaks generated by different compounds. The mass spectra were visually examined for multiple peaks within the same mass bin. All instances for which multiple peaks were identified were subsequently analyzed using a Gaussian based approach to examine each peak individually. Integrated signals for each peak were normalized to primary ion ($H3O^+$) concentrations, and concentrations for each mass peak were calculated. Only m/z values that had

concentrations in culture greater than two standard deviations above the blank growth medium concentration were considered in the downstream analysis. Mean concentrations of VOCs derived from mono-culture and co-cultures were then compared using a students t-test with a p-value significance cut-off of 0.05 (n=4). Since a t-test was performed for 82 different m/z values that had concentrations greater than the blank, resulting p-values were corrected for multiple hypothesis testing. The Benjimani-Hochberg procedure was applied with a Q-value cutoff ≤ 0.1 to reduce the likelihood of false positives.

Results

Culture Growth

In growth medium replete with its known required organic carbon and reduced sulfur sources [pyruvate, glycine and methionine; (Tripp *et al.*, 2008; Carini *et al.*, 2012)], HTCC1062 had a generation time of 45.2 ± 0.9 h in co-culture with *T. pseudonana* and grew faster than the HTCC1062 mono-culture (51.1 ± 1.3 hours; $p= 1.7x10^{-4}$, n=5). Both cultures continued growing in exponential phase until nearly $1x10^{8}$ cells mL^{-1}. There was no difference in generation times of *T. pseudonana* grown in mono- and co-cultures (42.0 ± 1.5 and 41.6 ± 1.2, p=0.63, n=5) [Fig. 1A, 1B]. The faster growth rate of HTCC1062 in co-culture prompted us to ask if the diatom could support HTCC1062 growth even when its required growth substrates were not added to the medium. In co-culture with no added pyruvate, glycine or methionine, HTCC1062

attained a maximum cell density that was four-fold higher (7.9 x 10^6 cells mL^{-1}) than the HTCC1062 mono-culture grown in the absence of pyruvate, glycine and methionine (1.2 x 10^6 cells mL^{-1}) [Fig. 1C]. After 528 hours, the HTCC1062 cell density in co-culture crashed contemporaneously with *T. pseudonana* reaching stationary phase (data not shown).

Production and consumption of volatile organic compounds (VOCs) in co-culture

We hypothesized that *T. pseudonana* produces VOCs that can be used as growth substrates by HTCC1062. PTR-TOF/MS was used to measure VOCs that had accumulated in the culture medium of *T. pseudonana* grown in mono-culture and in co-culture with HTCC1062 after about two weeks of growth. In the mono-culture and co-culture, 82 of 238 detected m/z values had concentrations greater than that of the fresh growth medium blank, and these m/z values ranged from 33.035 to 231.140 [Table 1]. Of these 82 m/z values, 50 m/z values had higher concentrations than the blank in both the co-culture and *T. pseudonana* mono-culture. 16 additional m/z values had concentrations that were higher in the *T. pseudonana* mono-culture, but not the co-culture when compared to the blank, while 16 others were higher in the co-culture, but not in the *T. pseudonana* mono-culture when compared to the blank [Table 1].

Nine m/z values were identified that significantly changed in concentration between the *T. pseudonana* mono-culture and co-culture [Fig. 2A, 2B]. Eight of the nine m/z values were lower in concentration in the co-culture compared to the *T. pseudonana* mono-culture, with m/z 101.096 showing the largest relative decrease in co-culture

concentration with a $\log_2$ fold-change of -1.24 [Fig. 2B]. Several m/z values that changed in concentration in the co-culture compared to the *T. pseudonana* mono-culture were putatively identified in Table 2 on the basis of their mass number and previous reports of biogenic production by phytoplankton (Cotsaris *et al.*, 1995; Colomb *et al.*, 2008b; Jüttner *et al.*, 2010; Dani and Loreto, 2017; Halsey *et al.*, 2017). As a result, we identified cyclohexanol, hexanal, cyclopentanol, acetaldehyde, acetonitrile, and acetone as compounds that changed significantly ($Q \leq 0.1$) in concentration in the co-culture compared to the diatom mono-culture [Fig. 2, Table 2]. Dimethyl sulfide (m/z 63.026) and isoprene (m/z 69.070), two important VOCs in the marine environment, marginally changed in concentration between the mono- and co-cultures [Fig. 2, Table 2]. VOCs at m/z 82.958 and 84.940 were also lower in concentration in the co-culture relative to the mono-culture. These two m/z values may be halogenated organic compounds, such as carbonyl chlorofluoride (m/z 82.958) or dichloromethane (m/z 84.940), which are reportedly produced in large quantities by diatoms (Colomb *et al.*, 2008a; Paul and Pohnert, 2011),. Halogenated compounds were not expected to be observed when running the PTR-TOF/MS in H_3O^+ mode, but ionization by contaminant O_2^+ ions originating from the ion source may have allowed for detection of some halogenated compounds. One m/z value, 49.011 (methanethiol), was higher in concentration in the co-culture compared to the *T. pseudonana* mono-culture, as might be anticipated since *Pelagibacter* has previously been identified as a methanethiol producer (Sun *et al.*, 2016). There were no differences in the concentrations of compounds with m/z values larger than 101.096.

ATP measurements

A sensitive luciferase-based assay to measure cellular ATP was used to test whether HTCC1062 could metabolize the compounds we identified using PTR-TOF/MS. VOCs we putatively identified based on molecular mass and previous reports of production by phytoplankton (Cotsaris *et al.*, 1995; Colomb *et al.*, 2008b; Jüttner *et al.*, 2010; Dani and Loreto, 2017; Halsey *et al.*, 2017) were fed to starved HTCC1062 cells. Acetone (m/z 59.049), isoprene (m/z 69.070), and two compounds representing m/z 101.096, hexanal and cyclohexanol, caused increases in cellular ATP content over the no-VOC-added control [Table 3]. 2-Hexanone and cis-3-hexen-1-ol, which were also candidate compounds representing m/z 101.096, did not result in increases in cellular ATP content. Acetonitrile (m/z 42.034) concentrations changed between the mono- and co-culture, and toluene appeared as a compound of interest early on in our analysis, but increased ATP content could not be confirmed in cells fed either of these compounds because of a large standard deviation across replicates in this particular experiment. These data confirm that HTCC1062 can utilize a variety of VOCs as energy sources, thus the metabolism of these compounds by HTCC1062 may have resulted in their lower concentrations measured in the co-cultures. Since many different compounds with a wide variety of elemental compositions and structures can have the same mass number, we could not screen all of the chemical compounds that could represent each m/z value identified in Table 2. Consequentially, we cannot rule out that other VOCs sharing the same molecular mass contribute to the observed concentration changes in the PTR-TOF/MS m/z values.

Carbon fixation and photophysiology

Even though the presence of HTCC1062 did not cause a change in the growth rate of *T. pseudonana* when compared to its growth rate in mono-culture [Fig 1B], we considered the possibility that other photo-physiological changes may have been stimulated by HTCC1062. F_v/F_m experienced a slight drop from 0.62 in mono-culture to 0.60 in co-culture, but there were no other evident differences in various measurements of diatom photo-physiology, including chlorophyll-a, total integrated cellular absorption, and measurements of other photo-pigment concentrations between the mono- and co-cultures [Table 4].

Photosynthetic carbon fixation was measured in seven independent pairs of *T. pseudonana* mono- and co-cultures. Carbon fixation varied between iterations of the experiment from 0.0249 to 0.0939 pmol C $cell^{-1}$ h^{-1}. Nevertheless, the average difference in carbon fixation between mono- and co-culture pairs was 0.0139 pmol C $cell^{-1}$ h^{-1} ($p = 0.05$, paired t-test, $n = 7$), equating to a mean increase of 20.3% in *T. pseudonana* carbon fixation in the co-culture compared to the mono-culture [Fig. 3A]. Accumulation of the ^{14}C tracer in bacterial biomass through inorganic carbon fixation was ruled out because the mean increase in carbon fixation by the diatoms in the co-cultures was 9.51×10^3 pmol C mL $culture^{-1}$ h^{-1}, but incorporation of the labeled inorganic carbon by HTCC1062 was only 1.07×10^1 pmol C mL $culture^{-1}$ h^{-1}, about three orders of magnitude less than the average difference in carbon fixation between the *T. pseudonana* mono and co-cultures.

We hypothesized that metabolism of VOCs by HTCC1062 stimulated the faster rate of carbon fixation in *T. pseudonana* in co-culture relative to the mono-culture. To

test this idea, we replaced the biological VOC sink (i.e., HTCC1062) with a physical VOC sink – a hydrocarbon trap in a circulating gas loop. When VOCs were continuously removed from the *T. pseudonana* cultures using the hydrocarbon trap, carbon fixation increased by an average of 0.0214 pmol $cell^{-1}$ h^{-1} (18.1%) compared to normal cultures containing VOCs [Fig. 3B, $p = 0.08$, paired t-test, n=6]. Similar to the growth experiments in the presence and absence of HTCC1062, *T. pseudonana* growth rates were unaffected by the presence or absence of VOCs (0.57 ± 0.02 and 0.56 ± 0.04 d^{-1}, respectively).

Discussion

The total VOC pool has attracted attention as a potentially significant component of phytoplankton-derived DOC in the marine environment (Myklestad, 2000; Thornton, 2014), but the magnitude of VOC flux between phytoplankton and bacterioplankton and the suite of compounds involved have not been characterized with enough precision and detail to draw definitive conclusions. Two studies suggested that 30 to 40% of marine DOC is composed of VOCs (Dachs *et al.*, 2005; Ruiz-Halpern *et al.*, 2010), but methodological issues confounded those results (Hauser *et al.*, 2013). There is also uncertainty about variation in the contributions of VOCs to the DOC pool across different ocean regions and time scales, which are needed to close the carbon budget and define the roles of VOCs in marine ecology and their impacts on atmospheric processes (O'Dowd and de Leeuw, 2007; Facchini *et al.*, 2008; Spracklen *et al.*, 2008).

We designed experiments with two taxa that are important carbon cycle contributors in productive temperate coastal ocean regions, and studied their VOC-

associated interactions with analytical methods that were not confined to known targeted VOCs. VOCs known to be produced by diatoms, including, acetone (m/z 59.049), and cyclohexanol (m/z 101.096) (Cotsaris *et al.*, 1995; Colomb *et al.*, 2008a; Dani and Loreto, 2017; Halsey *et al.*, 2017; Srikanta Dani *et al.*, 2017), were identified and shown to be metabolized by the common heterotroph *Pelagibacter*, which co-occurs in diatom habitats. Unexpectedly, consumption of these VOCs by *Pelagibacter* imposed a significant energetic tax on *T. pseudonana* by decoupling photosynthetic carbon fixation from growth. To explain these observations, we postulate that some VOCs used by *Pelagibacter* are volatile metabolic intermediates in phytoplankton biochemical pathways that enter a pool of public goods. In this conceptual model, *Pelagibacter* metabolism of these public goods imposes an energetic tax by requiring the diatom to more rapidly fix carbon to maintain intracellular pools of volatile metabolites.

Growth of HTCC1062 in co-culture with *T. pseudonana* caused VOCs at nine different m/z values to change in concentration relative to *T. pseudonana* mono-cultures. Eight of these m/z values decreased in concentration in the co-culture, suggesting that metabolism of VOCs by HTCC1062 resulted in their lower observed concentrations in co-culture. An alternative interpretation of these data is that, in the co-culture, production of these VOCs by *T. pseudonana* was diminished by the presence of HTCC1062. The first explanation is more likely because when VOCs representing several m/z values were fed to HTCC1062 in mono-culture, ATP content in the cells increased [Table 3]. Additionally, we observed a decrease in the concentrations of m/z 45.033 (acetaldehyde) and 63.026 (dimethyl sulfide [DMS]), as well as an increase in the concentration of m/z 49.011 (methanethiol), findings that are consistent with previous reports showing

HTCC1062 metabolism of acetaldehyde and DMS, and formation of methanethiol as a waste product of DMSP metabolism (Sun *et al.*, 2016; Halsey *et al.*, 2017). Thus, we can add acetone, isoprene, cyclohexanol, and hexanal to the growing list of VOC substrates used by *Pelagibacter*, but the rates and mechanisms of their metabolism remain to be determined. Acetonitrile and toluene marginally increased in ATP content; however, significant variability in this particular experiment prevented us from confirming HTCC1062 metabolism of these compounds by this approach. Significant, yet modest increases in cellular ATP content when supplied the VOCs shown in Table 3 indicate that certain VOCs can be utilized by HTCC1062, but they do not provide as much ATP as pyruvate, a required growth substrate. However, the collective impact of many different VOCs utilized simultaneously by HTCC1062 in co-cultures or in the environment could additively constitute a significant energy input for cell metabolism.

Recent work examining bacterial metabolism of VOCs in the marine environment has shown that a limited but diverse array of marine heterotrophic bacterioplankton are able to harvest VOC compounds and use them to supply elemental quotas or energy (Sun *et al.*, 2011; Halsey *et al.*, 2012, 2017; Dixon *et al.*, 2014; Johnston *et al.*, 2017; Sargeant *et al.*, 2018). For example, acetone metabolism rates in seawater were positively correlated with the abundance of low nucleic acid bacteria, which dominated the community and included *Rhodobacteriales* and SAR11/*Pelagibacter* (Dixon *et al.*, 2014). Similarly, the abundance of SAR11 was correlated with rates of methanol oxidation and explained up to 59% of methanol oxidation in oligotrophic environments (Sargeant *et al.*, 2018). *Rhodococcus, Gordonia*, and *Mycobacterium* were enriched in seawater incubated with isoprene (Johnston *et al.*, 2017), and the evolutionarily distant methylovore

HTCC2181 (Betaproteobacteria) metabolized a variety of VOCs, including methyl chloride and methanol (Halsey *et al.*, 2012). Aside from these few examples, the microbes responsible for metabolizing VOCs in the ocean and the biochemical pathways involved remain relatively unknown.

T. pseudonana supported growth of *Pelagibacter* HTCC1062 with no added pyruvate, glycine or methionine [Fig 1C], and enhanced HTCC1062 growth rates under carbon replete conditions in co-culture [Fig. 1A]. These data show that *T. pseudonana* produced compounds that met the unusual requirements of HTCC1062 for reduced sulfur compounds, glycine or glycine precursors, and alanine or alanine precursors (Tripp *et al.*, 2008; Carini *et al.*, 2012, 2014). The ubiquitous cyanobacterium, *Prochlorococcus,* was also observed to support growth of a related *Pelagibacter* strain, HTCC7211, in co-culture. Similar to HTCC1062 growing with *T. pseudonana*, HTCC7211 exhibited enhanced growth during the *Prochlorococcus* exponential phase and a rapid decline in cell density when *Prochlorococcus* reached stationary phase (Becker *et al.*, 2019), potentially due to a shift in the types of exometabolites produced as the phytoplankton reaches stationary phase (Barofsky *et al.*, 2009; Longnecker *et al.*, 2015). Exometabolite production, including VOCs, differs among phytoplankton (Halsey *et al.*, 2017; Landa *et al.*, 2017), but in the two examples of phytoplankton co-cultured with *Pelagibacter* reported so far, the phytoplankton exometabolites were sufficient to support growth when required growth substrates were omitted from the growth medium, with the exception of vitamins such as 4-amino-5-hydroxymethyl-2-methylpyrimidine (HMP), which were not tested in either study (Becker *et al.*, 2019). The volatile components of DOC produced by *T. pseudonana* were demonstrated to be sources of energy for HTCC1062, as some of the

identified VOCs stimulated ATP production by the bacteria, but their contribution to the observed growth enhancement of HTCC1062 in co-culture remains uncertain, with the exception of acetaldehyde (m/z 45.033), which can be incorporated into HTCC1062 biomass (Halsey *et al.*, 2017). Experiments examining the metabolism of VOCs by HTCC1062 in greater detail are necessary to understand their importance as substrates, but studies on the metabolism of other carbon substrates by the SAR11 clade indicate that many organic compounds are oxidized for energy, rather than used for growth (Sun *et al.*, 2011; Halsey *et al.*, 2017; S. J. Giovannoni *et al.*, 2019).

The propensity of low molecular weight, non-polar, or hydrophobic volatile compounds to diffuse through the cell membrane (Bjørrisen, 1988) means that they can be uncontrollably lost from cells. For photoautotrophs, this carbon loss can be taxing to the energetics of their growth, especially in small cells with low surface area to volume ratios, unless a relatively high environmental concentration of VOCs exists to maintain equilibrium with the VOCs inside the cell (Bjørrisen, 1988). In principle, the consumption of VOCs by heterotrophic organisms would promote the flux of VOC metabolites from the phytoplankton cells into the environment. We found support for this interpretation in the observation that we could simulate continuous bacterial VOC consumption by recirculating the headspace air in *T. pseudonana* mono-cultures through a hydrocarbon trap. Removal of VOCs using this method caused an 18.1% increase in carbon fixation compared to cultures containing VOCs, without altering growth [Fig. 3B]. Comparably, HTCC1062 caused *T. pseudonana* carbon fixation to increase by 20.3% in the co-culture [Fig. 3A]. These results suggest that removal of VOCs from the culture medium stimulated diffusional efflux of VOCs from *T. pseudonana*, and the cells

responded to this loss of carbon by increasing carbon fixation. This response implies that phytoplankton depend on the availability of volatile compounds to maintain metabolic efficiency and constant growth rates. A similar phenomenon is shown to occur in bacterial cultures producing siderophore public goods under iron limitation, where siderophore production by *Pseudomonas aeruginosa* was higher in the presence of cheater cells that steal, but do not synthesize siderophores (Weigert and Kümmerli, 2017). Thus, VOCs are another example of a public good that can be exploited by the broader microbial community at the expense of the VOC producer.

Phytoplankton are sources of diverse VOC compounds, some of which have been identified as by-products or intermediates in biochemical pathways, such as carotenoid synthesis (Schmidt *et al.*, 2015). Some VOCs are reported to function as antioxidants in higher plants and algae, and protect phytoplankton cells from reactive oxygen species, especially in high light conditions (Dani and Loreto, 2017). Although the roles of VOCs in metabolism are known in only a few cases, our findings are consistent with the interpretation that VOCs are metabolic intermediates and therefore the depletion of the VOC pool by physical or biological sinks requires cells to respond by increasing carbon fixation rates to make up for the loss flux. Despite there being no difference in *T. pseudonana* growth rates in either of our experiments, VOCs cannot be considered "costless public goods" (Pacheco *et al.*, 2019) because of the energetic costs associated with increasing carbon fixation to maintain *T. pseudonana* growth and homeostasis. Such cryptic physiological responses are challenging to measure but important for understanding the causes of variability in photosynthesis, which remain a major source of

error in estimates of global primary production (Cullen, 1990; Behrenfeld and Falkowski, 1997).

Elevated carbon fixation was observed in another diatom, *Phaeodactulum tricornutum*. In that study, it was hypothesized that catabolism of diatom-derived carbon by attached bacterial communities alleviated CO_2 limitation at the diatom cell surface, thus stimulating carbon fixation (Samo *et al.*, 2018). However, enhanced carbon fixation was heterogeneous in single cell measurements, and was only observed in one of two *P. tricornutum* co-cultures examined (Samo *et al.*, 2018). In another study, increased expression of transcripts associated with Photosystem I and chlorophyll synthesis occurred in *Prochlorococcus* when growing in a co-culture with *Alteromonas* (Biller *et al.*, 2016). Such changes may indicate that carbon fixation increased in *Prochlorococcus* in response to the heterotrophic consumption of carbon released by the algae, but carbon fixation was not directly measured (Biller *et al.*, 2016).

We offer a similar explanation for observed increases in photosynthesis when phytoplankton are co-cultured with heterotrophs. The evidence we provide supports a mechanism in which bacterial metabolism of VOCs lowers VOC concentrations in the environment, causing an increase in the leakage of VOC metabolites from phytoplankton cells. This scenario assumes that the VOC metabolites in question are not end-products that have no further metabolic purpose and would be wasted. Increasing the flux of such compounds from cells would force phytoplankton to increase carbon fixation to maintain their growth rate. If this interpretation is correct, then bacterial catabolism of diffusible public goods couples VOC production and consumption in a VOC cycle that has a

feedback mechanism, inducing more photosynthetic production and decreasing the efficiency of CO_2 conversion into phytoplankton biomass.

Our study, which used representatives of two of the most abundant microorganisms in the oceans, indicated VOC fluxes that we estimate are about 20% of carbon fixation. Rising awareness of VOC cycling has led to speculation about their contribution to the overall carbon cycle of the oceans. Across the entire ocean, gross primary production is estimated at 1.55×10^{17} g C y^{-1} (Marra, 2002; Westberry et al., 2008). If 20% of carbon fixed in the ocean is released from algae as VOCs, the total marine VOC production rate would be 3.10×10^{16} g C y^{-1}. This estimate is subject to large uncertainties, and likely depends on many unexplored factors, including growth conditions and community composition, but it establishes an approximate magnitude for the process we observed. Unexpectedly large fluxes of VOCs from phytoplankton and specialization in the oxidation of labile low molecular weight compounds, including VOCs, by SAR11 may partially explain how small, simple SAR11 cells capture an estimated 6-37% of gross primary production (White et al., 2018).

Our results suggest that the VOC cycle can be a very significant component of carbon transfer from phytoplankton to bacteria. Further exploration of this topic likely will take varied paths, which might include further studies with cultured cells to define the metabolic origins, turnover times, and fates of the wide variety of VOCs that are being detected in phytoplankton cultures. Also important will be field studies to measure these compounds in the environment, where, in many cases, they have seldom or never been reported. Defining the roles of VOCs will contribute to a better understanding of many features of the carbon cycle, for example uncoupling of gross and net carbon

fixation, the niches of heterotrophs, like SAR11, some of which paradoxically capture a large fraction of production with small genomes, and the variable influence of plankton on the atmosphere, where VOCs are engaged in complex chemistry.

Originality Significance Statement*:*

This research evaluated the contributions of VOCs to phytoplankton-bacterial interactions in the context of the marine microbial carbon cycle. We show that a wide variety of VOCs are transferred between a ubiquitous photosynthetic diatom and the heterotrophic bacteria *Pelagibacter*. Our results show for the first time that bacterial metabolism of VOCs reduces the efficiency of CO_2 conversion into biomass in phytoplankton by promoting loss of diffusible VOCs from those cells, and that phytoplankton rely on a publicly available pool of VOCs to remain metabolically efficient. These findings recognize VOCs as an important pool of public goods in microbial ecosystems, and their significant contributions to microbial interactions and the marine carbon cycle should not be overlooked.

Acknowledgements

The authors would like to thank Martin Schuster for use of the luminometer. This work was partially supported by the NASA North Atlantic Aerosols and Marine Ecosystems Study (NAAMES), award ID: NNX15AE70G, and the National Science Foundation, award ID: OCE-1436865.

Figures and Tables

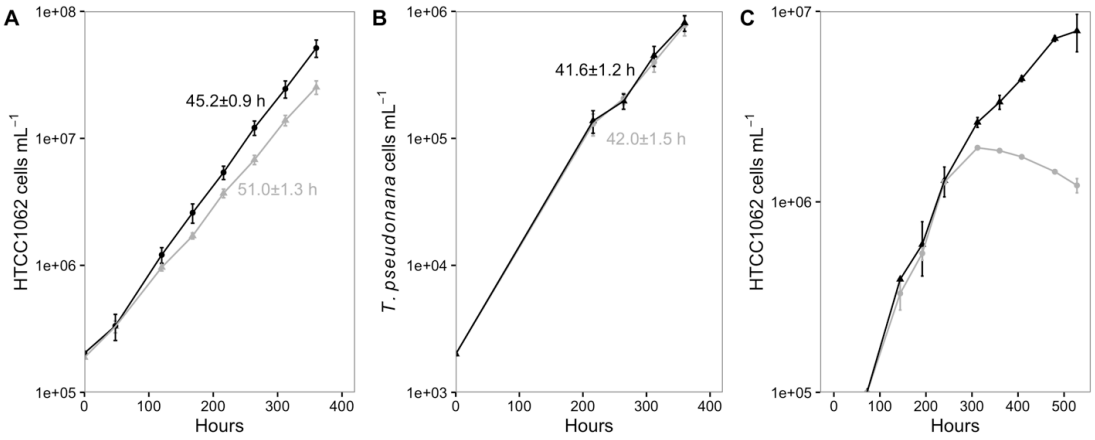

Fig.1: HTCC106*2* growth is enhanced by the presence of *T. pseudonana*. **A**: HTCC1062 generation times under carbon-replete conditions were nearly 6 hours faster in co-culture (black) with the diatom compared to growth in mono-culture (gray); ($p = 1 \times 10^{-4}$, n=5). **B:** *T. pseudonana* growth rates were unchanged in the presence of the heterotroph (black = co-culture, gray = mono-culture); (p=0.67, n=5). **C**: In medium lacking pyruvate, glycine and methionine, HTCC1062 was added to an exponentially growing *T. pseudonana* culture after 72h (black) and reached a maximum density that was four-fold higher than the density reached by cells in mono-culture also lacking pyruvate, glycine and methionine (gray) (n=3). Error bars show standard deviations, p-values calculated using a student's t-test.

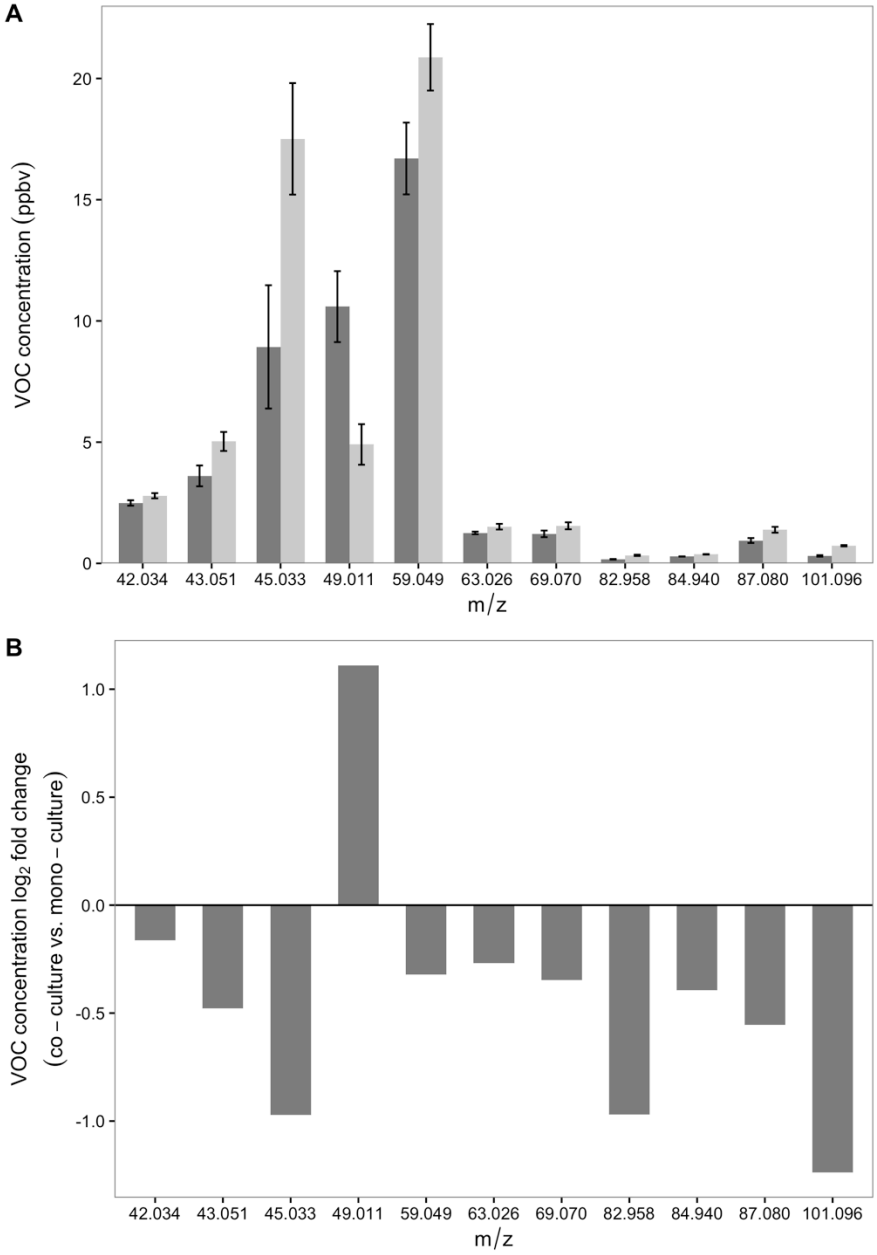

Fig. 2**:** HTCC1062 metabolizes a wide range of VOCs. **A**: Concentrations of VOCs (shown along x-axis as m/z, equal to a compound's un-fragmented mass + 1) that differed in concentration in the *T. pseudonana*-HTCC1062 co-culture (dark bars) relative to the *T. pseudonana* mono-culture (light bars). *T. pseudonana* cell densities were equal in all cultures. **B:** Log_2 fold-change of VOC concentrations in the co-culture relative to the *T. pseudonana* mono-culture for each m/z value. Putative identifications for each m/z are provided in Table 2.

m/z	Blank Conc. (ppbv)	TP Conc. (ppbv)	TP SD	CC Conc. (ppbv)	CC SD	Q-value	Culture
33.035	16.800	17.878	0.171	17.743	0.199	0.884	B
36.045	1.611	1.667	0.019	1.634	0.009	0.220	B
38.040	12.856	13.426	0.027	13.332	0.072	0.308	B
41.033	1.621	4.764	0.890	3.682	0.865	0.496	B
42.034	**1.821**	**2.790**	**0.107**	**2.491**	**0.112**	**0.092**	**B**
43.021	3.933	8.585	1.191	8.421	0.957	1.027	B
43.051	**1.775**	**5.029**	**0.392**	**3.609**	**0.429**	**0.039**	**B**
45.033	**11.463**	**17.510**	**2.300**	**8.930**	**2.542**	**0.041**	**T**
49.011	**3.600**	**4.905**	**0.836**	**10.591**	**1.463**	**0.032**	**C**
54.001	0.428	0.460	0.015	0.453	0.016	1.099	T
56.058	0.253	0.317	0.027	0.289	0.019	0.529	T
59.049	**8.863**	**20.874**	**1.372**	**16.700**	**1.482**	**0.076**	**B**
60.054	1.050	1.857	0.090	1.702	0.078	0.239	B
60.040	2.559	6.259	0.978	6.328	0.655	1.027	B
62.035	0.652	0.792	0.039	0.788	0.027	1.013	B
63.026	*0.866*	*1.513*	*0.117*	*1.256*	*0.052*	*0.145*	*B*
65.075	0.439	0.496	0.025	0.483	0.029	1.101	T
67.055	0.422	0.480	0.028	0.457	0.022	0.760	T
69.070	*0.920*	*1.550*	*0.144*	*1.218*	*0.137*	*0.140*	*B*
71.061	0.439	0.846	0.126	0.837	0.192	1.025	B
72.052	0.222	0.443	0.131	0.478	0.127	1.059	C
73.053	3.075	4.478	0.400	4.214	0.416	0.968	B
74.058	0.620	0.756	0.039	0.705	0.028	0.357	B
81.067	0.228	0.299	0.028	0.283	0.024	1.005	B
82.958	**0.157**	**0.332**	**0.027**	**0.169**	**0.010**	**0.015**	**T**
83.082	0.380	0.724	0.091	0.559	0.085	0.233	B
84.084	0.141	0.298	0.072	0.301	0.062	0.993	B
84.940	**0.286**	**0.374**	**0.011**	**0.285**	**0.004**	**0.005**	**T**
85.066	0.265	0.620	0.106	0.585	0.110	1.080	B
86.062	0.147	0.234	0.039	0.249	0.048	1.167	B
87.080	**0.660**	**1.387**	**0.120**	**0.944**	**0.101**	**0.029**	**B**
89.047	0.180	0.256	0.030	0.255	0.036	1.009	B
96.011	0.375	0.554	0.051	0.575	0.037	1.119	B
98.030	0.291	0.331	0.012	0.354	0.051	0.994	T
100.048	0.239	0.346	0.063	0.367	0.059	1.160	C
100.946	0.145	0.165	0.004	0.156	0.001	0.166	B
101.096	**0.218**	**0.728**	**0.027**	**0.309**	**0.031**	**0.000**	**B**
111.005	0.201	0.351	0.047	0.342	0.054	1.066	B
113.093	0.098	0.317	0.087	0.323	0.095	1.037	B
119.967	0.236	0.243	0.005	0.249	0.003	0.315	C
121.083	0.207	0.251	0.021	0.297	0.069	0.790	T

m/z	Blank	TP Mean	TP SD	CC Mean	CC SD	Q-value	T, C or B
121.985	0.127	0.136	0.004	0.144	0.011	0.780	T
123.105	0.126	0.188	0.029	0.197	0.029	1.055	B
123.960	0.211	0.217	0.006	0.220	0.003	1.080	C
125.978	0.127	0.151	0.011	0.151	0.016	0.999	T
127.097	0.141	0.417	0.073	0.370	0.067	0.963	B
128.095	0.085	0.122	0.012	0.118	0.008	1.119	B
129.115	0.141	0.235	0.024	0.217	0.023	0.874	B
130.080	0.079	0.099	0.005	0.094	0.008	0.906	T
135.087	0.123	0.180	0.025	0.168	0.020	1.080	B
138.036	0.066	0.098	0.012	0.095	0.012	1.074	B
140.100	0.065	0.089	0.012	0.086	0.011	1.148	T
141.100	0.078	0.179	0.029	0.150	0.023	0.573	B
143.133	0.098	0.180	0.027	0.176	0.030	1.042	B
143.948	0.079	0.091	0.004	0.090	0.005	1.064	B
145.107	0.062	0.073	0.004	0.071	0.005	1.122	T
149.037	0.099	0.161	0.027	0.161	0.030	1.001	B
151.096	0.065	0.152	0.055	0.146	0.040	1.008	C
153.084	0.066	1.203	0.443	1.028	0.292	1.099	B
153.256	0.025	0.209	0.081	0.187	0.054	1.114	B
155.080	0.072	0.233	0.078	0.236	0.070	0.983	B
156.116	0.046	0.070	0.009	0.069	0.008	1.055	B
157.131	0.063	0.103	0.016	0.100	0.016	1.045	B
167.095	0.051	0.093	0.025	0.123	0.025	0.517	C
169.127	0.052	0.131	0.041	0.126	0.031	1.024	C
171.133	0.048	0.071	0.009	0.074	0.011	1.097	B
177.122	0.045	0.068	0.015	0.072	0.013	1.077	C
183.152	0.039	0.245	0.089	0.127	0.038	0.314	B
184.159	0.035	0.064	0.014	0.045	0.005	0.314	T
185.149	0.041	0.086	0.013	0.066	0.010	0.275	B
191.128	0.041	0.067	0.020	0.068	0.013	1.020	C
195.163	0.037	0.098	0.032	0.080	0.021	0.945	C
197.140	0.107	1.077	0.271	0.702	0.171	0.321	B
198.100	0.047	0.186	0.043	0.134	0.026	0.377	B
199.153	0.035	0.121	0.037	0.116	0.043	0.993	T
210.144	0.036	0.094	0.025	0.098	0.026	1.031	B
205.951	0.052	0.082	0.021	0.088	0.018	1.063	C
207.032	0.038	0.049	0.009	0.049	0.005	0.998	C
209.145	0.035	0.168	0.064	0.155	0.042	1.080	B
210.145	0.032	0.071	0.023	0.075	0.019	1.056	C
220.191	0.040	0.234	0.160	0.252	0.102	1.021	C

231.140	0.026	0.028	0.004	0.032	0.002	0.527	C

Table 1**:** VOCs at 82 different m/z values were produced in the *T. pseudonana* mono- and co-cultures. Of 238 m/z values detected, 82 m/z values had mean concentrations greater than 2 standard deviations above the blank measurement made with fresh growth medium. Of these 82 m/z values identified, 50 had concentrations higher than the blank in both mono-culture and co-culture (B), 16 additional m/z values had concentrations higher in the *T. pseudonana* mono-culture only when compared to the blank (T), while 16 others were higher than the blank in the co-culture only (C) – refer to "Culture" column. Q-value shows the results of the Benjimani-Hochberg statistical test used to compare concentrations between the mono- and co-cultures. Rows in bold indicate a Q-value less than 0.1.

m/z	Putative VOC	Log_2 fold-change in co-culture	Q-value
42.034	Acetonitrile	- 0.163	0.08
43.051	*Propene* *Cyclopropane*	- 0.479	0.04
45.033	Acetaldehyde	- 0.971	0.03
49.011	Methanethiol	+ 1.110	0.03
59.049	Acetone	- 0.322	0.06
63.026	Dimethyl Sulfide	- 0.269	0.12
69.070	Isoprene	- 0.348	0.12
82.958	*Carbonyl chlorofluoride*	- 0.971	0.01
84.940	*Dichloromethane*	- 0.393	0.004
87.080	Cyclopentanol Pentanal	- 0.555	0.02
101.096	Cyclohexanol Hexanal	- 1.237	<0.001

Table 2**:** Putative identification of m/z values that differed in concentration in the co-culture relative to the *T. pseudonana* mono-culture. Chemical identifications made based on non-fragmented mass number, previous reports of the specific VOC being produced in phytoplankton, or metabolism by HTCC1062 determined by ATP assay (see Table 3). Compounds listed in italics are untested candidates for each respective m/z and provided on the basis of their molecular mass. The log_2 fold change (as in Fig. 2B) is the VOC concentration in co-culture relative to the VOC concentration in *T. pseudonana* mono-culture. Q-value shows the results of the Benjimani-Hochberg statistical test used to compare concentrations between the mono- and co-cultures.

	Isoprene	Acetone	Cyclo-hexanol	Hexanal	cis-3-hexen-1-ol	2-hexanone	Acetonitrile	Toluene
m/z	69.071	59.055	101.092	101.092	101.092	101.092	42.035	93.070
No VOC (- control)	2896 ± 247	3210 ± 172	3210 ± 172	3692 ± 108	3692 ± 108	3692 ± 108	4105 ± 2261	4105 ± 2261
VOC added	3318 ± 252	3631 ± 96	3845 ± 120	4185 ± 170	3739 ± 285	3501 ±152	6167 ± 3114	6864 ± 1032
Pyruvate (+ control)	10339 ± 1254	4533 ± 111	4533 ± 111	6629 ± 252	6629 ± 252	6629 ± 252	6707 ± 644	6707 ± 644
p-value	0.015	0.032	0.009	0.004	0.775	0.091	0.411	0.157

Table 3: VOCs were added to starved HTCC1062 (VOC added row) and cellular ATP content measured relative to negative controls (No VOC row). Increased cellular ATP content shows that the compound can be metabolized by HTCC1062 and supports our putative m/z value identification (Table 2). VOCs were supplied to HTCC1062 at 1μM. Values are mean zeptograms ATP $cell^{-1}$ ± SD and p-values were calculated using a student's t-test vs. the negative control values for each experiment (isoprene n = 6, acetone and cyclohexanol n = 4, all others n = 3). Pyruvate was used as the positive control. Experiments testing different compounds were conducted with independent cultures on four different days (separated by vertical lines in table). Within a given experiment, all replicates and treatments were prepared with samples of the same culture. Due to variability between the days and reagent batches used, variability exists between the four experiments, thus comparisons should only be made to the controls for a given experiment.

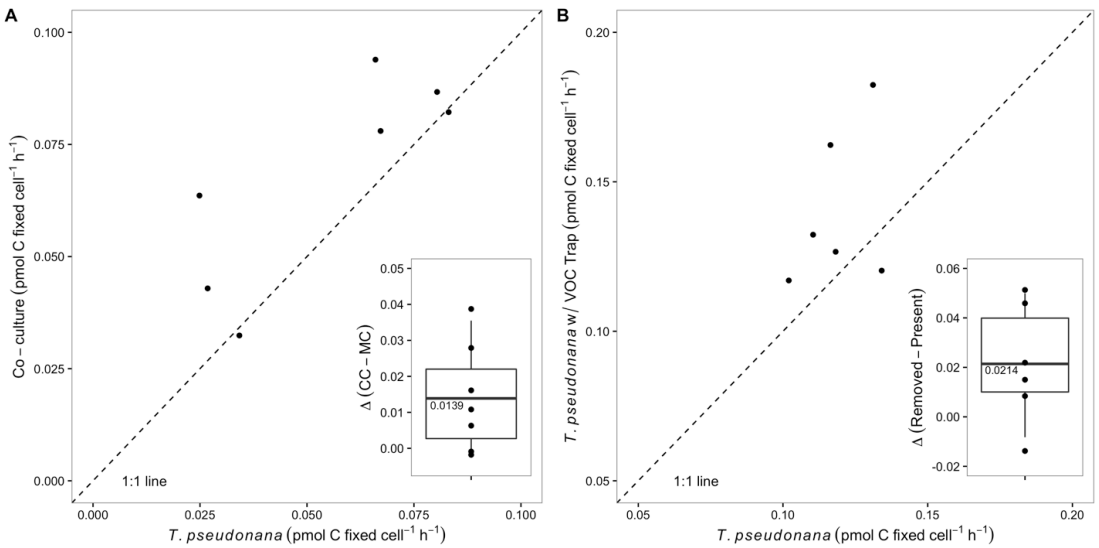

Fig. 3**:** VOC efflux causes an increase in photosynthetic carbon fixation in *T. pseudonana*. **A:** *T. pseudonana* carbon fixation increased an average of 0.0139 pmol C cell^{-1} h^{-1} ± 0.0139 pmol C cell^{-1} h^{-1}, (mean ± 95% CI, p = 0.050, paired t-test, n=7) in co-culture with HTCC1062 compared to *T. pseudonana* mono-cultures, a mean increase of 20.3%. **B:** Physical removal of VOCs in *T. pseudonana* mono-cultures using a hydrocarbon trap increased carbon fixation by an average of 0.0214± 0.0255 pmol C cell^{-1} h^{-1}, an 18.1% increase on average (mean ± 95% CI, p=0.083, paired t-test, n=6). Points in both A and B are measurements for independent pairs of mono- and co-cultures (A) or independent pairs of cultures with VOC-present and VOC-removed (B). Dashed line is the 1:1 relationship. Points falling above the 1:1 line indicate more carbon was fixed in co-culture or in the VOC-removed condition than in the mono-culture or in the VOC-present control. Differences (Δ) between carbon fixation for each pair are shown in the subplots, where the box shows the mean (value given), and upper and lower quartile divisions; whiskers show 95% confidence interval.

Parameter or pigment	*T. pseudonana* mono-culture	Co-culture	Units	p-value
F_v/F_m	0.62 ± 0.00	0.61 ± 0.01	unitless	0.05
Total absorbance	0.0116 ± 0.0012	0.0135 ± 0.0014	m^2 mg^{-1}	0.13
Chlorophyll a	0.7247 ± 0.0209	0.7541 ± 0.0617	pg $cell^{-1}$	0.50
19' Hexanoyloxyfucoxanthin	0.0018 ± 0.0003	0.0016 ± 0.0005	pg $cell^{-1}$	0.64
β Carotene	0.0219 ± 0.0012	0.0193 ± 0.0019	pg $cell^{-1}$	0.13
Chlorophyll b	0.0100 ± 0.0014	0.0099 ± 0.0009	pg $cell^{-1}$	0.95
Chlorophyll c	0.0758 ± 0.0117	0.0688 ± 0.0043	pg $cell^{-1}$	0.41
Chlorophyllide	0.0222 ± 0.0046	0.0293 ± 0.0043	pg $cell^{-1}$	0.12
Diadinoxanthin	0.0420 ± 0.0023	0.0394 ± 0.0039	pg $cell^{-1}$	0.37
Fucoxanthin	0.2737 ± 0.0105	0.2603 ± 0.0181	pg $cell^{-1}$	0.34
Lutein	0.0010 ± 0.0006	0.0012 ± 0.0003	pg $cell^{-1}$	0.51
Violaxanthin	0.0031 ± 0.0003	0.0027 ± 0.0002	pg $cell^{-1}$	0.16
Zeaxanthin	0.0015 ± 0.0008	0.0010 ± 0.0002	pg $cell^{-1}$	0.42
Total Carotenes	0.0219 ± 0.0012	0.0193 ± 0.0019	pg $cell^{-1}$	0.13

Table 4**:** Measurements of photo-physiological properties in *T. pseudonana* grown in mono-culture or co-culture showed little detectable variation between conditions. Values are the average of three biological replicates ± SD.

References

Amin, S.A., Hmelo, L.R., van Tol, H.M., Durham, B.P., Carlson, L.T., Heal, K.R., et al. (2015) Interaction and signalling between a cosmopolitan phytoplankton and associated bacteria. *Nature* **522**: 98–101.

Barofsky, A., Vidoudez, C., and Pohnert, G. (2009) Metabolic profiling reveals growth stage variability in diatom exudates. *Limnol Oceanogr Methods* **7**: 382–390.

Beale, R., Dixon, J.L., Arnold, S.R., Liss, P.S., and Nightingale, P.D. (2013) Methanol, acetaldehyde, and acetone in the surface waters of the Atlantic Ocean. *J Geophys Res Ocean* **118**: 5412–5425.

Becker, J.W., Hogle, S.L., Rosendo, K., and Chisholm, S.W. (2019) Co-culture and biogeography of Prochlorococcus and SAR11. *ISME J*.

Behrenfeld, M.J. and Falkowski, P.G. (1997) Photosynthetic rates derived from satellite-based chlorophyll concentration. *Limnol Oceanogr* **42**: 1–20.

Bidigare, R.R., Van Heukelem, L., and Trees, C.. (2005) Analysis of algal pigments by high performance liquid chromatography. In, Andersen,R. (ed), *Algal Culturing Techniques*. Academic Press, pp. 327–345.

Biller, S.J., Coe, A., and Chisholm, S.W. (2016) Torn apart and reunited: Impact of a heterotroph on the transcriptome of Prochlorococcus. *ISME J* **10**: 2831–2843.

Bisutti, I., Hilke, I., and Raessler, M. (2004) Determination of total organic carbon – an overview of current methods. *TrAC Trends Anal Chem* **23**: 716–726.

Bjørrisen, P.K. (1988) Phytoplankton exudation of organic matter: Why do healthy cells do it? *Limnol Oceanogr* **33**: 151–154.

Bromke, M.A., Giavalisco, P., Willmitzer, L., and Hesse, H. (2013) Metabolic Analysis of Adaptation to Short-Term Changes in Culture Conditions of the Marine Diatom Thalassiosira pseudonana. *PLoS One* **8**: e67340.

Buchan, A., LeCleir, G.R., Gulvik, C.A., and González, J.M. (2014) Master recyclers: features and functions of bacteria associated with phytoplankton blooms. *Nat Rev Microbiol* **12**: 686–698.

Carini, P., Campbell, E.O., Morré, J., Sañudo-Wilhelmy, S. a, Thrash, J.C., Bennett, S.E., et al. (2014) Discovery of a SAR11 growth requirement for thiamin's pyrimidine precursor and its distribution in the Sargasso Sea. *ISME J* **8**: 1727–38.

Carini, P., Steindler, L., Beszteri, S., and Giovannoni, S.J. (2012) Nutrient requirements for growth of the extreme oligotroph 'Candidatus Pelagibacter ubique' HTCC1062 on a defined medium. *ISME J* **7**: 592–602.

Colomb, A., Yassaa, N., Williams, J., Peeken, I., and Lochte, K. (2008a) Screening volatile organic compounds (VOCs) emissions from five marine phytoplankton species by head space gas chromatography/mass spectrometry (HS-GC/MS). *J Environ Monit* **10**: 325–330.

Colomb, A., Yassaa, N., Williams, J., Peeken, I., and Lochte, K. (2008b) Screening volatile organic compounds (VOCs) emissions from five marine phytoplankton species by head space gas chromatography/mass spectrometry (HS-GC/MS). *J Environ Monit* **10**: 325–330.

Cotsaris, E., Bruchet, A., Mallevialle, J., and Bursill, D.B. (1995) The identification of odorous metabolites produced from algal monocultures. *Water Sci Technol* **31**: 251–

258.
Cullen, J.J. (1990) On models of growth and photosynthesis in phytoplankton. *Deep Sea Res Part A Oceanogr Res Pap* **37**: 667–683.
Dachs, J., Calleja, M.L., Duarte, C.M., del Vento, S., Turpin, B., Polidori, A., et al. (2005) High atmosphere-ocean exchange of organic carbon in the NE subtropical Atlantic. *Geophys Res Lett* **32**: L21807.
Dani, K.G.S. and Loreto, F. (2017) Trade-Off Between Dimethyl Sulfide and Isoprene Emissions from Marine Phytoplankton. *Trends Plant Sci* **22**: 361–372.
Dixon, J.L., Beale, R., and Nightingale, P.D. (2013) Production of methanol, acetaldehyde, and acetone in the Atlantic Ocean. *Geophys Res Lett* **40**: 4700–4705.
Dixon, J.L., Beale, R., Sargeant, S.L., Tarran, G.A., and Nightingale, P.D. (2014) Microbial acetone oxidation in coastal seawater. *Front Microbiol* **5**: 1–9.
Facchini, M.C., Rinaldi, M., Decesari, S., Carbone, C., Finessi, E., Mircea, M., et al. (2008) Primary submicron marine aerosol dominated by insoluble organic colloids and aggregates. *Geophys Res Lett* **35**:.
Fink, P. (2007) Ecological functions of volatile organic compounds in aquatic systems. *Mar Freshw Behav Physiol* **40**: 155–168.
Giovannoni, S., Halsey, K., Saw, J., Muslin, O., Suffridge, C., Sun, J., et al. (2019) A parasitic arsenic cycle that shuttles energy from phytoplankton to heterotrophic bacterioplankton. *mBio (In Rev*.
Giovannoni, S.J. (2017) SAR11 Bacteria: The Most Abundant Plankton in the Oceans. *Ann Rev Mar Sci* **9**: 231–255.
Giovannoni, S.J., Halsey, K.H., Saw, J., Muslin, O., Suffridge, C.P., Sun, J., et al. (2019) A Parasitic Arsenic Cycle That Shuttles Energy from Phytoplankton to Heterotrophic Bacterioplankton. *MBio* **10**:.
Giovannoni, S.J., Tripp, H.J., Givan, S., Podar, M., Vergin, K.L., Baptista, D., et al. (2005) Genome streamlining in a cosmopolitan oceanic bacterium. *Science* **309**: 1242–1245.
Guillard, R.R.L. and Ryther, J.H. (1962) Studies of marine planktonic diatoms. I. Cyclotella nana Hustedt and Detonula confervacea Cleve. *Can J Microbiol* **8**: 229–239.
Halsey, K.H., Carter, A.E., and Giovannoni, S.J. (2012) Synergistic metabolism of a broad range of C1 compounds in the marine methylotrophic bacterium HTCC2181. *Environ Microbiol* **14**: 630–640.
Halsey, K.H., Giovannoni, S.J., Graus, M., Zhao, Y., Landry, Z., Thrash, J.C., et al. (2017) Biological cycling of volatile organic carbon by phytoplankton and bacterioplankton. *Limnol Oceanogr*.
Hauser, E.J., Dickhut, R.M., Falconer, R., and Wozniak, A.S. (2013) Improved method for quantifying the air-sea flux of volatile and semi-volatile organic carbon. *Limnol Oceanogr Methods* **11**: 287–297.
Johnston, A., Crombie, A.T., El Khawand, M., Sims, L., Whited, G.M., McGenity, T.J., and Colin Murrell, J. (2017) Identification and characterisation of isoprene-degrading bacteria in an estuarine environment. *Environ Microbiol* **19**: 3526–3537.
Jüttner, F., Messina, P., Patalano, C., and Zupo, V. (2010) Odour compounds of the diatom Cocconeis scutellum: Effects on benthic herbivores living on Posidonia oceanic. *Mar Ecol Prog Ser* **400**: 63–73.

Kolber, Z.S., Prášil, O., and Falkowski, P.G. (1998) Measurements of variable chlorophyll fluorescence using fast repetition rate techniques: defining methodology and experimental protocols. *Biochim Biophys Acta - Bioenerg* **1367**: 88–106.

Landa, M., Burns, A.S., Roth, S.J., and Moran, M.A. (2017) Bacterial transcriptome remodeling during sequential co-culture with a marine dinoflagellate and diatom. *ISME J* 1–14.

Longnecker, K., Kido Soule, M.C., and Kujawinski, E.B. (2015) Dissolved organic matter produced by Thalassiosira pseudonana. *Mar Chem* **168**: 114–123.

Marra, J. (2002) Approaches to the Measurement of Plankton Production. In, *Phytoplankton Productivity*. Oxford, UK: Blackwell Science Ltd, pp. 78–108.

Mitchell, B.G. and Kieper, D.A. (1988) Variability in pigment particulate fluorescence and absorption spectra in the northeastern Pacific Ocean. *Deep Res* **35**: 665–689.

Myklestad, S.M. (2000) Dissolved Organic Carbon from Phytoplankton. *Handb Environ Chem* **5**: 111–148.

O'Dowd, C.D. and de Leeuw, G. (2007) Marine aerosol production: a review of the current knowledge. *Philos Trans R Soc A* **365**: 1753–1774.

Pacheco, A.R., Moel, M., and Segrè, D. (2019) Costless metabolic secretions as drivers of interspecies interactions in microbial ecosystems. *Nat Commun* **10**: 103.

Paul, C., Mausz, M.A., and Pohnert, G. (2012) A co-culturing/metabolomics approach to investigate chemically mediated interactions of planktonic organisms reveals influence of bacteria on diatom metabolism. *Metabolomics* **9**: 349–359.

Paul, C. and Pohnert, G. (2011) Production and role of volatile halogenated compounds from marine algae. *Nat Prod Rep* **28**: 186–195.

Ritchie, R.J. (2006) Consistent sets of spectrophotometric chlorophyll equations for acetone, methanol and ethanol solvents. *Photosynth Res* **89**: 27–41.

Ruiz-Halpern, S., Sejr, M.K., Duarte, C.M., Krause-Jensen, D., Dalsgaard, T., Dachs, J., and Rysgaard, S. (2010) Air-water exchange and vertical profiles of organic carbon in a subarctic fjord. *Limnol Oceanogr* **55**: 1733–1740.

Samo, T.J., Kimbrel, J.A., Nilson, D.J., Pett-Ridge, J., Weber, P.K., and Mayali, X. (2018) Attachment between heterotrophic bacteria and microalgae influences symbiotic microscale interactions. *Environ Microbiol* **20**: 4385–4400.

Sargeant, S.L., Murrell, J.C., Nightingale, P.D., and Dixon, J.L. (2018) Basin-scale variability of microbial methanol uptake in the Atlantic Ocean. *Biogeosciences* **15**: 5155–5167.

Schmidt, R., Cordovez, V., De Boer, W., Raaijmakers, J., and Garbeva, P. (2015) Volatile affairs in microbial interactions. *ISME J* **9**: 2329–2335.

Shaw, S.L., Chisholm, S.W., and Prinn, R.G. (2003) Isoprene production by Prochlorococcus, a marine cyanobacterium, and other phytoplankton. *Mar Chem* **80**: 227–245.

Sinha, V., Williams, J., Meyerhöfer, M., Riebesell, U., Paulino, A.I., and Larsen, A. (2007) Air-sea fluxes of methanol, acetone, acetaldehyde, isoprene and DMS from a Norwegian fjord following a phytoplankton bloom in a mesocosm experiment.

Spracklen, D. V., Arnold, S.R., Sciare, J., Carslaw, K.S., and Pio, C. (2008) Globally significant oceanic source of organic carbon aerosol. *Geophys Res Lett* **35**: n/a-n/a.

Srikanta Dani, K.G., Silva Benavides, A.M., Michelozzi, M., Peluso, G., Torzillo, G., and

Loreto, F. (2017) Relationship between isoprene emission and photosynthesis in diatoms, and its implications for global marine isoprene estimates. *Mar Chem* **189**: 17–24.

Sun, J., Steindler, L., Thrash, J.C., Halsey, K.H., Smith, D.P., Carter, A.E., et al. (2011) One Carbon Metabolism in SAR11 Pelagic Marine Bacteria. *PLoS One* **6**: e23973.

Sun, J., Todd, J.D., Thrash, J.C., Qian, Y., Qian, M.C., Temperton, B., et al. (2016) The abundant marine bacterium Pelagibacter simultaneously catabolizes dimethylsulfoniopropionate to the gases dimethyl sulfide and methanethiol. *Nat Microbiol* **1**: 16065.

Thornton, D.C.O. (2014) Dissolved organic matter (DOM) release by phytoplankton in the contemporary and future ocean. *Eur J Phycol* **49**: 20–46.

Van Tol, H.M., Amin, S.A., and Armbrust, V. (2016) Ubiquitous marine bacterium inhibits diatom cell division. *ISME J* **11**: 31–42.

Tripp, H.J., Kitner, J.B., Schwalbach, M.S., Dacey, J.W.H., Wilhelm, L.J., and Giovannoni, S.J. (2008) SAR11 marine bacteria require exogenous reduced sulphur for growth. *Nature* **452**: 741–4.

Uitz, J., Claustre, H., Gentili, B., and Stramski, D. (2010) Phytoplankton class-specific primary production in the world's oceans: Seasonal and interannual variability from satellite observations. *Global Biogeochem Cycles* **24**: n/a-n/a.

Weigert, M. and Kümmerli, R. (2017) The physical boundaries of public goods cooperation between surface-attached bacterial cells. *Proc R Soc B* **284**:.

Westberry, T., Behrenfeld, M.J., Siegel, D.A., and Boss, E. (2008) Carbon-based primary productivity modeling with vertically resolved photoacclimation. *Global Biogeochem Cycles* **22**:.

White, A., Giovannoni, S., Zhao, Y., Vergin, K., and Carlson, C. (2018) Elemental content and stoichiometry of SAR11 chemoheterotrophic marine bacteria. *Limnol Oceanogr (In Rev*.

Wright, S.W., Jeffrey, S.W., Mantoura, R.F.C., Llewellyn, C.A., Bjørnland, T., Repeta, D., and Welschmeyer, N. (1991) Improved HPLC method for the analysis of chlorophylls and carotenoids from marine phytoplankton. *Mar Ecol Prog Ser* **77**: 183–196.

Metabolism of key atmospheric volatile organic compounds by the marine heterotrophic bacterium *Pelagibacter* (SAR11)

Eric R. Moore, Alec J. Weaver, Ed W. Davis, Stephen J. Giovannoni, and Kimberly H. Halsey

For submission to mBio

Abstract

Acetone and isoprene, volatile organic compounds (VOCs) produced by plants and phytoplankton, have important roles in atmospheric processes. These compounds diffuse between the ocean and atmosphere, with the ocean acting as either a net sink or source of these compounds. Large uncertainties exist about the significance of marine heterotrophic bacteria as a sink for acetone and isoprene and the control bacteria impose on the direction and magnitude of VOC fluxes. In this work, the metabolism of acetone and isoprene by a strain of the SAR11 family of α-proteobacteria was investigated, and its potential impact on marine acetone and isoprene cycling was studied using global ocean metagenomes. *Pelagibacter* strain HTCC1062 utilized acetone at rates similar to those observed in bacterial communities in whole seawater. Acetone could be oxidized to CO_2 or incorporated into biomass, where it could substitute for glycine, a required growth substrate. Homologs of an acetone monooxygenase-encoding gene were identified in the HTCC1062 genome and the genomes of a wide variety of other marine taxa, including SAR116 and Rhodobacteriaciae. Homologs of this gene were most abundant in metagenomes sampled in regions where the ocean is an acetone sink. *Pelagibacter*, which does not have a canonical isoprene degradation pathway, utilized isoprene supplied in culture to meet its isoprenoid requirements for growth. Acetone and isoprene metabolism by heterotrophic bacteria, including HTCC1062, likely consume substantial fractions of the total marine acetone and isoprene budgets, and therefore play key roles in regulating the emissions of these important climate active compounds from the ocean into the atmosphere.

Introduction

Acetone (C_3H_6O) and isoprene (C_5H_8) are abundant volatile organic compounds (VOCs) that are produced by phytoplankton in the ocean (Shaw *et al.*, 2003; Colomb *et al.*, 2008; Halsey *et al.*, 2017). Movement of these VOCs across the sea-air interface initiates complex chemical reactions that include important climate-relevant processes (Hense *et al.*, 2017). Acetone is a major source of ozone in the troposphere (Müller and Brasseur, 1999; Folkins and Chatfield, 2000) and is sometimes the dominant non-methane VOC in the atmosphere (Singh *et al.*, 1994). Acetone flux between the ocean and atmosphere is concentration-dependent and variable in direction and magnitude over time and space. Acetone sea-air flux ranges from -7 to +8 Tg yr^{-1}, with the ocean typically acting as a sink for acetone in temperate latitudes and a source in the tropics and sub-tropics (Sinha *et al.*, 2007; Fischer *et al.*, 2012; Beale *et al.*, 2013; Yang *et al.*, 2014). Biological isoprene emissions contribute to about half of the 1000 Tg C global VOC budget (Guenther *et al.*, 2012), are involved in secondary aerosol formation, and impact the oxidative capability of the atmosphere (Andreae and Crutzen, 1997; Liakakou *et al.*, 2007). Marine isoprene emissions are estimated at 0.1-11.6 Tg C y^{-1} (Palmer and Shaw, 2005; Sinha *et al.*, 2007; Hackenberg *et al.*, 2017), two to three orders of magnitude lower than terrestrial emissions. Discrepancies between measured and modeled flux rates suggest that there is a significant unknown sink for isoprene in the ocean (Palmer and Shaw, 2005; Booge *et al.*, 2017).

Microbial heterotrophic consumption of acetone and isoprene has been hypothesized to account for unexplained variability in sea-air flux rates and VOC budgets. Monthly variability in acetone oxidation rates in the ocean range from 1-380 pmol L^{-1} h^{-1} (Dixon *et al.*, 2014; Beale *et al.*, 2015). Oxidation rates were highest in the winter or when "low nucleic acid" bacteria, a classification that includes the ubiquitous clade of α-proteobacteria SAR11, were at their highest cell densities and dominant in the community (Dixon *et al.*, 2014). In soil systems, bacterial acetone metabolism occurs through a variety of biochemical pathways that are typically initiated by an acetone monooxygenase enzyme that converts acetone to acetol or methyl acetate (Levine and Krampitz, 1952; Taylor *et al.*, 1980; Kotani *et al.*, 2007). Acetol can be further converted to methylglyoxal then to pyruvate (Taylor *et al.*, 1980), to formaldehyde and acetic acid (Hartmans and de Bont, 1986), or possibly to formaldehyde and acetaldehyde (Levine and Krampitz, 1952), but this latter pathway requires further support (Hausinger, 2007). Methyl acetate, the alternative product of the monooxygenase, can be further converted to methanol and acetic acid (Kotani *et al.*, 2007).

Isoprene degrading bacterial communities have been described in estuarine surface water and sediments where heterotrophic consumption of isoprene was sufficient to prevent isoprene emission into the atmosphere (Alvarez *et al.*, 2009; Johnston *et al.*, 2017). Microbial isoprene metabolism has best been studied in a pathway that requires isoprene monooxygenases (van Hylckama Vlieg *et al.*, 2000), but may alternatively occur through promiscuous enzymatic reactions in cells lacking known isoprene degradation pathways (Patel *et al.*, 1982; Johnston *et al.*, 2017). Isoprene commonly occurs in both soil and marine systems, so it is surprising that other metabolic strategies, such as

isoprene incorporation into isoprenoid synthesis pathways, have not been observed. In the ocean, biological coupling of acetone and isoprene production by algae (Mckay *et al.*, 1996; Shaw *et al.*, 2003; Colomb *et al.*, 2008; Bonsang *et al.*, 2010; Halsey *et al.*, 2017) to degradation by heterotrophs directly impacts the net fluxes of these VOCs between the ocean and atmosphere. Thus, identifying the microbial taxa and metabolisms acting upon these VOCs are needed to explain how VOC fluxes are biologically controlled.

Pelagibacter is a cultured representative of the SAR11 clade of alpha-proteobacteria, the most abundant heterotrophic bacterial family in the ocean (Morris *et al.*, 2002). Recent reports show that *Pelagibacter* metabolizes a wide variety of volatile and methylated compounds, including acetone (Sun *et al.*, 2011; Halsey *et al.*, 2017; Giovannoni *et al.*, 2019, Moore *et al*., 2019), but evidence for isoprene consumption was less certain (Moore et al., 2019). A role for *Pelagibacter* in controlling sea-air acetone fluxes has been suggested (Dixon *et al.*, 2014), but the rates of consumption and mechanisms involved were not known. We hypothesized that *Pelagibacter* is an important sink for acetone and isoprene in the ocean. Cultures of *Pelagibacter* strain HTCC1062 were used to study acetone and isoprene metabolism and estimate the potential impacts of *Pelagibacter* and other heterotrophs on the distribution and flux of these important VOCs.

Experimental Procedures

Culturing

For all experiments described, *Pelagibacter* strain HTCC1062 (SAR11 group 1a.1) was grown in f/2 artificial seawater medium (Guillard and Ryther, 1962) that was modified to support growth of HTCC1062 (Moore *et al.*, 2019). Cultures were maintained in exponential growth at 16^{o} C, 25 μE light on a 12 hour light/dark cycle and shaken gently. Cultures were grown in sterile, acid-washed polycarbonate flasks or in 10-20 mL glass vials treated with a 5% solution of bovine serum albumin for 8 hours, rinsed with nanopure water then sterilized. Cell enumerations were conducted by staining 200 μL samples of culture with Sybr Green I for 1-2 hours then measured using a Guava flow cytometer.

Acetone incorporation/oxidation

Incubations of cells with radiolabeled acetone (1,3 ^{14}C acetone, American Radiolabeled Chemicals, St. Louis, MO) were performed to quantify rates of acetone incorporation into biomass and oxidation to CO_2 by HTCC1062. 300mL cultures of HTCC1062 were grown until late exponential phase. 60mL of the culture was heat killed at 55^{o} C for 45 min. Cell enumerations done immediately and two days following heat treatment showed no change in cell density compared to cell counts done immediately before heat treatment. 1μCi (1μM) acetone was spiked into the live and killed cells, activity samples were taken, then 10mL live cells and killed cells were aliquoted into 20mL BSA treated sterile vials and sealed with Teflon faced butyl stoppers. Partitioning of acetone to the headspace of the vial at 16^{o}C was expected to be less than 1%, and was therefore negligible. Vials were incubated at 16^{o}C in the dark for 0, 2, 5, 8 and 12 h

before the incubations were terminated. For measurements of acetone incorporation into biomass, incubations were terminated by adding 1.1 mL of 100% w/v trichloroacetic acid using a syringe. For measurements of combined acetone oxidation and incorporation to biomass, incubations were terminated by adding 0.5 mL 1 M sodium hydroxide, 0.25 mL 0.1 M sodium carbonate, and 0.5 mL 1 M barium chloride. Killed cell incubations were terminated after 12 hours. Cultures were stored at for 12 hours at 4^{o}C. The contents of each vial were filtered through 0.1 μm polycarbonate filters and washed three times with 100% w/v trichloroacetic acid or 0.2 μm filtered artificial seawater. Filters were submerged in Ecoscint scintillation cocktail overnight, sonicated to disrupt the contents of the filter, then measured using a scintillation counter (Beckman-Coulter, Brea, CA, USA). Acetone oxidation rates were calculated by subtracting the rate of incorporation measured from the combined oxidation and incorporation measurement.

Primary growth substrate replacement with acetone

To test whether acetone could substitute for pyruvate or glycine, which are known required growth substrates of HTCC1062 (Carini *et al.*, 2012), triplicate 5 mL cultures of HTCC1062 were grown in BSA prepared vials (see above) for each of the following conditions: negative control, growth medium lacking either pyruvate or glycine; positive control, pyruvate (100 μM) and glycine (50 μM) provided; test conditions, pyruvate or glycine omitted from the medium with acetone supplied at 0.5, 5, 50, 500, or 5000 μM. Cultures were sealed with Teflon-faced butyl septa and incubated at 16^{o} C under gentle

shaking with 25 μmol photons m^{-2} s^{-1} on a 12h L/D cycle. 200 μL samples were taken with a sterile syringe approximately every other day for cell enumerations.

Inactivation of the isoprenoid biosynthetic pathway

To test if HTCC1062 could utilize isoprene to meet its isoprenoid requirements for growth, the antibiotic fosmidomycin (Life Technologies, Eugene OR) was added to HTCC1062 cultures to block the methyl-erythritol phosphate (MEP) pathway of isoprenoid biosynthesis. The minimum inhibitory concentration for fosmidomycin and HTCC1062 was determined to be 20μg mL^{-1} (data not shown). Quadruplicate 5 mL cultures of HTCC1062 were grown in sealed, BSA treated glass vials under the following conditions: positive control 1, No isoprene or fosmidomycin added; positive control 2, isoprene (10μM, Sigma-Aldrich, 99.5% analytical standard) with no fosmidomycin; negative control, no isoprene with fosmidomycin added at 50μg mL^{-1}; test condition, isoprene (10 μM) and fosmidomycin (50 μg mL^{-1}) added. Using a Henry's constant of $1.3x10^{-4}$ mol m^{-3} Pa^{-1} (Sander, 2015), the initial concentration of the added isoprene in the aqueous phase after headspace partitioning was calculated to be 2.01 μM at 16^0 C. Cultures were grown for several weeks and sampled once to twice per week for cell enumerations.

Gene identification, phylogenetic distribution and environmental abundance

The acetone monooxygenase and other genes involved in the acetone metabolic pathway previously described in *Gordonia sp*. TY-5 by Kotani *et al.*, 2007 were used in an initial search for genes associated with acetone metabolism in HTCC1062. BlastP was used to search the HTCC1062 and 19 other *Pelagibacter* genomes for the published acetone monooxygenase. An acetone monooxygenase was identified (SAR11_0845) and the functional annotation of the identified gene was validated further by predicting and comparing three-dimensional protein structures to the Protein Data Bank using the program I-TASSER (Yang and Zhang, 2015). Additionally, the SAR11_0845 sequence was used in a BlastP search of the nr protein databases to identify similar sequences in other taxa. These sequences, two validated sequences of phenylacetone (Q47PU3) and cyclohexanone (P12015) monooxygenases from Swissprot, and the protein sequence from *Gordonia sp.* TY-5 (A1IHE6) were used to construct a phylogenetic tree comparing the relationship of these genes across taxa using the NGphylogeny web service (Lemoine *et al.*, 2019). Amino acid sequences were aligned using MAFFT, the alignment was curated with Noisy and a maximum-likelihood phylogenetic tree was constructed with PhyML using 100 bootstrap iterations and default settings for all programs (Dress *et al.*, 2008; Guindon *et al.*, 2010; Katoh and Standley, 2013). iTOL was used to visualize the output tree (Letunic and Bork, 2019), which was re-rooted by the branch representing the *Gordonia sp*. TY-5 acetone monooxygenase (Kotani *et al.*, 2007).

Identification of an acetone monooxygenase, a key enzyme in acetone metabolism, in the genome of HTCC1062 allowed us to search for homologs of this gene in the environment. Homologs of the HTCC1062 acetone monooxygenase (SAR11_0845) were searched for in the TARA Oceans metagenome using the Ocean

Gene Atlas web tool (Villar *et al.*, 2018). Using this tool with default settings and an expect threshold of 1 x 10^{-60}, the relative abundance of homologs was plotted as a function of latitude to make comparisons of gene abundance with acetone concentrations and flux measurements across major ocean regions. Gene abundance was calculated by dividing the read coverage of the homologs identified by the read coverage of all genes in the dataset (Villar *et al.*, 2018). Homologs identified in the TARA Oceans metagenome were aligned using MAFFT and a maximum-likelihood phylogenetic tree was constructed using iqtree (Nguyen *et al.*, 2015) to assess the taxonomic diversity of the homologs identified in the metagenomes.

Results and Discussion

Acetone metabolism in HTCC1062

Radiolabeled 1,3 ^{14}C acetone was used to measure rates of acetone utilization by HTCC1062. Cells growing in medium replete with pyruvate and glycine metabolized acetone at a rate of 101 pmol acetone 10^{10} $cell^{-1}$ h^{-1}. Acetone was oxidized to CO_2 at a rate of 89.7 pmol acetone 10^{10} $cell^{-1}$ h^{-1} ($P = 0.002$), but incorporation into biomass was not significantly different from zero at 11.7 pmol acetone 10^{10} $cell^{-1}$ h^{-1} ($P = 0.33$) (Fig. 1). However, unusually low values of "incorporation" samples taken at 8 hours suggested there may have been a problem during processing of those samples. Overlooking this time-point would result in a higher rate of acetone incorporation of 17.2 pmol acetone 10^{10} $cell^{-1}$ h^{-1} and P-value of 0.008, raising the possibility that a low amount of acetone

was incorporated to biomass, but this remains uncertain. Note that the acetone used in these experiments was radiolabeled on two carbon atoms, therefore if only one of the two radioactive carbons was oxidized or incorporated by the cell, then the rates measured would be two-fold underestimates.

Uncertainty about the ability of HTCC1062 to incorporate acetone into biomass prompted us to test whether HTCC1062 could utilize acetone to replace the known required growth substrates glycine and pyruvate (Carini *et al.*, 2012). Surprisingly, acetone could partially replace glycine as a primary growth substrate when supplied at 500 and 5000 μM. Cells growing without glycine or acetone (negative control) reached a maximum density of 3.57×10^6 cells mL^{-1}, but cells supplied acetone at 500 or 5000 μM in the absence of glycine grew approximately two generations more than the negative control ($p = 0.01, 0.002$ respectively, students t-test, n=3) (Fig. 2A). Cells supplied acetone at 0.5, 5 or 50 μM in the absence of glycine did not reach higher maximum cell densities than the negative control ($p= 0.07, 0.06, 0.13$ respectively, students t-test, $n = 3$) (Fig. 2A). Providing acetone to pyruvate-limited cultures did not result in cell densities greater than the negative controls, thus acetone was not able to replace pyruvate as a growth substrate at any of the concentrations used (Fig. 2B).

Genetics and mechanism

The surprising finding that acetone could be used not only as an energy source, but also as a replacement for glycine prompted us to examine the metabolic mechanisms involved in acetone metabolism in HTCC1062. A gene encoding a putative acetone

monooxygenase (SAR11_0845) was identified in the translated genome sequence of HTCC1062. The translated sequence is 32% identical and 53% similar to the amino acid sequence of the acetone monooxygenase described in *Gordonia sp.* TY-5 (Kotani *et al.*, 2007) across a coverage of 99%. Use of the program ITASSER to compare the predicted 3D structure of the SAR11_0845 protein also showed that this gene was similar to acetone, cyclohexanone or phenylacetone monooxygenases, enzymes that can have high activities on a variety of ketones (Kotani *et al.*, 2007). Acetone monooxygenase catalyzes the conversion of acetone to acetol or methyl acetate (Levine and Krampitz, 1952; Taylor *et al.*, 1980; Kotani *et al.*, 2007) while cyclohexanone monooxygenase oxidizes cyclohexanone to ε-caprolactone (Donoghue and Trudgill, 1975). A BlastP search of SAR11_0845 in the non-redundant protein database returned many matches to other annotated cyclohexanone monooxygenases in a diversity of taxa, most of which were around 50% similar and had a coverage of around 98%. Of particular interest were hits in the SAR116 clade, and Rhodobaceriaciae, the family that includes *Roseobacter*. Like *Pelagibacter*, these bacterial taxa are highly abundant and of significant importance in marine epipelagic microbial communities (González and Moran, 1997; Rappé and Giovannoni, 2003; Morris *et al.*, 2012). The topology of the tree suggests a close relationship between the SAR11 and SAR116 monooxygenases, suggesting the possibility that this gene has been horizontally transferred amongst these co-occurring, but evolutionary distinct organisms. Interestingly, Blast searches of SAR11_0845 only returned hits in 3 of 20 different SAR11 genomes examined, suggesting that the putative acetone monooxygenase is not well conserved in the SAR11 family. However, this result could also be attributed to the fact that many of these genome sequences are incomplete.

Further work to understand the distribution of the putative acetone monooxygenase in the SAR11 family is on going.

SAR11, and other bacteria with streamlined genomes, have evolved mechanisms to metabolize a wide variety of compounds using a limited genetic repertoire (Giovannoni, Tripp, *et al.*, 2005) It is possible that the putative acetone monooxygenase identified in the *Pelagibacter* genome serves multiple functions. The most similar matches to this protein sequence are annotated as cyclohexanone monooxygenase, and the predicted 3D structure of this protein product was also most similar to cyclohexanone monooxygenase (Fig. 3). Further, the acetone monooxygenase described in *Gordonia sp.* TY-5 was highly active on a variety of ketones, especially cyclic ketones such as cyclohexanone (Kotani *et al.*, 2007). In a co-culture with the diatom *Thalassiosira pseudonana*, HTCC1062 was able to metabolize cyclohexanol produced by the diatom (Moore *et al.*, 2019). Cyclohexanol could be oxidized to cyclohexanone by a dehydrogenase, and then further oxidized to ε-caprolactam by the monooxygenase (Donoghue and Trudgill, 1975). Downstream conversions may lead to the formation of adipate that is used in beta-oxidation pathways (Donoghue and Trudgill, 1975). This raises the possibility that the monooxygenase identified could also be active on cyclohexanone or other ketones, and may explain why HTCC1062 incorporated acetone at a low rate and required such a high concentration for growth. Nevertheless, HTCC1062 is capable of metabolizing acetone and may have an important role in the turnover of this compound in marine environments.

Acetone metabolism by HTCC1062 suggests that *Pelagibacter* has the potential to limit acetone emissions from the surface ocean. In the epipelagic zone of the Sargasso

Sea where phytoplankton are a source of acetone (Cotsaris *et al.*, 1995; Halsey *et al.*, 2017; Moore *et al.*, 2019), *Pelagibacter* abundance averaged 2 x 10^8 cells L^{-1} (Morris *et al.*, 2002). Using this value, we estimate that *Pelagibacter* populations in seawater can consume acetone up to 2-4 pmol acetone L^{-1} h^{-1}. This value is on the low end of acetone oxidation rates measured in seawater off the coast of the UK, which ranged from 1-42 pmol L^{-1} h^{-1}, and were highest when "low nucleic acid" bacteria, a classification that includes *Pelagibacter*, were most abundant (Dixon *et al.*, 2014). However, given the finding that the putative acetone monooxygenase may not be well conserved across the SAR11 family, other taxa may also contribute to acetone degradation and help explain higher acetone oxidation rates in seawater. Homologs of the SAR11_0845 acetone monooxygenase were identified in other abundant marine bacteria like SAR116 and Rhodobacteriaciae (Fig. 3), thus these bacteria are also likely to contribute significantly to acetone degradation in the surface ocean.

Organisms encoding acetone monooxygenases like HTCC1062 may be collectively important in limiting acetone emissions to the atmosphere by coupling heterotrophic degradation to production by phytoplankton (Sinha *et al.*, 2007; Fischer *et al.*, 2012; Beale *et al.*, 2013; Yang *et al.*, 2014). The average net flux of acetone across the entire ocean is near zero, but the ocean is sometimes a sink for acetone, particularly in temperate latitudes (Sinha *et al.*, 2007; Fischer *et al.*, 2012; Beale *et al.*, 2013; Yang *et al.*, 2014). We used the Ocean Gene Atlas web-tool (Villar *et al.*, 2018) to query the TARA Oceans metagenome and compare the abundance of the HTCC1062 acetone monooxygenase (SAR11_0845) homologs throughout the ocean. Homologs of SAR11_0845 in the TARA Oceans metagenomes were found in a diversity of taxa, and

therefore, the search was not restricted to only *Pelagibacter* or its close relatives (Fig. 4). The abundance of SAR11_0845 homologs, relative to total gene abundance, varied by nearly three orders of magnitude, ranging from 1.05×10^{-7} to 6.29×10^{-5}, and was generally more abundant in temperate latitudes compared to tropical and sub-tropical regions (Fig. 5). This latitudinal variation in gene abundance follows a pattern similar to acetone concentration and flux rates measured in the Atlantic Ocean (Beale *et al.*, 2013; Yang *et al.*, 2014).

Along a transect between 49^0 N and 39^0 S in the Atlantic ocean, acetone concentrations and flux across latitudes were highly dependent on temperature (Beale *et al.*, 2013; Yang *et al.*, 2014). Nevertheless, acetone flux was also negatively correlated with bacterial leucine uptake rates, suggesting bacterial metabolism was at least partially responsible for trends in acetone flux (Beale *et al.*, 2013; Yang *et al.*, 2014). In temperate regions, the primary habitat of HTCC1062, relatively high occurrences of acetone monooxygenase homologs suggested that microbial communities in these regions possess the metabolic capacity required for acetone metabolism, and that they are important drivers of net oceanic acetone flux. In contrast, subtropical gyre regions are a net source of acetone to the atmosphere, where acetone monooxygenase abundances are lower, thus acetone metabolic pathways may not be as prevalent in these microbial communities. Higher ocean temperatures in subtropical gyres compared to temperate or equatorial upwelling regions promotes acetone emission to the atmosphere by decreasing the Henry's Law partitioning rate (C_w/C_a) (Sinha *et al.*, 2007), thus reducing the availability of acetone as a substrate for biological metabolism in warm marine waters.

Isoprene metabolism

Previously, we found that isoprene stimulated ATP production in HTCC1062 (Moore *et al.*, 2019). Isoprene could not support growth of HTCC1062 in the absence of pyruvate or glycine (data not shown). We then asked whether isoprene could meet the isoprenoid requirements of HTCC1062 .Fosmidomycin is an antibiotic that competitively inhibits the 1-deoxy-D-xylulose 5-phosphate reductoisomerase (dxr) at the second step of the MEP isoprenoid synthesis pathway (Fig. 6). Growth of HTCC1062 was sensitive to 50 μg mL^{-1} fosmidomycin. Addition of 10 μM isoprene (2 μM in aqueous phase, see Methods) recovered growth of HTCC1062 in the presence of fosmidomycin (Fig. 7). These results show that HTCC1062 was able to utilize isoprene directly to bypass the isoprenoid biosynthetic pathway blocked by fosmidomycin.

Isoprene monooxygenase is a key enzyme in known isoprene metabolic pathways (van Hylckama Vlieg *et al.*, 2000; Johnston *et al.*, 2017), but protein sequences of previously described isoprene monooxygenases in *Rhodococcus* did not match to any sequences in the HTCC1062 genome. Our data suggests that HTCC1062 does not encode canonical isoprene degradation pathways, but rather, another biochemical mechanism allows isoprene to be used directly to meet isoprenoid requirements. In this model, isoprene or another unknown intermediate may be phosphorylated to form the isoprenoid subunits isopentenyl pyrophosphate and dimethylallyl pyrophosphate, though no enzymes capable of such a conversion have been described.

In HTCC1062, isoprenoids are primarily used for biosynthesis of electron carriers, including ubiquinone; poryphrin based compounds, or pigments such as retinal,

which is a key component of proteorhodopsin. Cells typically rely on small pools of electron carriers, so the demand for isoprenoids in HTCC1062 is likely small, but critical, ensuring maintenance of the isoprenoid biosynthesis pathway in the genome despite evolutionary streamlining (Giovannoni *et al.*, 2005). For organisms like *Pelagibacter*, bypassing energy-expensive pathways like isoprenoid synthesis, which uses 1 ATP, 1 CTP and 1 NADPH for every isoprenoid subunit molecule produced (Zhao *et al.*, 2013), could improve growth efficiency in these cells. However, phosphorylation of isoprene would likely require ATP as a source of pyrophosphate, and thus reduce some of this energy savings. We attempted to measure isoprene metabolic rates in HTCC1062 using PTR-ToF/MS, but we were unable to directly quantify isoprene consumption by *Pelagibacter*. Nevertheless, we estimated the potential magnitude of isoprene demand in *Pelagibacter* cells based on intracellular quantities of proteorhodopsin. Four isoprene (5 C) molecules are required for biosynthesis of each retinal molecule (20 C) in proteorhodopsin. There are about 10,000 proteorhodopsin per SAR11 cell (Giovannoni, *et al.*, 2005), thus a single *Pelagibacter* cell would require 40,000 isoprene molecules. Given a standing stock of 2.4×10^{28} *Pelagibacter* cells worldwide, and a turnover rate of 0.3 d^{-1} (White *et al.*, 2018), the maximum potential *Pelagibacter* contribution to global marine isoprene uptake is 11.9 Tg y^{-1}. This value is remarkably similar in magnitude to the entire marine isoprene budget of 0.1-11.6 Tg C y^{-1} (Palmer and Shaw, 2005; Sinha *et al.*, 2007; Hackenberg *et al.*, 2017), but is likely underestimated because it does not consider other isoprenoid demands, such as quinones or poryphrin compounds also needed by the cell. This estimate using proteorhodopsin as an example demonstrates the scale of isoprene turnover by bacterial communities in the ocean, but also does not

include the input of other taxa or metabolic strategies. Nevertheless, our data suggest that use of isoprene by *Pelagibacter* and other heterotrophic bacteria that do not encode canonical isoprene degradation pathways creates a substantial sink for isoprene in the ocean. This bacterial activity helps explain discrepancies in predicted versus measured isoprene flux rates that imply a bacterial sink for isoprene in the ocean and shows that marine heterotrophic bacteria are important in controlling the emissions of this significant climate active chemical from the ocean.

Here, we report that *Pelagibacter* strain HTCC1062 (SAR11),, can metabolize acetone and isoprene, two highly abundant VOCs with important roles in atmospheric chemistry. The data presented here give new evidence for how heterotrophic bacteria help regulate marine VOC emissions to the atmosphere. Nevertheless, our understanding of the microbial communities and biochemistry involved in VOC metabolism remains inadequate, thus future research that elucidates the contributions of other microbes to the production and degradation of VOCs is needed to understand the flux of these compounds in the ocean and atmosphere.

Figures and Tables

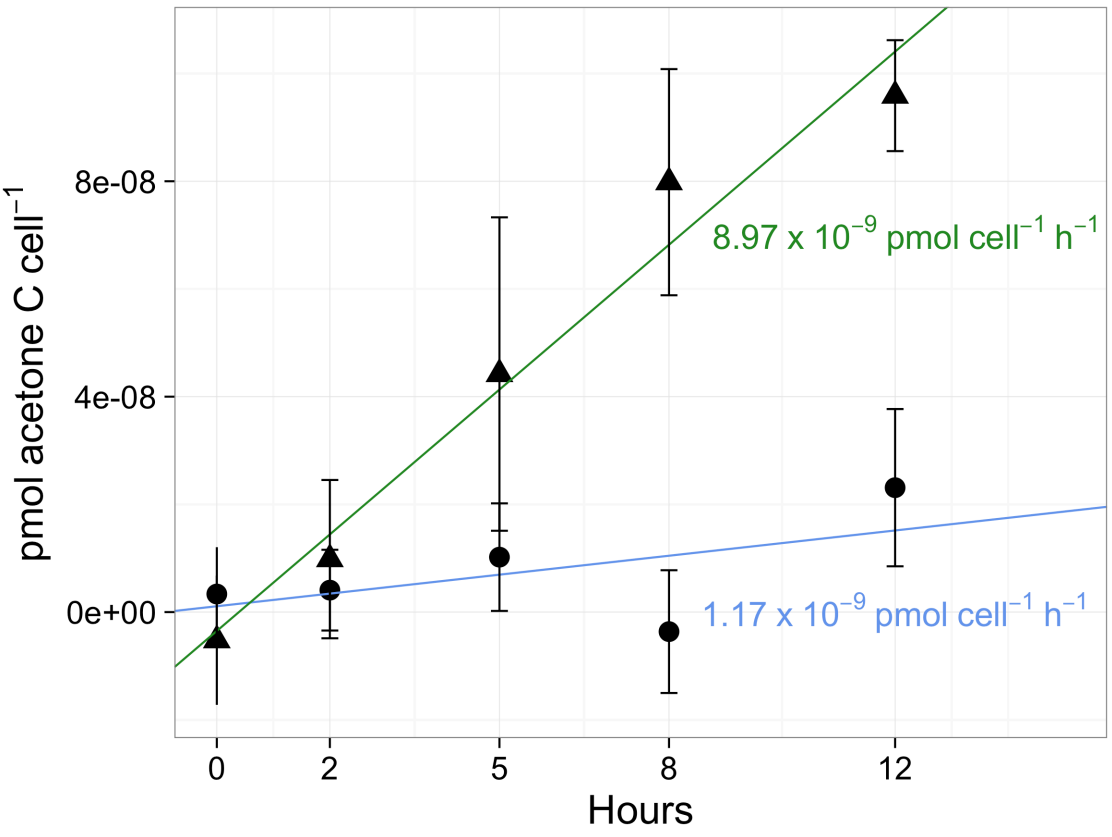

Fig. 1: HTCC1062 oxidizes acetone to CO_2 and incorporates acetone into biomass. ^{14}C acetone was oxidized (triangles) at a rate of 89.7 pmol acetone 10^{10} cell^{-1} h^{-1} (P = 0.002) and incorporated (circles) at 11.7 pmol acetone 10^{10} cell^{-1} h^{-1} (P = 0.33) over a 12 hour incubation period. Lines are linear regressions of oxidized (green) and TCA-insoluble radioactive acetone carbon incorporated to biomass (blue), which were used to calculate the rates shown. Points are averages of treatments minus the average of killed samples; error bars indicate the standard deviations for each time point. "Incorporation" samples taken at 8 hours appear to deviate significantly from other time-points, raising the possibility of errors introduced during sample collection and processing. Removal of this time-point results in a P-value of 0.008 and a higher rate of incorporation of 17.2 pmol acetone 10^{10} cell^{-1} h^{-1}, leaving the possibility of slow, but significant rates of acetone incorporation to biomass.

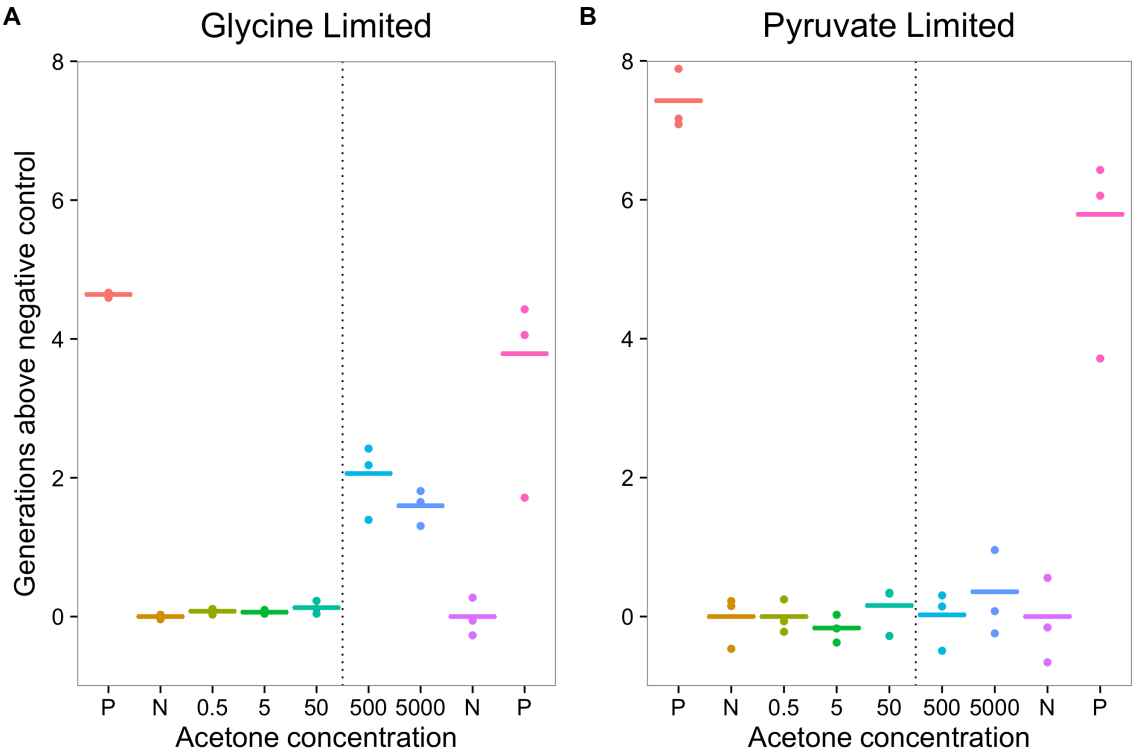

Fig. 2: Acetone replaced glycine as a required growth substrate at 500, and 5,000 µM, but did not replace pyruvate at any concentration. A: HTCC1062 generations of growth above the maximum cell yields of cultures grown without glycine (negative control, [N]). Positive controls [P] had both pyruvate and glycine supplied. Acetone was added at concentrations ranging from 0.5 to 5000 µM, glycine was added at 50 µM to the positive control (red/P). Acetone supplied at 500 and 5000 µM under glycine limitation caused significant growth over the control (P = 0.01 and 0.002 respectively, students t-test, n=3). B: Same as A, except pyruvate was omitted from the media instead of glycine. For all experimental conditions, bars indicate the mean of the three independent biological replicates shown as points. Individual experiments testing different concentrations of acetone are separated by the dotted line in each plot, and should be compared to the adjacent N (negative) and P (positive) controls.

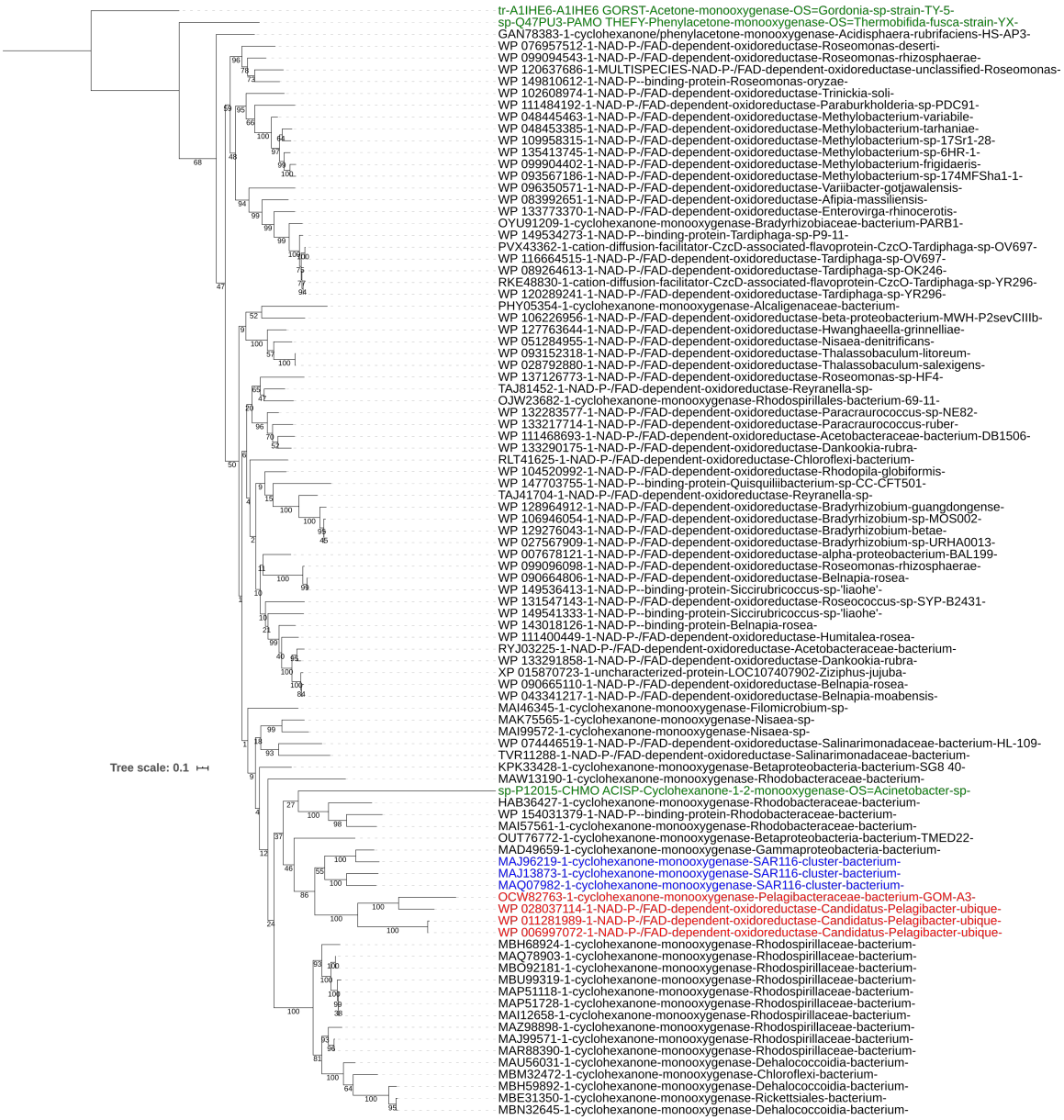

Fig. 3: Maximum likelihood phylogenetic tree showing the relationship of the putative SAR11 acetone monooxygenase (SAR11_0845) and the 100 most similar protein sequences in the nr protein database identified by BlastP. Tree was constructed using 100 bootstrap iterations and re-rooted by the previously described acetone monooxygenase of *Gordonia* strain TY-5 (green). Other validated cyclohexanone and phenylacetone monooxygenases from Swissprot are also included (green). Notably, putative acetone monooxygenases are found in important marine bacteria including SAR11 (red), SAR116 (blue) and Rhodobacteriaciae, the taxonomic family of the common marine bacteria *Roseobacter*; however, the exact taxonomic classification shown is not specific.

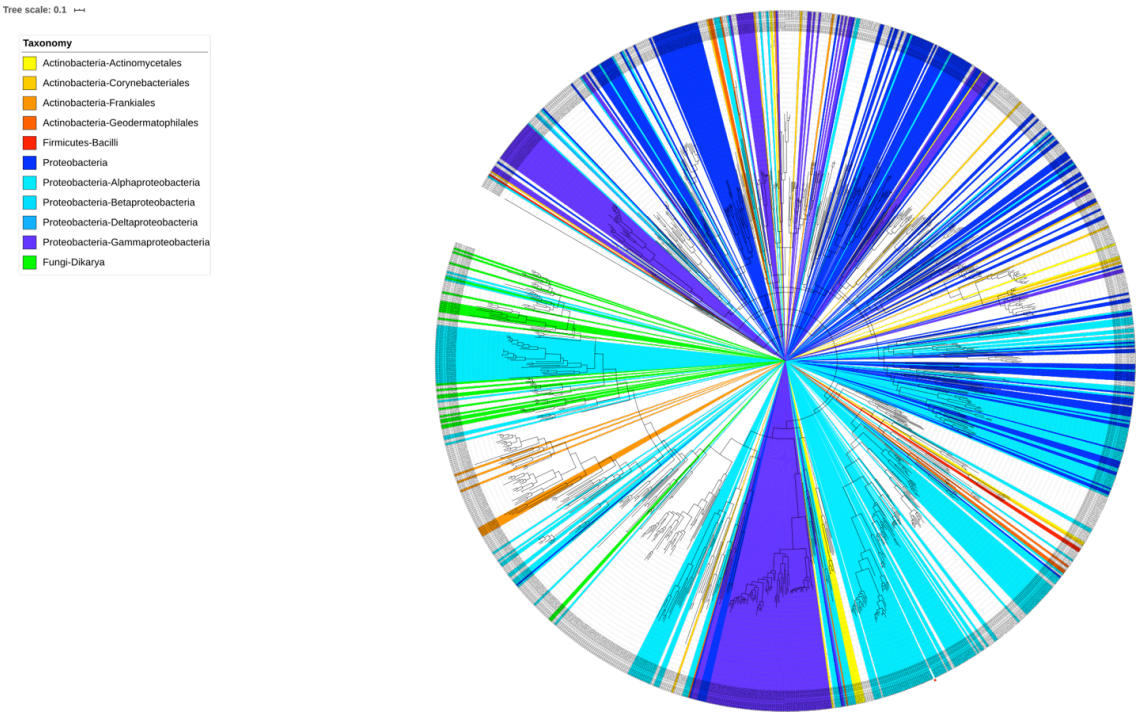

Fig. 4: Phylogenetic tree of sequences in the TARA Oceans metagenome sequences that were identified to be homologs of the putative acetone monooxygnease SAR11_0845. Homologs are distributed across a diverse variety of taxa, but are frequent in Proteobacteria. The tree was constructed with around 1100 gene sequences from the TARA Oceans metagenome with an expect score cutoff of $\leq 1x10^{-60}$.

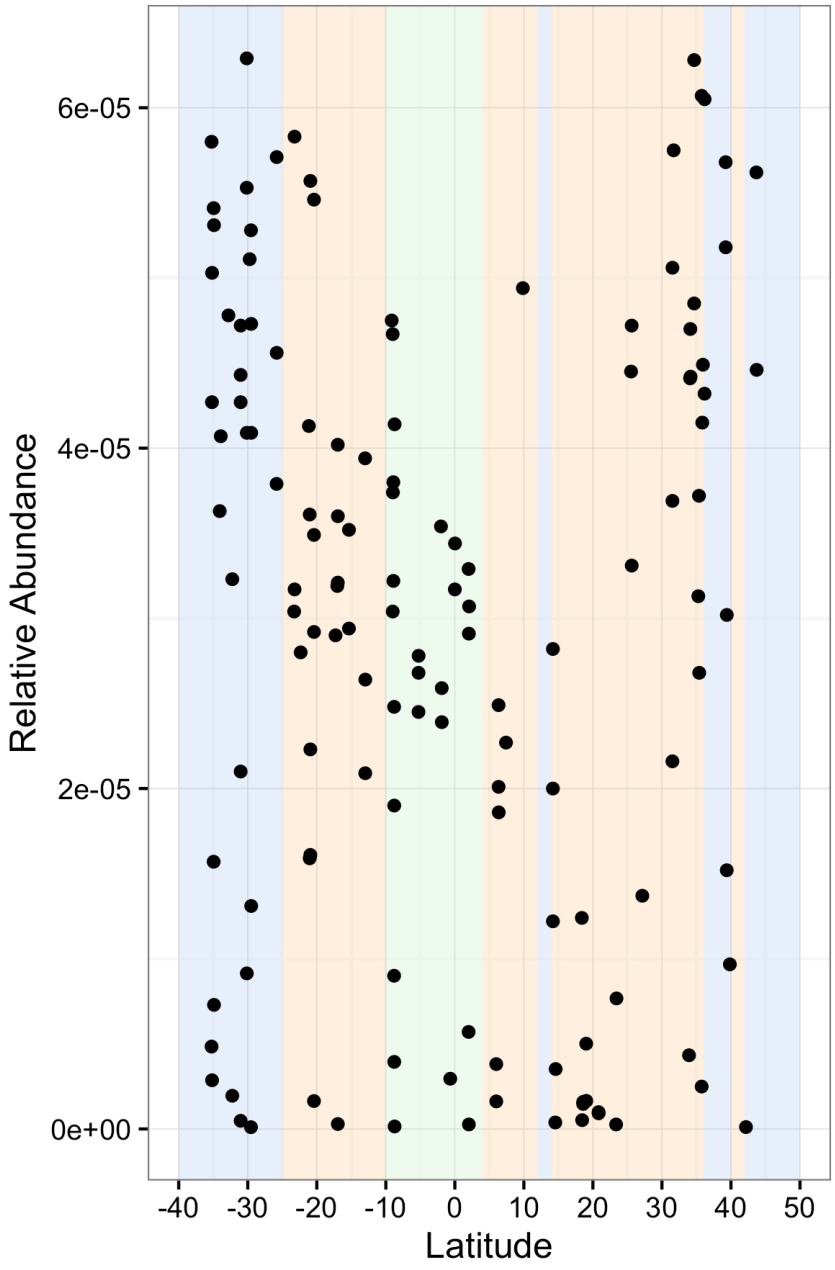

Fig. 5: Acetone monooxygenase gene abundance, normalized to total gene abundance, in the TARA Oceans metagenome is higher at temperate latitudes than in tropical and sub-tropical regions. Color shadings indicate where the ocean was a sink (blue), source (orange), or approximately net zero flux (green) for acetone during the Atlantic Meridional Transect (Beale *et al.*, 2013).

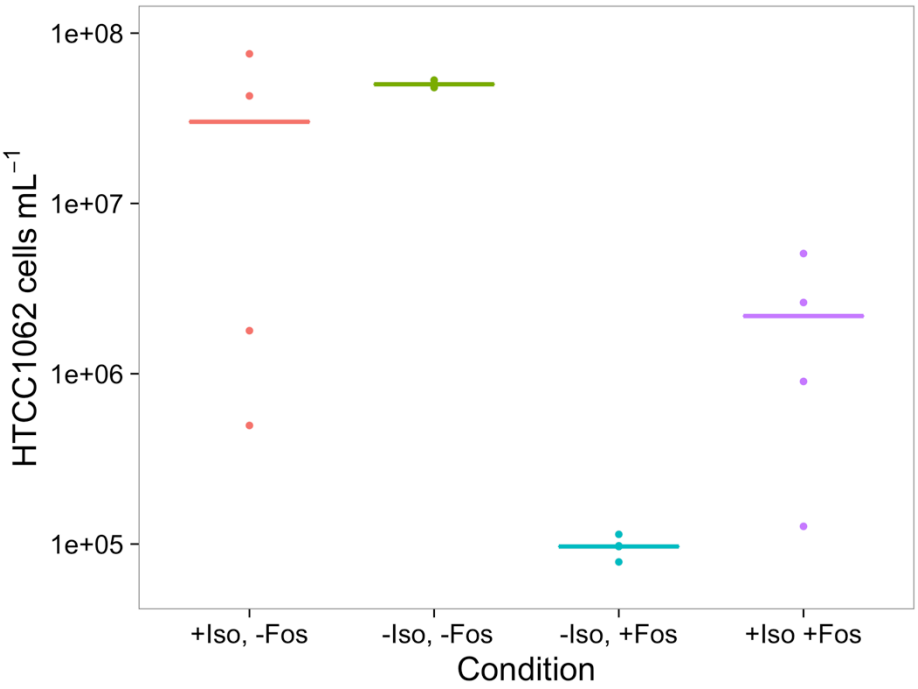

Fig. 6: 10µM isoprene partially rescued growth of HTCC1062 in the presence of the isoprenoid synthesis pathway inhibitor fosmidomycin. HTCC1062 growth was inhibited entirely by fosmidomycin in the absence of isoprene (blue). Addition of isoprene to cultures treated with fosmidomycin caused a nearly 10-fold increase in the final cell density (violet), but they did not grow as effectively as positive controls without fosmidomycin (red & green). Bars indicate mean final cell density of four biological replicates; individual replicates are shown as points.

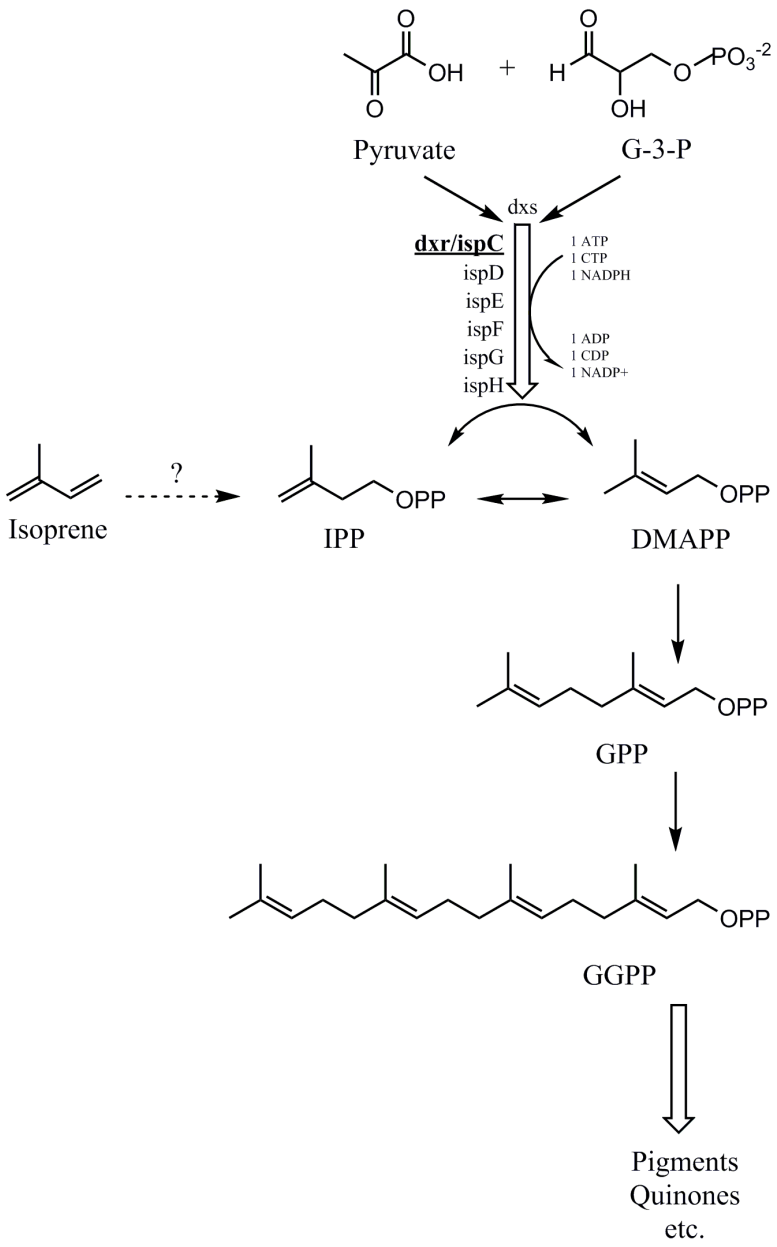

Fig. 7: Simplified view of the methyl erythritol phosphate (MEP) isoprenoid synthesis pathway HTCC1062 utilizes to produce the isoprenoid precursors isopentyl pyrophosphate (IPP) and dimethylallyl pyrophosphate (DMAPP) from pyruvate and glyceraldehyde-3-phosphate (G-3-P). The second enzyme of this pathway, *dxr*, is competitively inhibited by the antibiotic fosmidomycin (shown in bold/underline). Supplying isoprene rescued growth of HTCC1062 when this pathway was blocked with fosmidomycin. The dashed line indicates a hypothetical reaction that would allow HTCC1062 to utilize isoprene as a precursor for IPP and DMAPP. No enzyme has been shown to catalyze such a reaction.

References:

Alvarez, L.A., Exton, D.A., Timmis, K.N., Suggett, D.J., and McGenity, T.J. (2009) Characterization of marine isoprene-degrading communities. *Environ Microbiol* **11**: 3280–3291.

Andreae, M.O. and Crutzen, P.J. (1997) Atmospheric aerosols: Biogeochemical sources and role in atmospheric chemistry. *Science (80-)* **276**: 1052–1058.

Beale, R., Dixon, J.L., Arnold, S.R., Liss, P.S., and Nightingale, P.D. (2013) Methanol, acetaldehyde, and acetone in the surface waters of the Atlantic Ocean. *J Geophys Res Ocean* **118**: 5412–5425.

Beale, R., Dixon, J.L., Smyth, T.J., and Nightingale, P.D. (2015) Annual study of oxygenated volatile organic compounds in UK shelf waters. *Mar Chem* **171**: 96–106.

Bonsang, B., Gros, V., Peeken, I., Yassaa, N., Bluhm, K., Zoellner, E., et al. (2010) Isoprene emission from phytoplankton monocultures: The relationship with chlorophyll-a, cell volume and carbon content. *Environ Chem* **7**: 554–563.

Booge, D., Schlundt, C., Bracher, A., Endres, S., and Zäncker, B. (2017) Marine isoprene production and consumption in the mixed layer of the surface ocean – A field study over 2 oceanic regions. *Biogeosciences Discuss* 1–28.

Carini, P., Steindler, L., Beszteri, S., and Giovannoni, S.J. (2012) Nutrient requirements for growth of the extreme oligotroph 'Candidatus Pelagibacter ubique' HTCC1062 on a defined medium. *ISME J* **7**: 592–602.

Colomb, A., Yassaa, N., Williams, J., Peeken, I., and Lochte, K. (2008a) Screening volatile organic compounds (VOCs) emissions from five marine phytoplankton species by head space gas chromatography/mass spectrometry (HS-GC/MS). *J Environ Monit* **10**: 325–330.

Colomb, A., Yassaa, N., Williams, J., Peeken, I., and Lochte, K. (2008b) Screening volatile organic compounds (VOCs) emissions from five marine phytoplankton species by head space gas chromatography/mass spectrometry (HS-GC/MS). *J Environ Monit* **10**: 325–330.

Cotsaris, E., Bruchet, A., Mallevialle, J., and Bursill, D.B. (1995) The identification of odorous metabolites produced from algal monocultures. *Water Sci Technol* **31**: 251–258.

Dixon, J.L., Beale, R., Sargeant, S.L., Tarran, G.A., and Nightingale, P.D. (2014) Microbial acetone oxidation in coastal seawater. *Front Microbiol* **5**: 1–9.

Donoghue, N.A. and Trudgill, P.W. (1975) The Metabolism of Cyclohexanol by Acinetobacter NCIB 9871. *Eur J Biochem* **60**: 1–7.

Dress, A.W., Flamm, C., Fritzsch, G., Grünewald, S., Kruspe, M., Prohaska, S.J., and Stadler, P.F. (2008) Noisy: Identification of problematic columns in multiple sequence alignments. *Algorithms Mol Biol* **3**: 7.

Fischer, E. V., Jacob, D.J., Millet, D.B., Yantosca, R.M., and Mao, J. (2012) The role of the ocean in the global atmospheric budget of acetone. *Geophys Res Lett* **39**:.

Folkins, I. and Chatfield, R. (2000) Impact of acetone on ozone production and OH in the upper troposphere at high NOx. *J Geophys Res Atmos* **105**: 11585–11599.

Giovannoni, S., Bibbs, L., Cho, J.C., Stapels, M., Desiderio, R., Vergin, K., et al. (2005) Proteorhodopsin in the ubiquitous marine bacterium SAR11. *Nature* **438**: 82–85.

Giovannoni, S., Tripp, J., Givan, S., Podar, M., Vergin, K., Baptista, D., et al. (2005) Genome streamlining in a cosmopolitan oceanic bacterium. *Science* **309**: 1242–1245.

Giovannoni, S.J., Halsey, K.H., Saw, J., Muslin, O., Suffridge, C.P., Sun, J., et al. (2019) A Parasitic Arsenic Cycle That Shuttles Energy from Phytoplankton to Heterotrophic Bacterioplankton. *MBio* **10**:.

González, J.M. and Moran, M.A. (1997) Numerical dominance of a group of marine bacteria in the α-subclass of the class Proteobacteria in coastal seawater. *Appl Environ Microbiol* **63**: 4237–4242.

Guenther, A.B., Jiang, X., Heald, C.L., Sakulyanontvittaya, T., Duhl, T., Emmons, L.K., and Wang, X. (2012) The model of emissions of gases and aerosols from nature version 2.1 (MEGAN2.1): An extended and updated framework for modeling biogenic emissions. *Geosci Model Dev* **5**: 1471–1492.

Guillard, R.R.L. and Ryther, J.H. (1962) Studies of marine planktonic diatoms. I. Cyclotella nana Hustedt and Detonula confervacea Cleve. *Can J Microbiol* **8**: 229–239.

Guindon, S., Dufayard, J.-F., Lefort, V., Anisimova, M., Hordijk, W., and Gascuel, O. (2010) New Algorithms and Methods to Estimate Maximum-Likelihood Phylogenies: Assessing the Performance of PhyML 3.0. *Syst Biol* **59**: 307–321.

Hackenberg, S.C., Andrews, S.J., Airs, R., Arnold, S.R., Bouman, H.A., Brewin, R.J.W., et al. (2017) Potential controls of isoprene in the surface ocean. *Global Biogeochem Cycles* **31**: 644–662.

Halsey, K.H., Giovannoni, S.J., Graus, M., Zhao, Y., Landry, Z., Thrash, J.C., et al. (2017) Biological cycling of volatile organic carbon by phytoplankton and bacterioplankton. *Limnol Oceanogr*.

Hartmans, S. and de Bont, J.A.M. (1986) Acetol monooxygenase from Mycobacterium Py1 cleaves acetol into acetate and formaldehyde. *FEMS Microbiol* **36**: 155–158.

Hausinger, R.P. (2007) New Insights into Acetone Metabolism. *J Bacteriol* **189**: 671–673.

Hense, I., Stemmler, I., and Sonntag, S. (2017) Ideas and perspectives: Climate-relevant marine biologically driven mechanisms in Earth system models. *Biogeosciences* **14**: 403–413.

van Hylckama Vlieg, J.E.T., Leemhuis, H., Jeffrey, H., Spelberg, L., and Janssen, D.B. (2000) Characterization of the Gene Cluster Involved in Isoprene Metabolism in Rhodococcus sp . Strain AD45. *J Bacteriol* **187**: 1956–1963.

Johnston, A., Crombie, A.T., El Khawand, M., Sims, L., Whited, G.M., McGenity, T.J., and Colin Murrell, J. (2017) Identification and characterisation of isoprene-degrading bacteria in an estuarine environment. *Environ Microbiol* **19**: 3526–3537.

Katoh, K. and Standley, D.M. (2013) MAFFT Multiple Sequence Alignment Software Version 7: Improvements in Performance and Usability. *Mol Biol Evol* **30**: 772–780.

Kotani, T., Yurimoto, H., Kato, N., and Sakai, Y. (2007) Novel acetone metabolism in a propane-utilizing bacterium, Gordonia sp. strain TY-5. *J Bacteriol* **189**: 886–893.

Lemoine, F., Correia, D., Lefort, V., Doppelt-Azeroual, O., Mareuil, F., Cohen-Boulakia, S., and Gascuel, O. (2019) NGPhylogeny.fr: new generation phylogenetic services

for non-specialists. *Nucleic Acids Res* **47**: W260–W265.
Letunic, I. and Bork, P. (2019) Interactive Tree Of Life (iTOL) v4: recent updates and new developments. *Nucleic Acids Res* **47**: W256–W259.
Levine, S. and Krampitz, L.O. (1952) The oxidation of acetone by a soil diphtheroid.
Liakakou, E., Vrekoussis, M., Bonsang, B., Donousis, C., Kanakidou, M., and Mihalopoulos, N. (2007) Isoprene above the Eastern Mediterranean: Seasonal variation and contribution to the oxidation capacity of the atmosphere. *Atmos Environ* **41**: 1002–1010.
Mckay, W.A., Turner, M.F., Jones, B.M.R., and Halliwell, C.M. (1996) Emissions of hydrocarbons from marine phytoplankton - some results from controlled laboratory experiments. *Atmos Environ* **30**: 2583–2593.
Moore, E.R., Davie-Martin, C.L., Giovannoni, S.J., and Halsey, K.H. (2019) Pelagibacter metabolism of diatom-derived volatile organic compounds imposes an energetic tax on photosynthetic carbon fixation. *Environ Microbiol* **10.1111/14**:
Morris, R.M., Frazar, C.D., and Carlson, C.A. (2012) Basin-scale patterns in the abundance of SAR11 subclades, marine Actinobacteria (OM1), members of the Roseobacter clade and OCS116 in the South Atlantic. *Environ Microbiol* **14**: 1133–1144.
Morris, R.M., Rappé, M.S., Connon, S.A., Vergin, K.L., Siebold, W.A., Carlson, C.A., and Giovannoni, S.J. (2002) SAR11 clade dominates ocean surface bacterioplankton communities. *Nature* **420**: 806–810.
Müller, J.F. and Brasseur, G. (1999) Sources of upper tropospheric HOx: A three-dimensional study. *J Geophys Res Atmos* **104**: 1705–1715.
Nguyen, L.T., Schmidt, H.A., Von Haeseler, A., and Minh, B.Q. (2015) IQ-TREE: A fast and effective stochastic algorithm for estimating maximum-likelihood phylogenies. *Mol Biol Evol* **32**: 268–274.
Palmer, P.I. and Shaw, S.L. (2005) Quantifying global marine isoprene fluxes using MODIS chlorophyll observations. *Geophys Res Lett* **32**:.
Patel, R.N., Hou, C.T., Laskin, A.I., and Felix, A. (1982) Microbial oxidation of hydrocarbons: Properties of a soluble methane monooxygenase from a facultative methane-utilizing organism, Methylobacterium sp. strain CRL-26. *Appl Environ Microbiol* **44**: 1130–1137.
Rappé, M.S. and Giovannoni, S.J. (2003) The uncultured microbial majority. *Annu Rev Microbiol* **57**: 369–94.
Sander, R. (2015) Compilation of Henry's law constants (version 4.0) for water as solvent. *Atmos Chem Phys* **15**: 4399–4981.
Shaw, S.L., Chisholm, S.W., and Prinn, R.G. (2003) Isoprene production by Prochlorococcus, a marine cyanobacterium, and other phytoplankton. *Mar Chem* **80**: 227–245.
Singh, H.B., O'Hara, D., Herlth, D., Sachse, W., Blake, D.R., Bradshaw, J.D., et al. (1994) Acetone in the atmosphere: Distribution, sources, and sinks. *J Geophys Res* **99**: 1805.
Sinha, V., Williams, J., Meyerhöfer, M., Riebesell, U., Paulino, A.I., and Larsen, A. (2007) Air-sea fluxes of methanol, acetone, acetaldehyde, isoprene and DMS from a Norwegian fjord following a phytoplankton bloom in a mesocosm experiment.

Sun, J., Steindler, L., Thrash, J.C., Halsey, K.H., Smith, D.P., Carter, A.E., et al. (2011) One Carbon Metabolism in SAR11 Pelagic Marine Bacteria. *PLoS One* **6**: e23973.

Taylor, D.G., Trudgill, P.W., Cripps, R.E., and Harris, P.R. (1980) The Microbial Metabolism of Acetone. *J Gen Microbiol* **118**: 159–170.

Villar, E., Vannier, T., Vernette, C., Lescot, M., Cuenca, M., Alexandre, A., et al. (2018) The Ocean Gene Atlas: Exploring the biogeography of plankton genes online. *Nucleic Acids Res* **46**: W289–W295.

White, A., Giovannoni, S., Zhao, Y., Vergin, K., and Carlson, C. (2018) Elemental content and stoichiometry of SAR11 chemoheterotrophic marine bacteria. *Limnol Oceanogr (In Rev*.

Yang, J. and Zhang, Y. (2015) Protein Structure and Function Prediction Using I-TASSER. *Curr Protoc Bioinforma* **52**: 5.8.1-5.8.15.

Yang, M., Beale, R., Liss, P., Johnson, M., Blomquist, B., and Nightingale, P. (2014) Air-sea fluxes of oxygenated volatile organic compounds across the Atlantic Ocean. *Atmos Chem Phys* **14**: 7499–7517.

Zhao, L., Chang, W., Xiao, Y., Liu, H., and Liu, P. (2013) Methylerythritol Phosphate Pathway of Isoprenoid Biosynthesis. *Annu Rev Biochem* **82**: 497–530.

Morphological and transcriptomic evidence for ammonium induction of sexual reproduction in *Thalassiosira pseudonana* and other centric diatoms

Eric R. Moore[1], Briana S. Bullington[1], Alexandra J. Weisberg[2], Yuan Jiang[3], Jeff Chang[2], Kimberly H. Halsey[1]*

Published in PLoS ONE, July 2017
12(7): e0181098

Abstract

The reproductive strategy of diatoms includes asexual and sexual phases, but in many species, including the model centric diatom *Thalassiosira pseudonana*, sexual reproduction has never been observed. Furthermore, the environmental factors that trigger sexual reproduction in diatoms are not understood. Although genome sequences of a few diatoms are available, little is known about the molecular basis for sexual reproduction. Here we show that ammonium reliably induces the key sexual morphologies, including oogonia, auxospores, and spermatogonia, in two strains of *T. pseudonana*, *T. weissflogii*, and *Cyclotella cryptica*. RNA sequencing revealed 1,274 genes whose expression patterns changed when *T. pseudonana* was induced into sexual reproduction by ammonium. Some of the induced genes are linked to meiosis or encode flagellar structures of heterokont and cryptophyte algae. The identification of ammonium as an environmental trigger suggests an unexpected link between diatom bloom dynamics and strategies for enhancing population genetic diversity.

Introduction

Diatoms are protists that form massive annual spring and fall blooms in aquatic environments and are estimated to be responsible for about half of photosynthesis in the global oceans (Nelson et al., 1995). This predictable annual bloom dynamic fuels higher trophic levels and initiates delivery of carbon into the deep ocean biome. Diatoms have complex life history strategies that are presumed to have contributed to their rapid genetic diversification into ~200,000 species (Mann, 1999) that are distributed between the two major diatom groups: centrics and pennates (Simonsen, 1979). A defining characteristic of all diatoms is their restrictive and bipartite silica cell wall that causes them to progressively shrink during asexual cell division. At a critically small cell size and under certain conditions, auxosporulation restitutes cell size and prevents clonal death (Drebes, 1977; Lewis, 1984; Chepurnov et al., 2004). The entire lifecycles of only a few diatoms have been described and rarely have sexual events been captured in the environment (Jewson, 1992; Koester et al., 2008; Holtermann et al., 2010).

So far, all centric diatoms appear to share the process of oogamous sexual reproduction (Fig 1). The average cell size of a population of asexually dividing diatoms decreases as a result of differential thecae inheritance. At a critically small size, cells become eligible to differentiate into male and female cells. Meiosis in the male spermatogonangium produces multinucleate spermatogonia that divide into individual haploid spermatocytes. Meiosis in the female oogonia produces a single functional haploid nucleus that is fertilized by a flagellated spermatocyte through an opening in the oogonia thecae. Fertilized oogonia expand into a large auxospore where new, large thecae are formed for the new, enlarged initial cell. Auxosporulation can also occur asexually,

but it is considered an ancillary pathway for cell size restitution in diatom species that have a sexual path for reproduction (Chepurnov et al., 2004).

The environmental factors that trigger formation of sexual cells and sexual reproduction in centric diatoms are not well understood (Chepurnov et al., 2008; Von Dassow and Montresor, 2011), but sexualization appears to be strongly associated with conditions causing synchronous sexuality in cells experiencing growth stress (Edlund and Stoermer, 1997). Besides the size threshold requirement, previous observations indicate that sexualization is possible when active growth has ceased, causing cell cycle arrest (Armbrust et al., 1990; Huysman et al., 2014) and cell densities are sufficient to permit successful fertilization of the oogonia by the spermatocyte (Assmy et al., 2006). Light interruption with an extended dark period (Armbrust et al., 1990), changing salinities, and nutrient shifts (Godhe et al., 2014), have sometimes been successful in inducing sexual reproduction, probably by causing cell cycle arrest. Recently, pheromones produced by the pennate diatom, *Seminavis robusta,* have been identified that cause cell cycle arrest and induce the sexual pathway (Moeys et al., 2016). However, we are aware of no method that reliably causes induction of all of the sexual stages of centric diatoms shown in figure 1.

The ecological importance of diatoms, combined with their potential uses in materials chemistry, drug delivery, biosensing (Kroth, 2007; Ezzati et al., 2011), and bioenergy (Hildebrand et al., 2012; d'Ippolito et al., 2015), prompted genome sequencing of *T. pseudonana* CCMP1335 (a ‘centric’ diatom collected from the North Atlantic Ocean) and *Phaeodactulum tricornutum* (a ‘pennate’ diatom), which have become model organisms for experimental studies (Armbrust et al., 2004; Bowler et al., 2008).

However, sexual morphologies have never been observed in either of these species or in the vast majority of diatoms (Chepurnov et al., 2008). The inability to reliably control the sexual cycle in centric diatoms has severely hindered studies to understand the silica deposition process, as well as the genetic regulation, ecology, and evolution of sex (Apt et al., 1996; Chepurnov et al., 2008; Chepurnov et al., 2011). Both of the model diatoms were thought to have repurposed their extant genetic toolkits and lost the need and ability for a sexual lifestyle (Chepurnov et al., 2008; Von Dassow and Montresor, 2011; Patil et al., 2015).

Here we show that two strains of *T. pseudonana* and two other centric species, *T. weisflogii* and *Cyclotella cryptica,* can be reliably induced into the sexual reproductive pathway when cells are below the critical size threshold and exposed to ammonium during the stationary phase of growth. Ammonium induced oogonia, auxospore, and spermatocyte formation in each of these species. Induction of sexuality was further supported by RNA sequencing (RNAseq) which revealed 1,274 genes whose expression patterns changed when *T. pseudonana* became sexualized by ammonium. Meiosis genes and genes associated with flagellar structures of heterokont and cryptophyte algae were differentially expressed in ammonium-induced cells compared to nitrate grown cells. We anticipate that this discovery will open opportunities to study the evolution of diatom lifecycles and facilitate expansion of diatom breeding to explore functional genetics for molecular ecology, nanotechnology and biofuels applications.

Results and discussion

Ammonium triggers sexual morphologies

We observed *T. pseudonana* CCMP1335 cell morphologies consistent with sexual reproduction when cells were propagated in artificial seawater medium supplemented with ammonium. The proportion of cells that differentiated into sexual cell types was dependent on ammonium concentration, with up to 39% of the population identified as oogonia or auxospores in cultures supplemented with 800 μM NH_4Cl (Fig 2A). Oogonia and auxospores were first observed at the onset of stationary phase and reached maximum population proportions in late stationary phase (Fig 2A). Ammonium also induced oogonia and auxospore production in *T. pseudonana* CCMP1015 (collected from the North Pacific Ocean), *T. weissflogii*, and *Cyclotella cryptica* (S1 Fig). A few oogonia and auxospores were observed in nitrate grown cultures with no added ammonium (Fig 2A and S1). However, with the exception of nitrate grown *C. cryptica* cultures, which generated oogonia and auxospores constituting 11% of the total population, oogonia and auxospores were only a small percentage of the total population in nitrate-grown *T. pseudonana* and *T. weissflogii.* Even though auxospores can have diameters 3-4 times that of asexual cells, such small population proportions do not lead to discernable shifts in cell size distributions obtained by particle size analysis (e.g., Coulter counter, a commonly used method to assess population size). We initially observed auxospores when performing visual inspections using a light microscope of our cultures that were growing in ammonium. For the data reported here, oogonia and auxospores were quantified by manually counting the cell types using a hemocytometer. We suspect that reliance on laboratory instruments such as particle counters and flow cytometers in place of microscopic analysis is one reason that sexual morphologies in these well-studied

diatom species have gone undetected until now. Laboratory stock cultures are typically maintained in media with low concentrations of nitrogen, especially when ammonium is supplied as the nitrogen source because it has been considered to be toxic to diatoms in high concentrations (Yoshiyama and Sharp, 2006). Therefore, it may not be surprising that sexual cells have gone un-noticed due to the low rates of sexual induction in the presence of low ammonium concentrations (Fig. 2A).

Cells differentiated into oogonia and auxospores regardless of whether ammonium was supplied at inoculation or at the onset of stationary phase (Fig. 1B). Thus, it appears that stationary phase and ammonium availability are key factors that trigger formation of sexual cells in centric diatoms. Resource depletion can arrest the cell cycle (Huysman et al., 2014), and the presence of ammonium at the onset of stationary phase appears to activate the sexual cycle. Auxospore formation was observed in *Cyclotella meneghiniana* during stationary phase (Hoops and Floyd, 1979), and other protists initiate sex under stress in response to nutrient depletion or oxidative DNA damage (Bernstein and Bernstein, 2010). Ammonium can inhibit photosynthesis (Yoshiyama and Sharp, 2006); however, diatoms, including *T. pseudonana*, can acclimate to millimolar ammonium concentrations (Collos and Harrison, 2014). It is possible that high ammonium concentrations intensify the stress condition required for the sexual pathway. Nevertheless, ammonium consistently caused formation of ten-fold more sexualized cells than the same concentrations of nitrate (Fig 2 and S1).

Our results showing that ammonium induced formation of sexual cells in several centric diatom species suggests that it may serve as a key environmental factor regulating the sexual lifecycle across centric diatoms. Ammonium is typically present in very low

concentrations in aquatic ecosystems. However, ammonium reached 12.6 mM in a eutrophic lake where the centric diatom, *Aulacoseira subarctica,* was observed undergoing sexual reproduction (Jewson, 1992). Clearly, ammonium was not the growth-limiting nutrient under those conditions or in our laboratory cultures (Fig 2). *Pseudo-nitzschia* auxospore formation was positively correlated with ammonium, which was measured to be 14 μM during a major bloom event off the coast of Washington (Holtermann et al., 2010). Thus, the formation of sexual cells appears to be triggered by the presence of ammonium while at least one other growth factor becomes limiting, such as light (discussed below), phosphorous, silica (Holtermann et al., 2010), vitamins, or trace elements.

Cell differentiation in *T. pseudonana* was induced irrespective of growth rate in exponential phase, light intensity, or light regime. However, the growth parameters did affect the proportion of differentiated cells. Oogonia and auxospores were only 0.5% of the population when grown under very low light (5 μE) with 200 μM NH_4Cl and increased to 39% when grown under moderate light (100 μE) and 800 μM NH_4Cl (Table 1). The proportions of oogonia and auxospores increased with light up to moderate intensities (70-100 μE) but decreased at high (220 μE) intensities (Table 1), suggesting that photon flux has an important role in meeting the energetic demands of sexual reproduction. Other work showed sexualization was more prevalent at light <50 μE (Mouget et al., 2009) or with the addition of a dark period (Vaulot and Chisholm, 1987; Armbrust et al., 1990; Mills and Kaczmarska, 2006). Likely, the optimum light intensity or need for a dark period to precede sexual induction (Gillard et al., 2008) is species-specific and linked to adaptive life histories (Chepurnov et al., 2004).

Visualization of sexual morphologies

Confocal, light, and scanning electron microscopy were used to document the cell morphologies at various stages in the life history cycle of *T. pseudonana* (Fig 3 and S2). Oogonia were elongated relative to asexually growing vegetative cells and exhibited a bent morphology and swelling of the plasma membrane at the junction of the hypotheca and epitheca (Figs 3B, 3C and S2B-D). In oogonia, cellular contents became localized to the ends of the cell resulting in an apparent empty space near the area of membrane swelling where fertilization likely occurs (Chepurnov et al., 2004).

T. pseudonana spermatogonium harbored at least eight nuclei (Fig 3D), suggesting that a depauperating mitosis preceded meiosis (Von Dassow and Montresor, 2011; Kaczmarska et al., 2013). Sperm released were very small, about 1 μm, and flagellated (Figs 3E and S2E, S2F), but they often became entangled with other cells and debris (French III and Hargraves, 1985; Jewson, 1992; Idei et al., 2012). Sperm cells attached to oogonia at the junction of the thecae for fertilization (Figs 3F, 3G and S2I, S2J) as shown in *T. punctigera* (Chepurnov et al., 2006). Also similar to *T. punctigera*, flagella were not visible at that stage, possibly because flagella are abandoned upon attachment to the oogonia (French III and Hargraves, 1985).

Oogonia developed into auxospores and these conspicuous cell morphologies were always observed in cultures induced by ammonium. Auxospores were larger than vegetative cells and oogonia, ranging from about 6 to 20 μm in diameter, with most being 10-15 μm in diameter (Figs 3H, 3I and S2G, S2H, S2L). Auxospores were spherical, with most of the cellular contents localized to one side (Fig 3H, 3I and S2G, S2H, S2L) and sometimes showing slight distention where the mother valve was shed (Fig 3I), as

described in *Stephanodiscus niagarae* (Edlund and Stoermer, 1991). Thecae remained attached in some cases, especially on smaller cells. Oogonia, auxospores, and spermatogonia in the other species studied displayed similar morphologies to those observed in *T. pseudonana* and other centric diatoms (Figs 3L-O, S2M-P and 4A) (Hoops and Floyd, 1979; Chepurnov et al., 2006; Mills and Kaczmarska, 2006; Von Dassow and Montresor, 2011; Idei et al., 2012; Kaczmarska et al., 2013; Shirokawa and Shimada, 2013; Godhe et al., 2014; Idei et al., 2015).

Changes in DNA content in *T. pseudonana* cells induced into sexuality by ammonium were observed using flow cytometry-based analysis. Fluorescence-activated cell sorting (FACS) analysis showed that as the culture progressed from exponential into stationary growth phases, the diploid population (Fig 4B) expanded to include DNA fluorescence intensities that were consistent with the presence of spermatogonangia and spermatogonia containing multiple gametes (Fig 4C). In late stationary phase, a new population was observed that had DNA fluorescence signals consistent with haploid sperm cells with little to no chlorophyll (Armbrust et al., 1990) (Fig 4D).

Cell size restitution via auxosporulation produced progeny cells that were considerably larger than the parent cells from nitrate stock cultures. To induce a high proportion of the eligible cells into the sexual pathway we repeatedly propagated cultures in 800 μM ammonium with inoculum of 25%. This strategy raises the ratio between the exposure of cells to ammonium in stationary phase and the total number of cell divisions. Our findings can be explained by assuming that cells in nitrate stock cultures are already at or below the critical size threshold for induction into sexuality, but with each passage through growth and stationary phases in batch culture, only a fraction of the eligible cells

are induced into the sexual cycle. The average cell diameters of the resulting cultures were larger relative to stock cultures maintained in nitrate (Fig 4E and S3). The *T. pseudonana* initial cells were 7-12 μm, the largest size reported for this species (Figs 3J, 3K, S2K). Presuming that cell size reduction during vegetative growth occurs in *T. pseudonana,* this process of cell size reduction and cell size restitution via ammonium induction have opposing influences on the average size of populations. These processes confound the ability to observe the impacts of sexual induction without experimental designs that maximize the percentage of the population induced into the sexual pathway and minimize the number of vegetative replications between episodes of induction.

We identified oogonia, male gametes, auxospores, and initial cells in cultures of the model centric diatom, *T. pseudonana* providing new evidence for sexuality in this species that was previously assumed to be asexual (Chepurnov et al., 2008). Although cell enlargement through asexual/apomictic mechanisms has been recorded in other species (Gallagher, 1983; Nagai et al., 1995; Sabbe, 2004), the presence of all sexual cell types, and the expression of meiotic genes (discussed below), suggest apomixis is not the mechanism being used by *T. pseudonana* for cell enlargement. Furthermore, apomixis typically occurs in species that also undergo sexual reproduction (Chepurnov et al., 2004). Only spermatogenesis had previously been reported in *T. weissflogii* (Armbrust et al., 1990; Armbrust, 1999), but we have now also documented induction of oogonia and auxospores by ammonium and subsequent formation of initial cells in this species. A major challenge in visualizing the morphological characteristics of these species is their smaller cell sizes compared to other species for which morphological details have been documented. Now that we have determined a reliable method for inducing the sexual

morphologies, future studies will dissect additional details associated with the sexual pathways in these, and perhaps other species inducible by ammonium, to determine their variation from other centric diatoms. For example, the presence of auxospore scales, precise timing of fertilization and meiotic activity, repeated auxosporulation, and polyspermy events (e.g., (Chepurnov et al., 2006)). The case of *T. pseudonana* also presents interesting questions about whether this species has retained the ability to reduce in cell size. It appears that *T. pseudonana* has the capacity to avoid clonal death by maintaining a relatively constant cell size (3-9 μM) (Round, 1972; Hildebrand et al., 2006; Hildebrand et al., 2007). Our experiments show that cells in this size range are inducible into the sexual pathway. Nevertheless, the question remains whether the progeny of induced small cells of *T. pseudonana* are capable of cell size reduction.

Gene expression analysis of ammonium induced sexual morphologies

We used RNAseq to identify genes that were differentially expressed in conditions that triggered cell differentiation into sexual morphologies. We compared the transcriptomes of *T. pseudonana* harvested in exponential (EXP), stationary (STA), and late stationary phases (L-STA). Cells were grown in 100 μM $NaNO_3$ or, to capture a dose-dependent change in gene expression, either 100 or 800 μM NH_4Cl (S4 Fig). We identified genes that were significantly differentially expressed in multiple pairwise comparisons of growth phases and nitrogen sources (S1-S11 Tables). Next, we examined the statistical interactions of pairwise condition comparisons to identify genes with significantly greater or lesser magnitude changes in expression between growth stages in the presence of ammonium relative to 100 μM $NaNO_3$ (Fig 5A and S5).

This conservative approach yielded a total of 1,274 genes in the four analyses of statistical interactions (S12-S15 Tables). A total of 89 of the genes have an annotated function (Fig. 5A;S16 Table). The set of 89 genes includes four meiotic genes (*mcm2, mcm8, mcm9, and mlh1*, Fig 4B and S6) that were also up-regulated in pennate diatoms during sexual reproduction (Patil et al., 2015). The Mcm family of DNA helicases function in DNA replication, with *mcm8, mcm9,* and *mlh1* having roles in double stranded break repair (Baker et al., 1996; Lutzmann et al., 2012; Park et al., 2013). Mcm8 was one of the four genes related to meiosis that were upregulated in the pennate diatom, *Seminavis robusta* during treatment with a sex-inducing pheromone (Moeys et al., 2016). Eight genes in our list are homologous to yeast genes involved in meiosis (Butler et al., 2009) (Fig 5B,S17 Table), including genes that regulate the meiotic anaphase promoting complex (*cdc16*, *cdc23*, *ama1*) (Zachariae et al., 1998; Cooper et al., 2000) and *rad54*, a motor protein that regulates branch migration of Holliday junctions during homologous recombination (Mazin et al., 2010). Expression of genes encoding other RAD proteins (*rad50 and rad 51*) increased in pennate diatoms induced into meiosis (Patil et al., 2015; Moeys et al., 2016).

Of three 'sexually induced genes' that were up-regulated in *T. weissflogii* at the initiation of gametogenesis (Armbrust, 1999) and associated with sperm flagella mastigonemes (Honda et al., 2007), one, *sig3*, was significantly up-regulated in stationary phase compared to exponential phase (Fig 5B). In addition, a gene encoding an intraflagellar transport protein (IFT88) was also up-regulated in ammonium induced cells during stationary phase (Fig. 5B). An IFT system is required for flagellar assembly (Rosenbaum and Witman, 2002) and five genes encoding IFT particle proteins, including

IFT88, and a kinesin-associated protein involved in anterograde transport were found in the *T. pseudonana* genome (Merchant et al., 2007). The genes encoding Sig3 and IFT88 are unique to flagellar structures, and their differential expression in ammonium induced *T. pseudonana* compared to the nitrate-grown control treatments provide additional evidence that ammonium induced spermatogenesis in this species.

The MYB factor and bZIP families of proteins are transcriptional regulators that control a variety of cell processes including stress responses, development, and differentiation in plants (Ambawat et al., 2013). Expression of two genes having the characteristic R2R3 MYB DNA binding domains common in plants, *myb24 and myb16,* was generally lower in ammonium induced cultures compared to the nitrate grown controls (Fig 5B). In *Arabidopsis thaliana*, hormonal activation of *myb24* is required for stamen development and male fertility (Cheng et al., 2009). Whether *myb24, myb16,* and *bzip2* play roles in regulating gamete development or sex differentiation in diatoms remains to be determined.

The 1,274 genes provide new avenues to understand the evolution of sexuality in the Heterokont eukaryotic lineage. Diatoms emerged ~ 200 Mya, about 800 My after a eukaryotic heterotroph engulfed a red alga in the secondary endosymbiosis event that gave rise to the SAR eukaryotic supergroup (Archibald, 2009). Of 171 diatom genes of red algal origin (Archibald, 2009), 17 were identified as differentially expressed in conditions that induced sexual reproduction (S18 Table). None of these genes are annotated in the *T. pseudonana* genome, but in red algae they are predicted to function in transport and plastid-targeted processes (Bowler et al., 2008).

Conclusions

That some of the most well studied centric diatoms were never observed undergoing sexual reproduction was a mystery. Possibly even more elusive was the ability to reliably control or induce the sexual pathway of centric diatoms in the laboratory (Chepurnov et al., 2008) despite a myriad of efforts that ranged from sweet-talk to torture. Factors that have limited progress in this field center on the problem that even under 'favorable environmental conditions' that result in the sexual lifecycle, only a fraction of cells undergo sexual reproduction (Fig 2). Thus, capturing the sexual event requires near constant visual observation because (a) only cells that have become sufficiently small and reach the critical size threshold can undergo sexual reproduction (Geitler, 1932), (b) only a fraction of those size-eligible cells may undergo sexual reproduction (Jewson, 1992; Assmy et al., 2006; Mouget et al., 2009; Godhe et al., 2014), (c) there has been a lack of understanding about what constitutes conditions that are 'favorable' for triggering diatom sex (Chepurnov et al., 2004; Holtermann et al., 2010), and (d) morphological changes indicative of sex may not be recognized by untrained scientists (Mann, 1988).

Our results provide strong evidence that *T. pseudonana* is a sexual organism, expressing the major morphologies associated with the sexual pathway that result in enlarged initial cells. Furthermore, the sexual pathway was reliably induced in *T. pseudonana*, and two other centric diatom species by exposure of size-eligible cells to ammonium. Ammonium triggered formation of sexual cells in a dose-dependent manner and significant changes in expression of genes involved in meiosis, spermatocyte flagellar structures and assembly, and sex differentiation. RNAseq analysis revealed

many more genes with unknown functions that were expressed under conditions of sexual differentiation. Other genes involved in sex are likely to have been missed by our analysis because their changes in expression were masked by the mixed population of asexual and sexual cells, or they were not captured in the coarse time-resolution of sampling used in this study. Nevertheless, our discoveries resolve two persistent mysteries that have plagued diatom researchers. Furthermore, the RNAseq data provide a subset of genes that can be used to study the molecular ecology of diatoms.

The ecology of centric diatom sexual reproduction that can be inferred from our findings appears best described as synchronous sexuality (Edlund and Stoermer, 1997) triggered by ammonium in cells experiencing growth stress. Asexual cell cycle arrest appears to be prerequisite to activation of the diatom sexual life cycle (Hoops and Floyd, 1979; Armbrust et al., 1990; Bernstein and Bernstein, 2010; Huysman et al., 2014). In the environment, diatoms bloom following elevated nutrient concentrations driven by vertical mixing, coastal upwelling, or river inputs and the bloom reaches its peak biomass when essential nutrients are depleted. Within a week, the bulk of a bloom can be consumed by heterotrophic protists (Tillmann, 2004) that excrete ammonium to maintain homeostatic elemental composition (Sterner and Elser, 2002). We propose that ammonium released by grazers at bloom climax may be a principal ecological trigger for sexual morphologies in centric diatoms. Synchronization of sexuality at the onset of resource depletion (stationary phase) increases the chances for successful fertilization because cell density is at its maximum (Edlund and Stoermer, 1997). Environmental concentrations of ammonium in the environment rarely reach the concentrations used in this study to demonstrate the dose response effect on sexuality. Other methods that have

sometimes successfully triggered sexual reproduction in other species are similarly unusual compared to environmental conditions. For example, the magnitude of the salinity shifts used to induce sexual reproduction in *Skeletonema marioni* in the laboratory do not occur in the Baltic sea (Godhe et al., 2014). Nevertheless, pulses of ammonium, shifts in salinity, and other environmental fluctuations do occur in aquatic ecosystems, and provided the other conditions for sexuality are met (e.g., cell size threshold, stress, population density), are likely to induce sexuality in at least a small fraction of a population. The presence of ammonium and the onset of stationary phase also point to involvement of another growth factor whose depletion triggers sexual reproduction. The specific collection of factors that lead to sexual reproduction in diatoms in the environment is not yet known and neither is whether ammonium is a direct or indirect trigger of sexuality (Lewis, 1984). Nevertheless, this work suggests an intriguing ecological role for ammonium in the mechanisms underlying sexuality in centric diatoms and will certainly be a valuable tool to control sexuality in the laboratory.

The identification of ammonium as a reliable inducer of sexuality in *T. pseudonana* and other centric diatoms has the potential to shift perspectives on diatom ecology, open avenues for the experimental investigation of diatom reproductive mechanisms, and provide tools for genetic manipulation of centric diatoms that have not heretofore been available. Diatom blooms have a global impact but the factors that control these blooms and their demise are complex and a consensus has not been reached about these processes. Our evidence suggests that induction of sexuality may play a vital role in diatom bloom conclusion and the production of genetic diversity that seeds future blooms (Chen and Rynearson, 2016). Our analysis suggests an involvement of genes of

red-algal origin, providing new lines of evolutionary enquiry. Interest in diatoms for biotechnological applications is high due to their uses in biofuels, materials chemistry and medicine. Our work will likely propel this exploration by enabling improved breeding and genetic modification to control and understand unique diatom traits.

Experimental Procedures

Stock cultures of *T. pseudonana* (CCMP1335) were maintained in f/2 medium (Guillard, 1975) with 200 μM $NaNO_3$ under continuous sub-saturating light at 18°C. Sexual cells were quantified in triplicate cultures of *T. pseudonana* (CCMP1335 and CCMP1015)*, T. weissflogii* (CCMP1336) and *C. cryptica* (CCMP332) (all obtained from NCMA) grown in f/2 amended with $NaNO_3$ or NH_4Cl and grown at 18^{o}C under 50 μE continuous light, or under variable light intensities/cycles as shown in Table 1. Cell populations were quantified using a Coulter counter (Beckman-Coulter, Indianapolis, Indiana). Oogonia and auxospores were counted using a hemocytometer.

We found that a modified f/2 medium yielded better cell images using light and confocal microscopy. This medium contained 0.939 mM KCl, 0.802 mM NO_3^-, 1 mM NH_4Cl, 0.05 mM glycine, 0.01 mM methionine, 0.078 mM pyruvate, 0.84 μM pantothenate, 0.985 μM 4-amino-5-hydroxymethyl-2-methylpyrimidine, 0.3 μM thiamine, 0.002 μM biotin, 0.117 μM $FeCl_3*6H_2O$, 0.009 μM $MnCl_2*4H_2O$, 0.0008 μM $ZnSO_4*7H_2O$, 0.0005 μM $CoCl_2*6H_2O$, 0.0003 μM $Na_2MoO_4*2H_2O$, 0.001 μM Na_2SeO_3, and 0.001 μM $NiCl_2*6H_2O$, and sparged with filter-sterilized carbon dioxide and air for 8 hours and overnight respectively. To view DNA, 1 ml live samples were stained with 5 μl 1.62 μM Hoescht 33342 (0.2 μm filtered) for 10 min. For scanning

electron microscopy (SEM), 1 ml samples were diluted 1:3 with sterile f/2 and syringe filtered onto 13 mm 0.2 μm polycarbonate filters using a Swinnex filter unit. The filter was washed with 4 ml f/2 containing 0.5% gluteraldehyde and left submerged for at least 24 hours, followed by a series of 4 ml washes: 0.2 μm filtered 80%, 60%, 40%, 20% and 0% f/2, followed by 20%, 40%, 60% 80% and 100% ethanol, before critical point drying. SEM imaging was done at the Oregon State University Electron Microscope facility.

For flow cytometry 1 ml culture samples were fixed with 1 μl gluteraldehyde (50%) and stained with 10 μl Sybr green mix (1:25 dilution Sybr green in 0.01M Tris-EDTA, pH 8.0) for 30 min. Samples were run on a FACScan flow cytometer (Becton Dickinson, Franklin Lakes, New Jersey). Settings were FL1=582 and FL3=450 for unstained cells and FL1=450 and FL3=450 for stained cells.

For RNAseq analysis, $1.61x10^{8}$ – $1.10x10^{9}$ cells from triplicate independent cultures were filtered onto 0.8 μm 47 mm polycarbonate filters during exponential, stationary and late stationary phases and flash frozen in liquid nitrogen. RNA was extracted using a Qiagen RNeasy midi kit according to modified manufacturer's instructions (Dyhrman et al., 2012). Silica beads (0.5 mm) were added to the cells and lysis buffer and vortexed until homogeneous before being filtered through Qiashredder columns to remove large particles. Eluted RNA was subjected to off column RNase free DNase I treatment and secondary purification according to manufacturer's recommendations. Total RNA was prepared and sequenced as a 150 bp single end library on an Illumina HiSeq 3000 at the Center for Genome Research and Biocomputing at Oregon State University. Sequencing data/interaction analyses were conducted using the Ballgown pipeline (Pertea et al., 2016). Sequencing reads were trimmed to remove

sequencing adapters using BBDuk v. with the parameters " ktrim=r k=23 mink=9 hdist=1 minlength=100 tpe tbo" (Bushnell, 2016). Reads aligned to the *T. pseudonana* reference genome (NCBI accession GCA_000149405.2) using HISAT2 v. 2.0.4 with the parameters " --min-intronlen 20 --max-intronlen 1500 --rna-strandness F --dta-cufflinks" (Kim et al., 2015). Transcripts were assembled for each dataset and merged using Stringtie v 1.2.4 (Pertea et al., 2015). Pairwise differential expression analyses for genes were performed using the "stattest" function in Ballgown version 2.2.0 (Frazee et al., 2015). Interaction effects were tested by comparing the models with (timepoint + treatment + timepoint * treatment) and without (timepoint + treatment) the interaction term using the custom model option in the "stattest" function.

For construction of the phylogenetic tree, 18s rRNA sequences were obtained from the Silva database and aligned using Muscle v3.8.31 (default settings) (Edgar, 2004). A genome editor (BioEdit) was used to manually trim off overhanging sequence. The tree was built using RAxML-HPC v8.0.26 using the GTRCAT model, "-f a" option, and 1000 bootstrap replicates (Stamatakis, 2006). A visual representation was created using the TreeDyn (Chevenet et al., 2006) tool through LIRMM (phylogeny.fr) (Dereeper et al., 2008).

All RNAseq data have been deposited to NCBI under BioProject ID PRJNA391000.

Acknowledgements

The authors thank Kelsey McBeain for assistance with confocal microscopy imaging and the Electron Microscope Facility at Oregon State University for scanning electron micrographs.

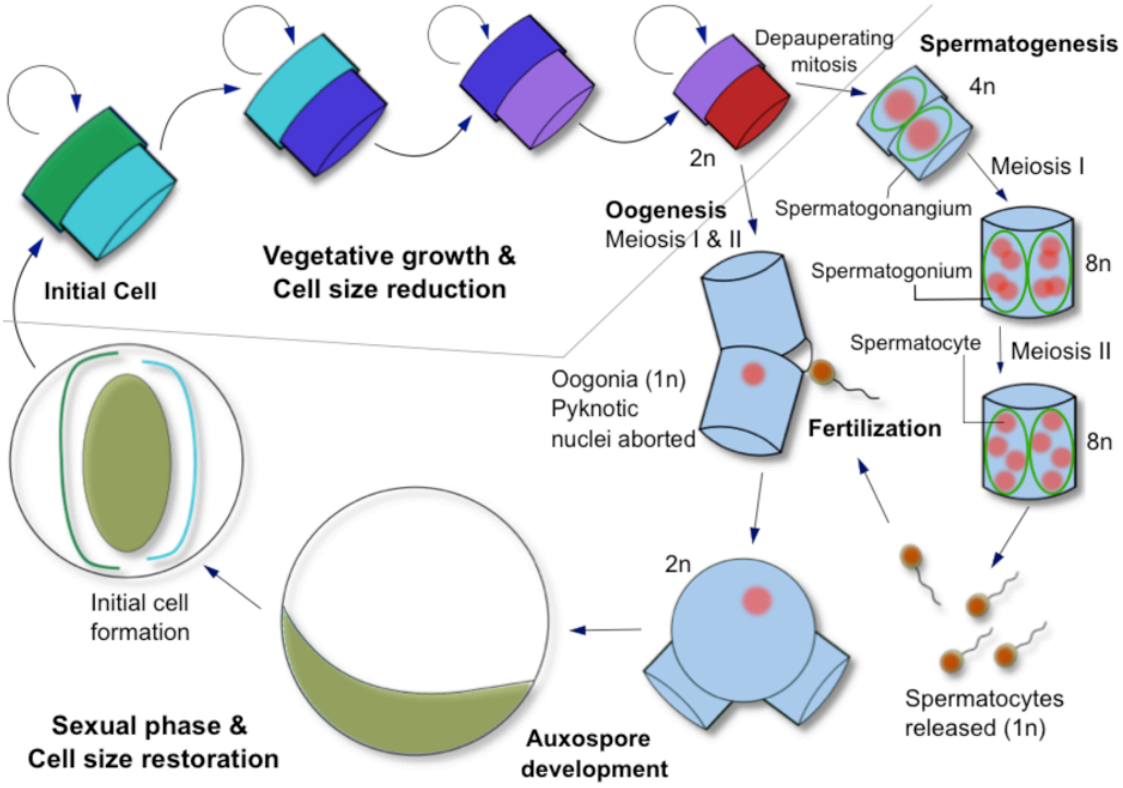

Fig 1. The life cycle of a centric diatom. The average cell size of a population of asexually dividing diatoms decreases as a result of differential thecae inheritance. At a critically small size, cells can initiate sexual reproduction and differentiate into male and female cells. Meiosis in the male spermatogonangium produces multinucleate spermatogonia that divide into individual haploid spermatocytes. Meiosis in the female oogonia produces a single functional haploid nucleus that is fertilized by a flagellated spermatocyte through an opening in the oogonia thecae. Fertilized oogonia expand into a large auxospore where new, large thecae are formed for the new initial cell.

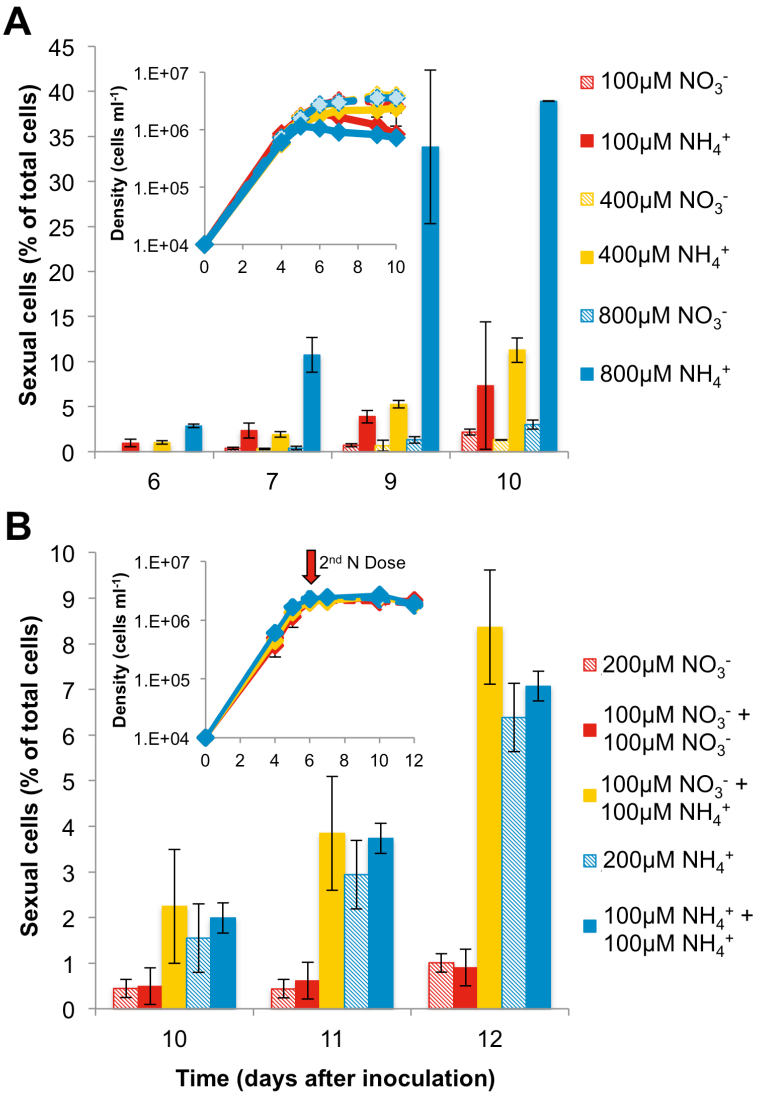

Fig 2. Ammonium induces sexual morphologies in *T. pseudonana* CCMP1335. (A) Proportion of sexual cells (oogonia and auxospores) relative to the total population in cultures of *T. pseudonana* grown in the presence of NH_4Cl or $NaNO_3$; n=3 independent cultures, average of 300 cells counted per replicate. Oogonia and auxospores were only observed beginning in stationary phase, data are mean values, error bars are s.d.. Inset: corresponding growth curve linking the onset of stationary phase with first appearance of sexual cells on day six. (B) Sexual cells were observed in cultures with NH_4Cl present at inoculation (blue hatched and solid blue bars) or following NH_4Cl addition at the onset of stationary phase (yellow bars). Legend shows concentration of nitrogen source provided at inoculation and concentration of nitrogen source added at the time of the second dosing. Two control treatments were supplied 200 μM nitrogen source at inoculation only. Inset: corresponding growth curve showing the onset stationary phase and timing of 2nd nitrogen addition; n=3 independent cultures, average of 281 cells counted per replicate, data are mean values, error bars are s.d.

Species	Light intensity (μE)	Light regime	Nitrogen concentration (μM)	Specific growth rate (d^{-1})	Oogonia and auxospores in NO_3^- (%)	Oogonia and auxospores in NH_4^+ (%)
T. pseudonana	5	24 h	200	0.28	0.21 ± 0.22	0.52 ± 0.52
	50	24 h	200	0.89	3.67 ± 0.55	7.67 ± 0.50
	50	12 h/12 h L/D	200	0.80	0.67 ± 0.27	2.32 ± 0.52
	220	24 h	200	1.2	0.26 ± 0.26	1.30 ± 0.91
	70	24 h	800	0.98	3.01 ± 0.52	38.9 ± 0.04
C. cryptica	100	24 h	800	0.38	11.1 ± 2.27	37.6 ± 3.71
T. weissflogii	100	24 h	800	0.52	4.50 ± 2.36	39.8 ± 5.65

Table 1. Effects of growth parameters on induction of sexual reproduction in *T. pseudonana* CCMP1335, *T. weissflogii* and *C. cryptica*. Oogonia and auxospores always appeared in stationary phase. The percentage of the total population (at least 300 cells counted per replicate) differentiated into oogonia or auxospores when grown in nitrate or ammonium is shown for the day they were at their maximum number; data are mean values ± s.d., biological replicates n=3.

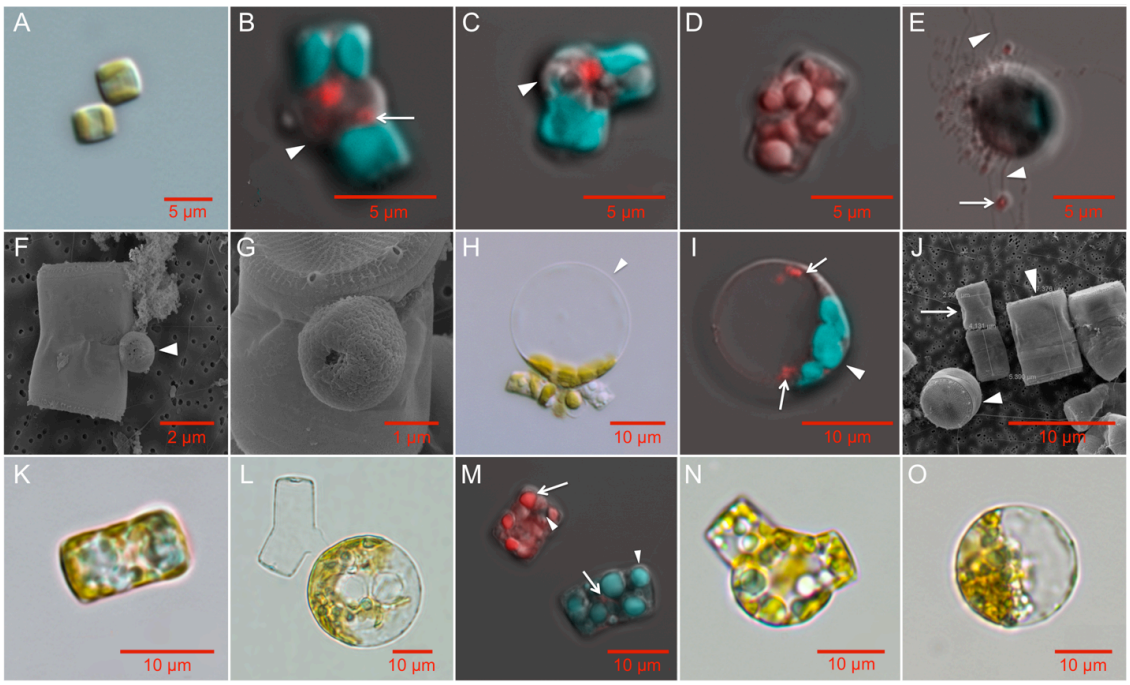

Fig 3. The life cycle stages of *T. pseudonana* (A-K), T. weissflogii (L) and C. cryptica (M-O) imaged using scanning electron microscopy (SEM), light (LM), and confocal microscopy (CFM). A: Two vegetative cells (LM, CCMP1335). B: Oogonium displaying separation of thecae (arrowhead) and putative pycnotic nucleus indicated by the arrow (CFM, CCMP1015). C: Oogonium sharply bending at the thecae junction. Arrowhead indicates protrusion of the plasma membrane (CFM, CCMP1335). Oogonia images are representative of 38 total images. D: Spermatogonium containing multiple spermatocytes seen as individual red (DNA stained) clusters (CFM, CCMP1335); representative of 8 images. E: Motile spermatocytes (in red, arrow) with moving flagella (arrowheads, CFM, CCMP1335, representative of 10 images). F-G: SEM images of spermatocytes (arrowhead) attached to early oogonia (SEM, CCMP1335, representative of 20 images). H,I: Auxospores; representative of 60 images in CCMP1015 (H, LM) and CCMP1335 (I, CFM) showing bulging where mother valve was attached (arrowhead). Two nuclei are visible in red following non-cytokinetic mitosis. J: Small parental cell (arrow) with initial cells produced by sexual reproduction to the left (partial valve view) and right (girdle view) indicated by the arrowheads (SEM, CCMP1335). K: 7 x 12 µm initial cell (LM); j and k representative of 12 images of CCMP1335. L: *T. weissflogii* auxospore (LM); representative of 12 similar images. M: *C. cryptica* spermatogonium (upper left) and vegetative cell (lower right). CFM shows stained DNA (red, arrow) and multiple nuclei in the spermatogonium. Arrowheads indicate chlorophyll autofluorescence (green). Oogonium (N, representative of 6 images) and auxospore (O, representative of 4 similar images) of *C. cryptica* (LM). Confocal microscopy images (b-e, i, m) show chlorophyll autofluorescence (green) and Hoescht 33342 stained DNA (red). Scale bars: A: 5 µm; B-E: 5 µm; F: 2 µm; G: 1 µm; H-O: 10 µm.

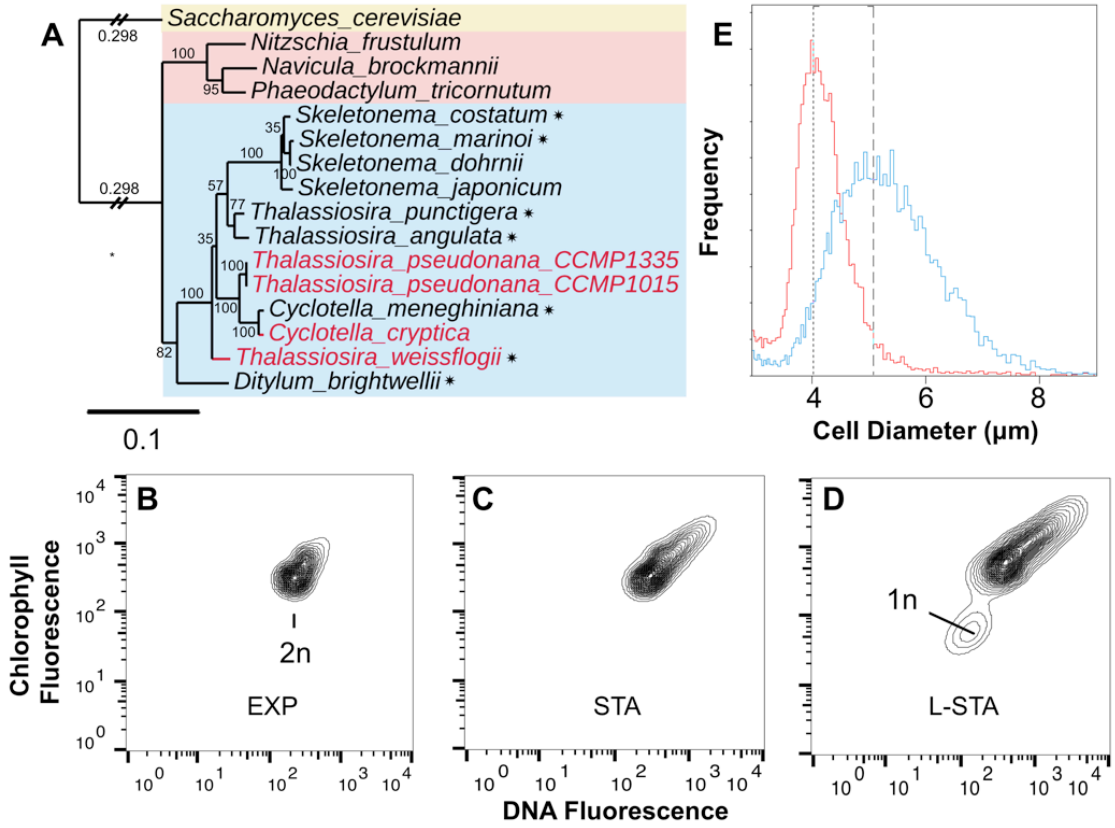

Fig 4. Evidence for meiosis and initial cells. A: 18s rRNA phylogeny of diatoms including pennates (pink rectangle), centrics (blue rectangle). Highlighted in red are the four strains induced into sexual reproduction in this study. Species for which some evidence already exists for sexual reproduction are starred [9, 13, 16, 28, 33, 38]. B-D: Changes in DNA and chlorophyll fluorescence in exponential (EXP), stationary (STA) and late stationary (L-STA) growth phases of *T. pseudonana* induced by ammonium; 30,000 events recorded, representative of two biological replicates. E: Coulter Counter distributions of cell diameter for *T. pseudonana* cultures in exponential phase of growth and maintained in $NaNO_3$ (red) and after six successive 25% transfers to medium with ammonium (blue). Each new culture was allowed to remain in stationary phase for three days before the next 25% transfer was made. Single replicates of cultures with cell densities of 2.4×10^6 ml^{-1} ($NaNO_3$) and 2.3×10^6 ml^{-1} (ammonium). Dashed lines are the mode for each peak.

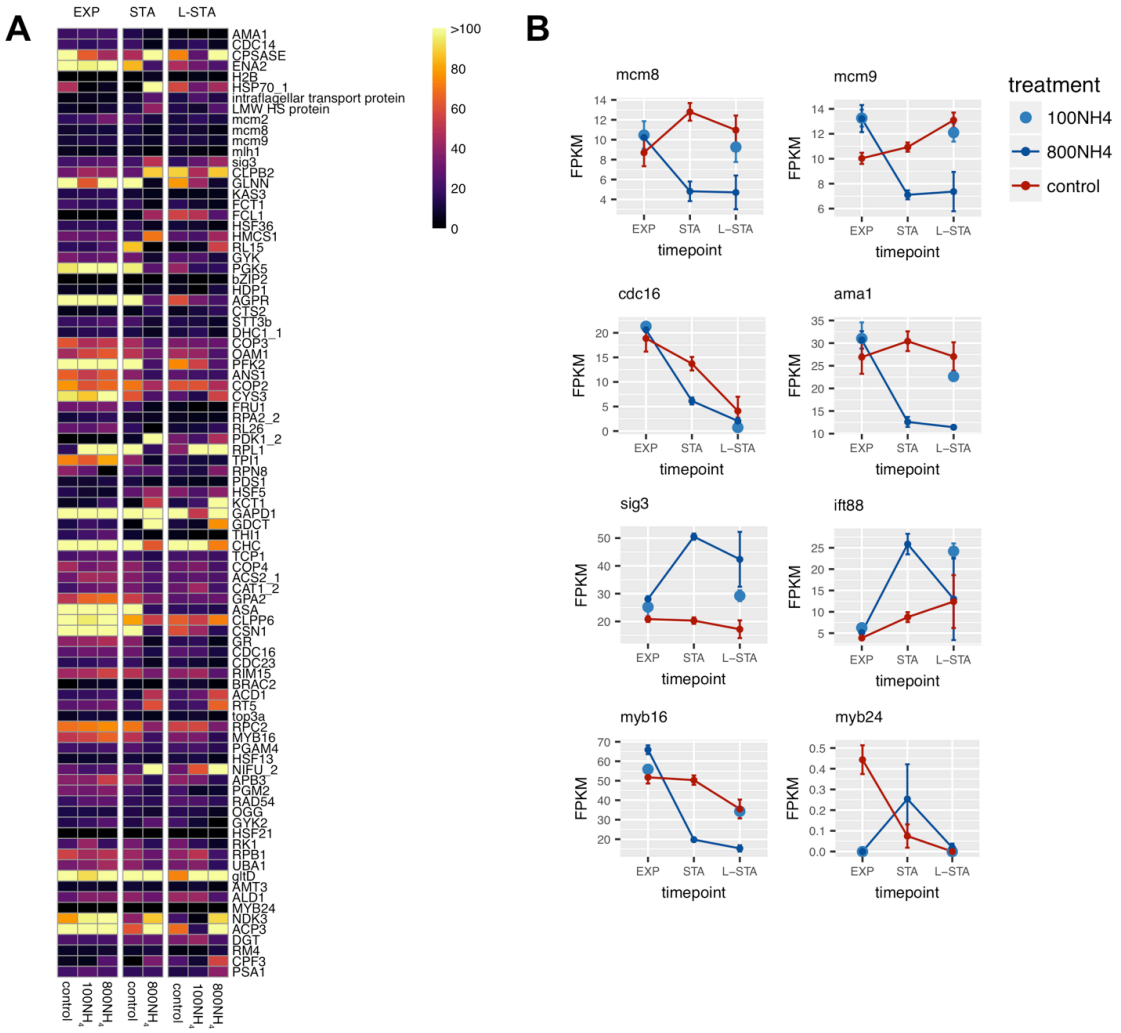

Fig 5. Transcriptomic evidence for sexual reproduction in *T. pseudonana*. A: Heat map of 89 genes having annotated functions that were differentially expressed during differentiation and sexual reproduction in *T. pseudonana* CCMP1335. Color indicates normalized expression value (FPKM) for each nitrogen treatment (control = 100 µM NO_3^-; 100NH4 = 100 µM NH_4^+; 800NH4 = 800 µM NH_4^+) and growth phase (EXP, STA, L-STA). B: FPKM values of select genes across growth phases for each nitrogen treatment.

Supporting Information

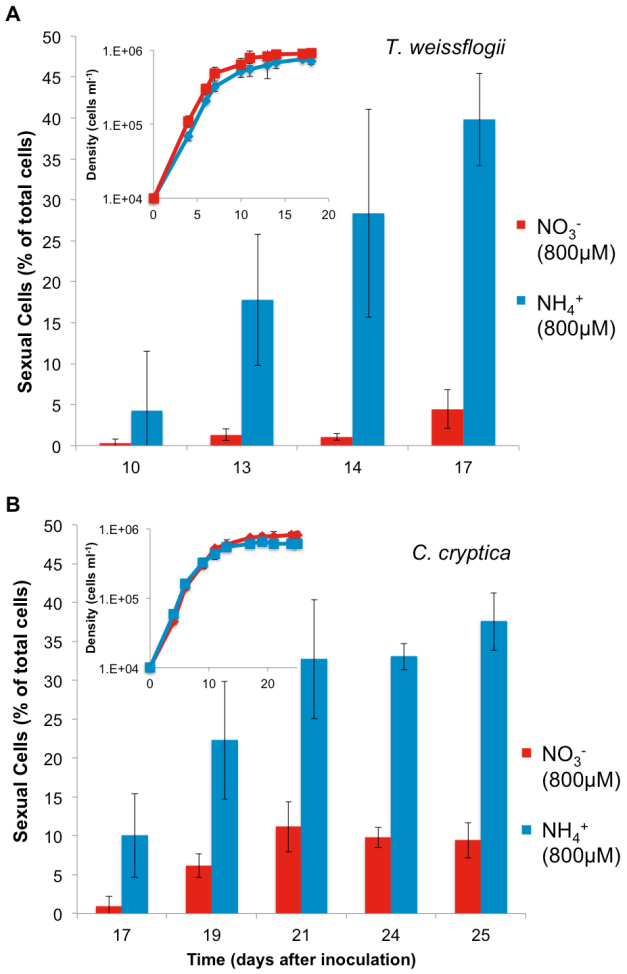

S1 Fig. Ammonium induces sexual morphologies in *T. weissflogii* (A) and *C. cryptica* (B). Proportion of sexual cells (oogonia and auxospores) relative to the total population in cultures supplemented with NH_4Cl or $NaNO_3$. An average of 120 and 107 cells were counted per replicate of *T. weissflogii* and *C. cryptica*, respectively, throughout the growth curve, but oogonia and auxospores were only observed beginning in stationary phase; independent cultures n=3, data are mean values, error bars are s.d.. Inset: corresponding growth curve linking the onset of stationary phase with first appearance of sexual cells on day 10 (A) and 17 (B).

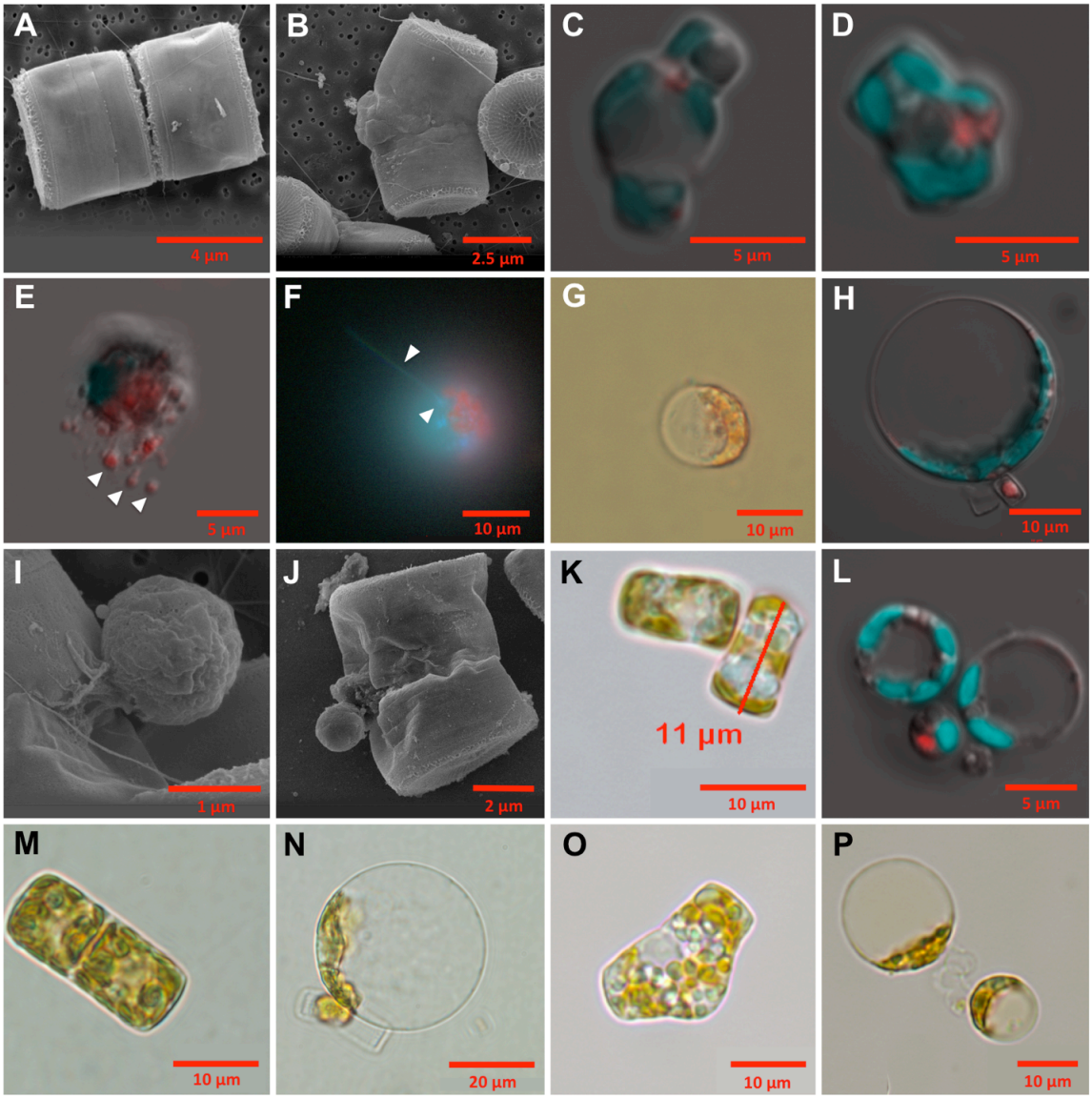

S2 Fig. The different life stages in *T. pseudonana* (A-L), *T. weissflogii* (M,N) and *C. cryptica* (O,P). A: SEM of vegetative cells (CCMP1335). B-D: SEM (B) and CFM images of CCMP1335 oogonia, displaying separation of the thecae and expansion of the membrane. E: CFM image of flagellated spermatocytes with stained DNA (arrowheads), F, G. Epifluorescence (F) and LM images of the same view. In F, an active, flagellated spermatocyte (arrowhead) possibly associated with an auxospore surface is revealed by lateral light from fluorescence of DNA (blue) and chlorophyll (red). H,L: Auxospores of CCMP1015 and CCMP1335 respectively (CFM). I,J: Individual spermatocytes attached to oogonia (SEM). K: Initial cells of *T. pseudonana* CCMP1335 (LM). M,N: *T. weissflogii* vegetative cells (M; LM) and auxospore (N; LM). O,P: *C. cryptica* oogonia (O; LM) and auxospores (P; LM). CFM images (C-E, H, L) show fluorescence of DNA in red and chlorophyll in green.

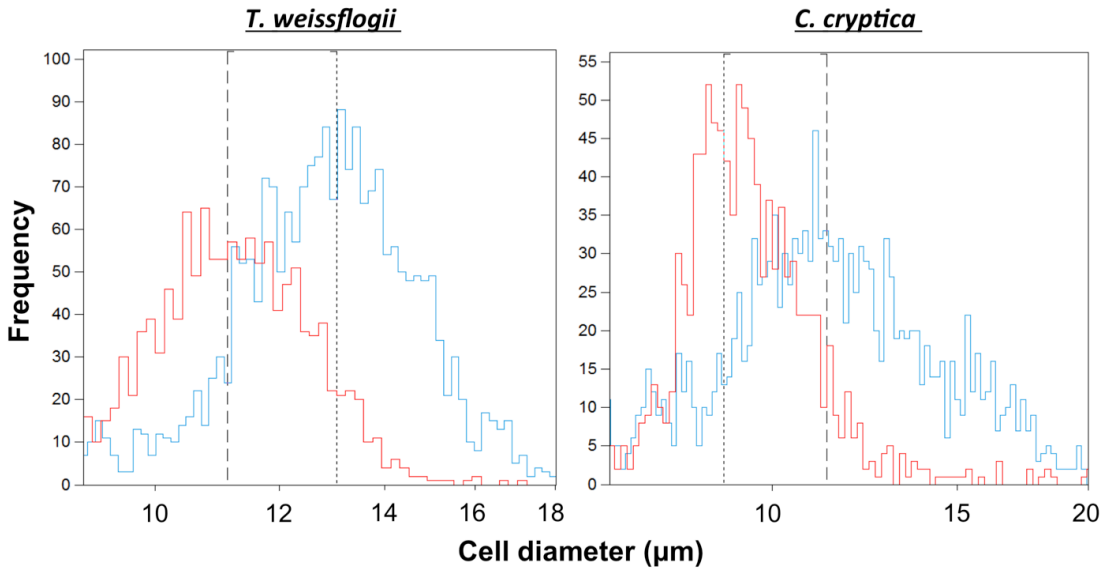

S3 Fig. Coulter Counter distributions of cell diameter for *T. weissflogii* (A) and *C. cryptica* (B) cultures in exponential phases of growth and maintained in $NaNO_3$ (red) and after two successive 25% transfers to media with ammonium (blue), each new culture was allowed to remain in stationary phase for three days before the next 25% transfer was made. Single replicates. Dashed lines are the mode for each peak. Cell densities in (A) are 2.2 x 10^5 ml^{-1} ($NaNO_3$) and 3.3 x 10^5 ml^{-1} (ammonium) and (B) are 1.6 x 10^6 ml^{-1} ($NaNO_3$) and 2.2 x 10^6 ml^{-1} (ammonium).

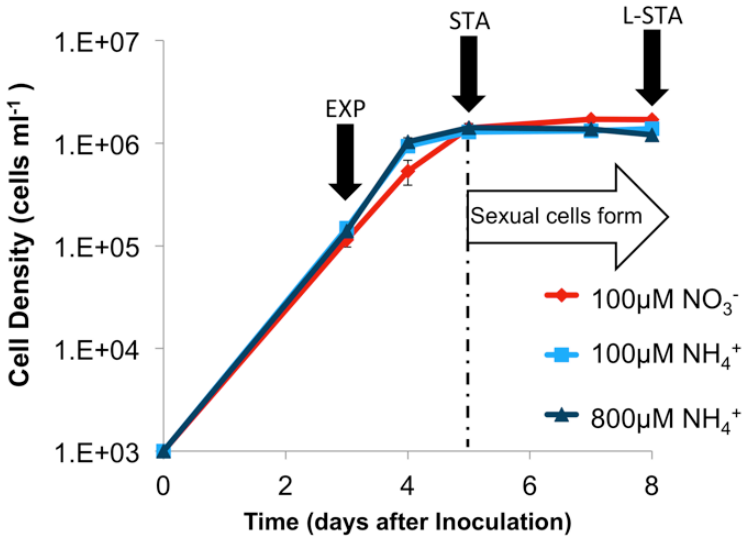

S4 Fig. *T. pseudonana* CCMP1335 growth and collection for RNAseq analysis. Three independent cultures of each nitrogen treatment were harvested 3, 5, and 8 days after inoculation (down arrows) in exponential (EXP), stationary (STA) and late stationary phases (L-STA). The 100uM NH_4^+ STA treatment did not yield sufficient RNA for analysis.

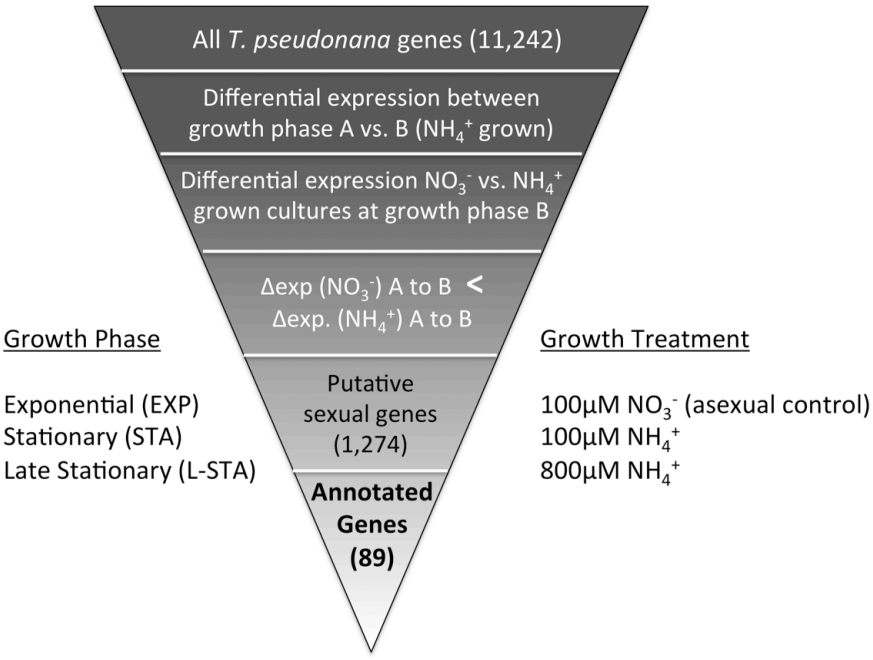

S5 Fig. Interaction analysis workflow of RNAseq data. Growth phase A vs. B is EXP vs. STA, EXP vs. L-STA, or STA vs. L-STA, respectively. Δexp is the magnitude of change in gene expression between growth phases for the different nitrogen treatments.

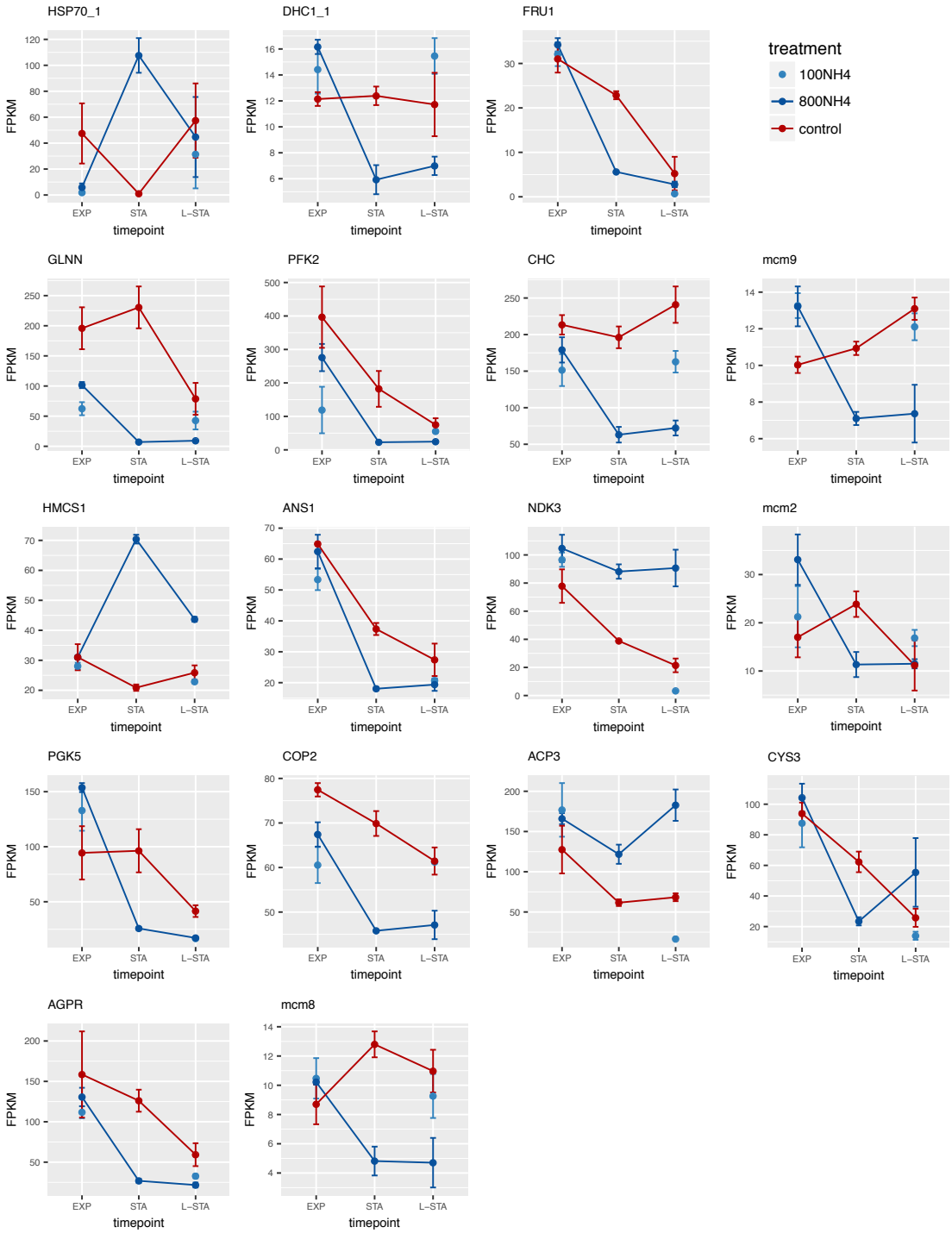

S6 Fig. Expression values (FPKM) of 15 selected genes across the three growth phases for each nitrogen treatment.

References

Ambawat, S., Sharma, P., Yadav, N.R., and Yadav, R.C. (2013) MYB transcription factor genes as regulators for plant responses: an overview. *Physiology and Molecular Biology of Plants* 19: 307-321. doi:10.1007/s12298-013-0179-1

Apt, K.E., Kroth-Pancic, P.G., and Grossman, A. (1996) Stable nuclear transformation of the diatom Phaeodactylum tricornutum. *Molecular and General Genetics* 252: 572-579.

Archibald, J.M. (2009) The puzzle of plastid evolution. *Current Biology* 19: R81-R88.

Armbrust, E.V. (1999) Identification of a new gene family expressed during the onset of sexual reproduction in the centric diatom *Thalassiosira weissflogii*. *Applied and Environmental Microbiology* 65: 3121-3128.

Armbrust, E.V., Chisholm, S.W., and Olson, R.J. (1990) Role of light and the cell cycle on the induction of spermatogenesis in a centric diatom. *Journal of Phycology* 26: 470-478. doi:10.1111/j.0022-3646.1990.00470.x

Armbrust, E.V., Berges, J.A., Bowler, C., Green, B.R., Martinez, D., Putnam, N.H., Zhou, S., Allen, A.E., Apt, K.E., Bechner, M.B., Brzezinski, M.A., Chaal, B.K., Chiovitti, A., Davis, A.K., Demarest, M.S., Detter, J.C., Glavina, T., Goodstein, D., Hadi, M.Z., Hellsten, U., Heildebrand, M., Jenkins, B.D., Jurka, J., Kapitonov, V.V., Kroger, N., Lau, W.W.Y., Lane, T.W., Larimer, F.W., Lippmeier, J.C., Lucas, S., Medina, M., Montsant, A., Obornik, M., Parker, M.S., Palenik, B., Pazour, G.J., Richardson, P.M., Rynearson, T.A., Saito, M.A., Schwartz, D.C., Thamatrakoln, K., Valentin, K., Vardi, A., Wilkerson, F.P., and Rokhsar, D.S. (2004) The genome of the diatom *Thalassiosira pseudonana*: Ecology, evolution, and metabolism. *Science* 306: 79-86.

Assmy, P., Henjes, J., Smetacek, V., and Montresor, M. (2006) Auxospore formation in the silica-sinking oceanic diatom *Fragilariopsis kerguelensis* (Bacillariophyceae). *Journal of Phycology* 42: 1002-1006.

Baker, S.M., Plug, A.W., Prolla, T.A., Bronner, C.E., Harris, A.C., Yao, X., Chreistie, D.M., Monell, C., Arnheim, N., Bradley, A., Ashley, T., and Liskay, R.M. (1996) Involvement of mouse Mlh1 in DNA mismatch repair and meiotic crossing over. *Nature Genetics* 13: 336-342.

Bernstein, H., and Bernstein, C. (2010) Evolutionary origin of recombination during meiosis. *BioScience* 60: 498-505. doi:10.1525/bio.2010.60.7.5

Bowler, C.B., Allen, A.E., Badger, J.H., Grimwood, J., Jabbari, K., Kuo, A., Maheswari, U., Martens, C., Maumus, F., Otillar, R.P., Rayko, E., Salamov, A., and Vanedpoele, K. (2008) The *Phaeodactylum* genome reveals the evolutionary history of diatom genomes. *Nature* 456: 239-244.

Bushnell, B. (2016). BBtools

Butler, G., Rasmussen, M.D., Lin, M.F., Santos, M.A.S., Sakthikumar, S., Munro, C.A., Rheinbay, E., Grabherr, M., Forche, A., Reedy, J.L., Agafioti, I., Arnaud, M.B., Bates, S., Brown, A.J.P., Brunke, S., Costanzo, M.C., Fitzpatrick, D.A., de Groot, P.W.J., Harris, D., Hoyer, L.L., Hube, B., Klis, F.M., Kodira, C., Lennard, N., Logue, M.E., Martin, R., Neiman, A.M., Nikolaou, E., Quail, M.A., Quinn, J., Santos, M.C., Schmitzberger, F.F., Sherlock, G., Shah, P., Silverstein, K.A.T., Skrzypek, M.S., Soll, D., Staggs, R., Stansfield, I., Stumpf, M.P.H., Sudbery,

P.E., Srikantha, T., Zeng, Q., Berman, J., Berriman, M., Heitman, J., Gow, N.A.R., Lorenz, M.C., Birren, B.W., Kellis, M., and Cuomo, C.A. (2009) Evolution of pathogenicity and sexual reproduction in eight *Candida* genomes. *Nature* 459: 657-662. doi:10.1038/nature08064

Chen, G., and Rynearson, T.A. (2016) Genetically distinct populations of a diatom co-exist during the North Atlantic spring bloom. *Limnology and Oceanography* 61: 2165-2179. doi:10.1002/lno.10361

Cheng, H., Song, S., Xiao, L.X., Soo, H.M., cheng, Z., Xie, D., and Peng, J. (2009) Gibberellin acts through jasmonate to control the expression of MYB21, MYB24, and MYB57 to promote stamen filament growth in *Arabidopsis*. *PLOS Genetics* 5doi:10.1371/journal.pgen.1000440

Chepurnov, V.A., Mann, D.G., Sabbe, K., and Vyverman, W. (2004) Experimental studies on sexual reproduction in diatoms. *In A Survey of Cell Biology*. Jeon, K.W. (ed). London, UK: Elsevier Academic Press, pp. 91-154.

Chepurnov, V.A., Chaerle, P., Roef, L., Van Meirhaeghe, A., and Vanhoutte, K. (2011) Classical breeding in diatoms: Scientific background and practical perspectives. In *Diatom Biology*: Springer, pp. 167-194.

Chepurnov, V.A., Mann, D.G., Von Dassow, P., Armbrust, E.V., Sabbe, K., Dasseville, R., and Vyverman, W. (2006) Oogamous reproduction, with two-step auxosporulation, in the centric diatom *Thalassiosira punctigera* (Bacillariophyta). *Journal of Phycology* 42: 845-858. doi:10.1111/j.1529-8817.2006.00244.x

Chepurnov, V.A., Mann, D.G., von Dassow, P., Vanormelingen, P., Gillard, J., Inze, D., Sabbe, K., and Vyverman, W. (2008) In search of new tractable diatoms for experimental biology. *BioEssays* 30: 692-702.

Chevenet, F., Brun, C., Bañuls, A.L., Jacq, B., and Christen, R. (2006) TreeDyn: towards dynamic graphics and annotations for analyses of trees. *BMC Bioinformatics* 7: 439.

Collos, Y., and Harrison, P.J. (2014) Acclimation and toxicity of high ammonium concentrations to unicellular alage. *Marine Pollution Bulletin* 80: 8-23. doi:10.1016/j.marpolbul.2014.01.006

Cooper, K.F., Mallory, J.J., Egeland, D.B., Jarnik, M., and Strich, R. (2000) Ama1p is a meiosis-specific regulator of the anaphase promoting complex/cyclosome in yeast. *Proceedings of the National Academy of Sciences* 97: 14548-14553. doi:10.1073/pnas.250351297

d'Ippolito, G., Sardo, A., Paris, D., Vella, F.M., Adelfi, M.G., Botte, P., Gallo, C., and Fontana, A. (2015) Potential of lipid metabolism in marine diatoms for biofuel production. *Biotechnology for Biofuels* 8: 28-38. doi:10.1186/s13068-015-0212-4

Dereeper, A., Guignon, V., Blanc, G., Audic, S., Buffet, S., Chevenet, F., Dufayard, J.F., Guindon, S., Lefort, V., Lescot, M., Claverie, J.M., and Gascuel, O. (2008) Phylogeny.fr: robust phylogenetic analysis for the non-specialist. *Nucleic Acids Research* 1: W465-W469.

Drebes (1977) Sexuality. In *The Biology of Diatoms.* Werner, D. (ed). Oxford: Blackwell Scientific Publications, pp. 250-283.

Dyhrman, S.T., Jenkins, B.D., Rynearson, T.A., Saito, M.A., Mercier, M.L., Alexander, H., Whitney, L., Drzewianowski, A., Bulygin, V.V., Bertrand, E.M., Wu, Z., Benitez-Nelson, C., and Heithoff, A. (2012) The transcriptome and proteome of

the diatom *Thalassiosira pseudonana* reveal a diverse phosphorus stress response. *PLoS One* 7: e33768. doi:10.1371/journal.pone.0033768

Edgar, R.C. (2004) MUSCLE: a multiple sequence alignment method with reduced time and space complexity. *BMC Bioinformatics* 19: 113.

Edlund, M.B., and Stoermer, E.F. (1991) Sexual reproduction in *Stephanodiscus niagarae* (Bacillariophyta). *Journal of Phycology* 27: 780-793.

Edlund, M.B., and Stoermer, E.F. (1997) Ecological, evolutionary, and systematic significance of diatom life histories. *Journal of Phycology* 33: 897-918.

Ezzati, J., Dolatabadi, N., and de la Guardia, M. (2011) Applications of diatoms and silica nanotechnology in biosensing, drug and gene delivery, and formation of complex metal nanostructures. *Trends in Analytical Chemistry* 30: 1538-1548.

Frazee, A.C., Pertea, G.M., Jaffe, A.E., Langmead, B., Salzberg, S.L., and Leek, J.T. (2015) Ballgown bridges the gap between transcriptome assembly and expression analysis. *Nature Biotechnology* 33: 243-246.

French III, F.W., and Hargraves, P.E. (1985) Spore formation in the life cycles of the diatoms *Chaetoceros diadema* and *Leptocylindrus danicus*. *Journal of Phycology* 21: 477-483.

Gallagher, J.C. (1983) Cell Enlargement in *Skeletonema costatum* (Bacillariophyceae). *Journal of Phycology* 19: 539-542.

Geitler, L. (1932) Der Formwechsel der pennaten Diatomeen. Arch Protistenk 78: 1-226.

Gillard, J., Devos, V., Huysman, M.J.J., De Veylder, L., D'Hondt, S., Martens, C., Vanormelingen, P., Vuylsteke, M., and Vyverman, W. (2008) Physiological and transcriptomic evidence for a close coupling between chloroplast ontogeny and cell cycle progression in the pennate diatom *Seminavis robusta*. *Plant Physiology* 148: 1394-1411. doi:10.1104/pp.108.122176

Godhe, A., Kremp, A., and Montresor, M. (2014) Genetic and microscopic evidence for sexual reproduction in the centric diatom *Skeletonema marinoi. Protist* 165: 401-416. doi:10.1046/j.protis.2014.04.006

Guillard, R.R.L. (1975) Culture of phytoplankton for feeding marine invertebrates. In *Culture of Marine Invertebrate Animals*. Smith, W.L., and Chanley, M.H. (eds). New York: Plenum Press, pp. 26-60.

Hildebrand, D., Smith, S.R., Traller, J.C., and Abbriano, R.M. (2012) The place of diatoms in the biofuels industry. *Biofuels* 3: 221-240.

Hildebrand, M., Frigeri, L.G., and Davis, A.K. (2007) Synchronized growth of *Thalassiosira pseudonana* (Bacillariophyceae) provides novel insights into cell-wall synthesis processes in relation to the cell cycle. *Journal of Phycology* 43: 730-740.

Hildebrand, M., York, E., Kelz, J.I., Davis, A.K., Frigeri, L.G., Allison, D.P., and Doktycz, M.J. (2006) Nanoscale control of silica morphology and three-dimensional structure during diatom cell wall formation. *Journal of Materials Research* 21: 2689-2698.

Holtermann, K.E., Bates, S.S., Trainer, V.L., Odell, A., and Armbrust, E.V. (2010) Mass sexual reproduction in the toxigenic diatoms *Pseudo-Nitzscia australis* and *P. pungens* (Bacillariophyceaea) on the Washington coast, USA. *Journal of Phycology* 46: 41-52. doi:10.1111/j.1529-8817.2009.00792.x

Honda, D., Shono, T., Kimura, K., Fujita, S., Iseki, M., Makino, Y., and Murakami, A.

(2007) Homologs of the sexually induced gene 1 (sig1) product constitute the Stramenopile mastigonemes. *Protist* 158: 77-88.

Hoops, H.J., and Floyd, G.L. (1979) Ultrastructure of the centric diatom, *Cyclotella meneghiniana*: vegetative cell and auxospore development. *Phycologia* 18: 424-435.

Huysman, M.J.J., Vyverman, W., and De Veylder, L. (2014) Molecular regulation of the diatom cell cycle. *Journal of Experimental Botany* 65: 2573-2584.

Idei, M., Osada, K., Sato, S., Toyoda, K., Nagumo, T., and Mann, D.G. (2012) Gametogenesis and auxospore development in *Actinocyclus* (Bacillariophyta). *PLoS One* 7: e41890.

Idei, M., Sato, S., Nagasato, C., Motomura, T., Toyoda, K., Nagumo, T., and Mann, D.G. (2015) Spermatogenesis and auxospore structure in the multipolar centric diatom *Hydrosera*. *Journal of Phycology* 51: 144-158.

Jewson, D.H. (1992) Size reduction, reproductive strategy and the life cycle of a centric diatom. *Philosophical Transactions of the Royal Society B-Biological Sciences* 336: 191-213.

Kaczmarska, I., Poulíčková, A., Sato, S., Edlund, M.B., Idei, M., Watanabe, T., and Mann, D.G. (2013) Proposals for a terminology for diatom sexual reproduction, auxospores and resting stages. *Journal of Diatom Research* 28: 263-294.

Kim, D., Langmead, B., and Salzberg, S.L. (2015) HISAT: a fast spliced aligner with low memory requirements. *Nature Methods* 12: 357-360.

Koester, J.A., Brawley, S.H., Karp-Boss, L., and Mann, D.G. (2008) Sexual reproduction in the marine centric diatom *Ditylum brightwellii* (Bacillariophyta). *European Journal of Phycology* 42: 351-366.

Kroth, P. (2007) Molecular biology and the biotechnological potential of diatoms. *Advances in Experimental Medicine and Biology* 616: 23-33.

Lewis, W.M. (1984) The diatom sex clock and its evolutionary importance. *American Naturalist* 123: 73-80.

Lutzmann, M., Grey, C., Traver, S., Ganier, O., Maya-Mendoza, A., Ranisavljevic, N., Bernex, F., Nishiyama, A., Montel, N., Gavois, E., Forichon, L., de Massy, B., and Méchali, M. (2012) MCM8- and MCM9-deficient mice reveal gametogenesis defects and genome instability due to impaired homologous recombination. *Molecular Cell* 47: 523-534.

Mann, D.G. (1988) Why didn't Lund see sex in *Asterionella*? A discussion of the diatom life cycle in nature. In *Algae and the Aquatic Environment*, contributions in honour of JWG Lund. Round, F.E. (ed). Bristol: Biopress, pp. 384-412.

Mann, D.G. (1999) The species concept in diatoms. *Phycologia* 38: 437-495.

Mazin, A.V., Mazina, O.M., Bugreev, D.V., and Rossi, M.J. (2010) Rad54, the motor of homologous recombination. *DNA Repair* 9: 286-302.

Merchant, S.S., Prochnik, S.E., Vallon, O., Harris, E.H., Karpowicz, S.J., Witman, G.B., Terry, A., Salamov, A., Fritz-Laylin, L.K., Maréchal-Drouard, L., Marshall, W.F., Qu, L.-H., Nelson, D.R., Sanderfoot, A.A., Spalding, M.H., Kapitonov, V.V., Ren, Q., Ferris, P., Lindquist, E., Shapiro, H., Lucas, S.M., Grimwood, J., Schmutz, J., Cardol, P., Cerutti, H., Chanfreau, G., Chen, C.-L., Cognat, V., Croft, M.T., Dent, R., Dutcher, S., Fernández, E., Fukuzawa, H., González-Ballester, D., González-Halphen, D., Hallmann, A., Hanikenne, M., Hippler, M., Inwood, W.,

Jabbari, K., Kalanon, M., Kuras, R., Lefebvre, P.A., Lemaire, S.D., Lobanov, A.V., Lohr, M., Manuell, A., Meier, I., Mets, L., Mittag, M., Mittelmeier, T., Moroney, J.V., Moseley, J., Napoli, C., Nedelcu, A.M., Niyogi, K., Novoselov, S.V., Paulsen, I.T., Pazour, G., Purton, S., Ral, J.-P., Riaño-Pachón, D.M., Riekhof, W., Rymarquis, L., Schroda, M., Stern, D., Umen, J., Willows, R., Wilson, N., Zimmer, S.L., Allmer, J., Balk, J., Bisova, K., Chen, C.-J., Elias, M., Gendler, K., Hauser, C., Lamb, M.R., Ledford, H., Long, J.C., Minagawa, J., Page, M.D., Pan, J., Pootakham, W., Roje, S., Rose, A., Stahlberg, E., Terauchi, A.M., Yang, P., Ball, S., Bowler, C., Dieckmann, C.L., Gladyshev, V.N., Green, P., Jorgensen, R., Mayfield, S., Mueller-Roeber, B., Rajamani, S., Sayre, R.T., Brokstein, P., Dubchak, I., Goodstein, D., Hornick, L., Huang, Y.W., Jhaveri, J., Luo, Y., Martínez, D., Ngau, W.C.A., Otillar, B., Poliakov, A., Porter, A., Szajkowski, L., Werner, G., Zhou, K., Grigoriev, I.V., Rokhsar, D.S., and Grossman, A.R. (2007) The *Chlamydomonas* genome reveals the evolution of key animal and plant functions. *Science* 318: 245-250. doi:10.1126/science.1143609

Mills, K.E., and Kaczmarska, I. (2006) Autogamic reproductive behavior and sex cell structure in *Thalassiosira angulata* (Bacillariophyta). *Botanica Marina* 49: 417-430. doi:10.1515/BOT.2006.053

Moeys, S., Frenkel, J., Lembke, C., Gillard, J.T.F., Devos, V., Van den Berge, K., Bouillon, B., Huysman, M.J.J., De Decker, S., Scharf, J., Bones, A., Brembu, T., Winge, P., Sabbe, K., Vuylsteke, M., Clement, L., De Veylder, L., Pohnert, G., and Vyverman, W. (2016) A sex-inducing pheromone triggers cell cycle arrest and mate attraction in the diatom *Seminavis robusta*. *Scientific Reports* 6: 19252. doi:10.1038/srep19252

Mouget, J.-L., Gastineau, R., Davidovich, O., Gaudin, P., and Davidovich, N.A. (2009) Light is a key factor in triggering sexual reproduction in the pennate diatom *Haslea ostrearia. FEMS Microbiology Ecology* 69: 194-201.

Nagai, S., Hori, Y., Manabe, T., and Imai, I. (1995) Restoration of cell size by vegetative cell enlargement in *Coscinodiscus wailesii* (Bacillariophyceae). *Phycologia* 34: 533-535.

Nelson, D.M., Tréguer, P., Brzezinski, M.A., Leynaert, A., and Quéguiner, B. (1995) Production and dissolution of biogenic silica in the ocean: Revised global estimates, comparison with regional data and relationship to biogenic sedimentation. *Biogeochemical Cycles* 9: 359-372.

Park, J., Long, D.T., Lee, K.Y., Abbas, T., Shibata, E., Negishi, M., Luo, Y., Schimenti, J.C., Gambus, A., Walter, J.C., and Dutta, A. (2013) The MCM8-MCM9 complex promotes RAD51 recruitment at DNA damage sites to facilitate homologous recombination. *Molecular and Cellular Biology* 33: 1632-1644.

Patil, S., Moeys, S., Von Dassow, P., Huysman, M.J.J., Mapleson, D., De Veylder, L., Sanges, R., Vyverman, W., Montresor, M., and Immacolata, M. (2015) Identification of the meitic toolkit in diatoms and exploration of meiosis-specific SPO11 and RAD51 homologs in the sexual species *Pseudo-nitzchia multistriata* and *Seminavis robusta. BMC Genomics* 2015doi:10.1186/s12864-015-1983-5

Pertea, M., Kim, D., Pertea, G.M., Leek, J.T., and Salzberg, S.L. (2016) Transcript-level expression analysis of RNA-seq experiments with HISAT, StringTie and Ballgown. *Nature Protocols* 11: 1650-1667. doi:10.1038/nprot.2016.095

Pertea, M., Pertea, G.M., Antonescu, C.M., Chang, T.C., Mendell, J.T., and Salzberg, S.L. (2015) StringTie enables improved reconstruction of a transcriptome from RNA-seq reads. *Nature Biotechnology* 33: 290-295.

Rosenbaum, J.L., and Witman, G.B. (2002) Intraflagellar transport. *Nature Reviews Molecular Cell Biology* 3: 813-825.

Round, F.E. (1972) The problem of size reduction in diatoms. *Nova Hedwigia* 23: 291-303.

Sabbe, K. (2004) Apomixis in Achnanthes (Bacillariophyceae); development of a model system for diatom reproductive biology. *European Journal of Phycology* 39: 327-341.

Shirokawa, Y., and Shimada, M. (2013) Sex allocation pattern of the diatom *Cyclotella meneghiniana. Proceedings of the Royal Society B: Biological Sciences* 280: 20130503.

Simonsen, R. (1979) The diatom system: Ideas on phylogeny. *Bacillaria* 2: 9-71.

Stamatakis, A. (2006) RAxML-VI-HPC: maximum likelihood-based phylogenetic analyses with thousands of taxa and mixed models. Bioinformatics 22: 2688-2690.

Sterner, R.W., and Elser, J.J. (2002) Ecological stoichiometry: the biology of elements from molecules to the biosphere. Princeton, New Jersey, USA: Princeton University Press.

Tillmann, U. (2004) Interactions between planktonic microalgae and protozoan grazers. *Journal of Eukaryotic Microbiology* 51: 156-168.

Vaulot, D., and Chisholm, S.W. (1987) A simple model for the growth of phytoplankton populations in light/dark cycles. *Journal of Plankton Research* 9: 345-366.

Von Dassow, P., and Montresor, M. (2011) Unveiling the mysteries of phytoplankton life cycles: patterns and opportunities behind complexity. *Journal of Plankton Research* 33: 3-12.

Yoshiyama, K., and Sharp, J.H. (2006) Phytoplankton response to nutrient enrichment in an urbanized estuary: Apparent inhibition of primary production by overeutrophication. *Limnology and Oceanography* 51: 424-434.

Zachariae, W., Shevchenko, A., Andrews, P.D., Ciosk, R., Galova, M., Stark, M.J.R., Mann, M., and Nasmyth, K. (1998) Mass spectrometric analysis of the anaphase-promoting complex from yeast: Identificaiton of a subunit related to cullins. *Science* 279: 1216-1219.

Conclusion

The marine chemical environment has a substantial influence on microbial physiology and behavior. The studies reported here examined how the production and metabolism of chemicals in the marine environment can trigger changes in the physiology and life cycle of two important groups of marine plankton. Photoautotrophs, like the diatom *Thalassiosira pseudonana*, devote a significant portion of primary production to produce volatile organic compounds that serve as intermediates in biochemical pathways, metabolic waste of overflow, and chemical signals. Significant release of VOCs into the environment through passive diffusion supplies a pool of volatile public goods that are an important source of carbon and energy for heterotrophic bacteria. VOC production could promote growth of particular bacteria or archaea that can metabolize these ubiquitous chemicals, leading to changes in microbial communities and the interactions that occur. *Pelagibacter*, the most abundant bacteria in the ocean, is able to metabolize a wide variety of volatile organic compounds. VOC metabolism by heterotrophs like *Pelagibacter* taxes primary production by stimulating efflux of VOCs from phytoplankton that rely on VOCs as intermediates in metabolism. This effect has major implications for carbon cycling and is important in controlling the emission of phytoplankton produced VOCs to the atmosphere, where VOCs have important roles in atmospheric chemistry. However, the microorganisms and biochemistry involved in the heterotrophic metabolism of VOCs has barely been studied.

The discovery that *Pelagibacter* is capable of metabolizing a wide variety of VOCs prompted questions about the impact *Pelagibacter* has on ocean-atmospheric fluxes of acetone and isoprene, two VOCs that have significant impacts on atmospheric

processes, and how cells were utilizing these compounds. The *Pelagibacter* genome encodes an acetone monooxygenase that facilitates acetone metabolism, allowing the cell to oxidize and grow on acetone. This gene was also found in other important marine taxa, and its distribution in the environment may help explain trends of acetone flux in the ocean. Additionally, *Pelagibacter* was able to directly utilize isoprene to meet isoprenoid demands, a process that has the potential to occur in other cells. These findings show that *Pelagibacter*, and possibly other marine bacteria, are a major factor in controlling acetone and isoprene emissions from the ocean.

Future studies that clarify the significance of biological VOC sources and sinks are needed to understand the greater significance of VOCs in biological systems, the carbon cycle, and climate. More specifically, understanding how VOC production rates vary across many species and under a variety of growth conditions will lead to improved estimates of the gross biological production of these compounds in the ocean and the significance of VOCs as a conduit of carbon and energy in the microbial carbon cycle. Further, the field would be benefitted by studies that identify taxa and biochemistries involved in VOC metabolism, and quantifying VOC uptake by heterotrophic bacteria, measurements that will provide clarity on the scale of proposed biological VOC sinks. Information gathered from studies on biological VOC sources and sinks that are combined with broad scale measurements or predictions of microbial community composition and metabolic potential will facilitate improvements in VOC flux models by more accurately summarizing the large scale contributions of living organisms to VOC emissions in marine environments. Additionally, a greater understanding of how abiotic

factors modify phytoplankton physiology are needed to improve predictions of phytoplankton impacts on chemical cycles at a global scale.

A variety of factors, including nutrient and light availability, growth stage, and stressors, such as oxidative stress or grazing, induce changes in phytoplankton physiology that also lead to changes in VOC production. Physiological responses to chemical triggers that are controlled by other microbes are important adaptations that allow phytoplankton to survive challenges posed by their environment or life strategy. In diatoms, stress induced by excess ammonium was an important factor that controlled the induction of the essential sexual reproductive phase of the life cycle that facilitates survival of cell lineages and introduces genetic diversity in populations. While the chemical status of an environment may control physiology, changes in physiology can also control the chemical environment, establishing a highly complex, cyclic feedback of interactions amongst the microbial community, where any one perturbation can cause a cascade of effects. The studies presented here begin to unravel the complexities of chemically mediated interactions between marine plankton, and they also show that chemically-driven interactions can have major influences over global biogeochemical processes.

Bibliography

Acharya, A. and Desai, A.J. (1999) Acetonitrile-hydrolysing enzymes in Rhodococcus erythropolis A10. World J Microbiol Biotechnol 15: 111–113.

Alvarez, L.A., Exton, D.A., Timmis, K.N., Suggett, D.J., and McGenity, T.J. (2009) Characterization of marine isoprene-degrading communities. Environ Microbiol 11: 3280–3291.

Ambawat, S., Sharma, P., Yadav, N.R., and Yadav, R.C. (2013) MYB transcription factor genes as regulators for plant responses: an overview. Physiology and Molecular Biology of Plants 19: 307-321. doi:10.1007/s12298-013-0179-1

Amin, S.A., Hmelo, L.R., van Tol, H.M., Durham, B.P., Carlson, L.T., Heal, K.R., et al. (2015) Interaction and signalling between a cosmopolitan phytoplankton and associated bacteria. Nature 522: 98–101.

Amin, S.A., Parker, M.S., and Armbrust, E. V. (2012) Interactions between Diatoms and Bacteria. Microbiol Mol Biol Rev 76: 667–684.

Anbar, A.D., Yung, Y.L., and Chavez, F.P. (1996) Methyl bromide: Ocean sources, ocean sinks, and climate sensitivity. Global Biogeochem Cycles 10: 175–190.

Andreae, M.O. and Crutzen, P.J. (1997) Atmospheric aerosols: Biogeochemical sources and role in atmospheric chemistry. Science (80-) 276: 1052–1058.

Apt, K.E., Kroth-Pancic, P.G., and Grossman, A. (1996) Stable nuclear transformation of the diatom Phaeodactylum tricornutum. Molecular and General Genetics 252: 572-579.

Arandia-Gorostidi, N., Weber, P.K., Alonso-Sáez, L., Anxelu, X., Morán, G., and Mayali, X. (2017) Elevated temperature increases carbon and nitrogen fluxes between phytoplankton and heterotrophic bacteria through physical attachment. ISME J 11: 641–650.

Archibald, J.M. (2009) The puzzle of plastid evolution. Current Biology 19: R81-R88.

Armbrust, E.V. (1999) Identification of a new gene family expressed during the onset of sexual reproduction in the centric diatom Thalassiosira weissflogii. Applied and Environmental Microbiology 65: 3121-3128.

Armbrust, E.V., Berges, J.A., Bowler, C., Green, B.R., Martinez, D., Putnam, N.H., Zhou, S., Allen, A.E., Apt, K.E., Bechner, M.B., Brzezinski, M.A., Chaal, B.K., Chiovitti, A., Davis, A.K., Demarest, M.S., Detter, J.C., Glavina, T., Goodstein, D., Hadi, M.Z., Hellsten, U., Heildebrand, M., Jenkins, B.D., Jurka, J., Kapitonov, V.V., Kroger, N., Lau, W.W.Y., Lane, T.W., Larimer, F.W., Lippmeier, J.C., Lucas, S., Medina, M., Montsant, A., Obornik, M., Parker, M.S., Palenik, B., Pazour, G.J., Richardson, P.M., Rynearson, T.A., Saito, M.A., Schwartz, D.C., Thamatrakoln, K., Valentin, K., Vardi, A., Wilkerson, F.P., and Rokhsar, D.S. (2004) The genome of the diatom Thalassiosira pseudonana: Ecology, evolution, and metabolism. Science 306: 79-86.

Armbrust, E.V., Chisholm, S.W., and Olson, R.J. (1990) Role of light and the cell cycle on the induction of spermatogenesis in a centric diatom. Journal of Phycology 26: 470-478. doi:10.1111/j.0022-3646.1990.00470.x

Arnold, S.R., Spracklen, D. V, Williams, J., Yassaa, N., Sciare, J., Bonsang, B., et al. (2009) Evaluation of the global oceanic isoprene source and its impacts on marine organic carbon aerosol. Atmos Chem Phys 9: 1253–1262.

Assmy, P., Henjes, J., Smetacek, V., and Montresor, M. (2006) Auxospore formation in the silica-sinking oceanic diatom Fragilariopsis kerguelensis (Bacillariophyceae). Journal of Phycology 42: 1002-1006.

Audrain, B., Farag, M.A., Ryu, C.-M., and Ghigo, J.-M. (2015) Role of bacterial volatile compounds in bacterial biology. FEMS Microbiol Rev 39: 222–233.

Azam, F. and Malfatti, F. (2007) Microbial structuring of marine ecosystems. Nat Rev Microbiol 5: 782–791.

Baker, S.M., Plug, A.W., Prolla, T.A., Bronner, C.E., Harris, A.C., Yao, X., Chreistie, D.M., Monell, C., Arnheim, N., Bradley, A., Ashley, T., and Liskay, R.M. (1996) Involvement of mouse Mlh1 in DNA mismatch repair and meiotic crossing over. Nature Genetics 13: 336-342.

Bange, H.W. and Williams, J. (2000) New Directions: Acetonitrile in atmospheric and biogeochemical cycles. Atmos Environ 34: 4959–4960.

Barofsky, A., Vidoudez, C., and Pohnert, G. (2009) Metabolic profiling reveals growth stage variability in diatom exudates. Limnol Oceanogr Methods 7: 382–390.

Beale, R., Dixon, J.L., Arnold, S.R., Liss, P.S., and Nightingale, P.D. (2013) Methanol, acetaldehyde, and acetone in the surface waters of the Atlantic Ocean. J Geophys Res Ocean 118: 5412–5425.

Beale, R., Dixon, J.L., Smyth, T.J., and Nightingale, P.D. (2015) Annual study of oxygenated volatile organic compounds in UK shelf waters. Mar Chem 171: 96–106.

Becker, J.W., Hogle, S.L., Rosendo, K., and Chisholm, S.W. (2019) Co-culture and biogeography of Prochlorococcus and SAR11. ISME J.

Behrenfeld, M.J. and Falkowski, P.G. (1997) Photosynthetic rates derived from satellite-based chlorophyll concentration. Limnol Oceanogr 42: 1–20.

Bernstein, H., and Bernstein, C. (2010) Evolutionary origin of recombination during meiosis. BioScience 60: 498-505. doi:10.1525/bio.2010.60.7.5

Bidigare, R.R., Van Heukelem, L., and Trees, C.. (2005) Analysis of algal pigments by high performance liquid chromatography. In, Andersen,R. (ed), Algal Culturing Techniques. Academic Press, pp. 327–345.

Biller, S.J., Coe, A., and Chisholm, S.W. (2016) Torn apart and reunited: Impact of a heterotroph on the transcriptome of Prochlorococcus. ISME J 10: 2831–2843.

Bisutti, I., Hilke, I., and Raessler, M. (2004) Determination of total organic carbon – an overview of current methods. TrAC Trends Anal Chem 23: 716–726.

Bitas, V., Kim, H.-S., Bennett, J.W., and Kang, S. (2013) Sniffing on Microbes: Diverse Roles of Microbial Volatile Organic Compounds in Plant Health. / 835 MPMI 26:.

Bjørrisen, P.K. (1988) Phytoplankton exudation of organic matter: Why do healthy cells do it? Limnol Oceanogr 33: 151–154.

Bonsang, B., Gros, V., Peeken, I., Yassaa, N., Bluhm, K., Zoellner, E., et al. (2010) Isoprene emission from phytoplankton monocultures: The relationship with chlorophyll-a, cell volume and carbon content. Environ Chem 7: 554–563.

Booge, D., Schlundt, C., Bracher, A., Endres, S., and Zäncker, B. (2017) Marine isoprene production and consumption in the mixed layer of the surface ocean – A field study over 2 oceanic regions. Biogeosciences Discuss 1–28.

Bowler, C.B., Allen, A.E., Badger, J.H., Grimwood, J., Jabbari, K., Kuo, A., Maheswari, U., Martens, C., Maumus, F., Otillar, R.P., Rayko, E., Salamov, A., and Vanedpoele, K. (2008) The Phaeodactylum genome reveals the evolutionary history of diatom genomes. Nature 456: 239-244.

Boyd, P.W., Strzepek, R., Chiswell, S., Chang, H., DeBruyn, J.M., Ellwood, M., et al. (2012) Microbial control of diatom bloom dynamics in the open ocean. Geophys Res Lett 39: 2–7.

Bromke, M.A., Giavalisco, P., Willmitzer, L., and Hesse, H. (2013) Metabolic Analysis of Adaptation to Short-Term Changes in Culture Conditions of the Marine Diatom Thalassiosira pseudonana. PLoS One 8: e67340.

Brooks, S.D. and Thornton, D.C.O. (2018) Marine Aerosols and Clouds. Ann Rev Mar Sci 10: 289–313.

Bucciarelli, E. and Sunda, W.G. (2003) Influence of CO2, nitrate, phosphate, and silicate limitation on intracellular dimethylsulfoniopropionate in batch cultures of the coastal diatom Thalassiosira pseudonana. Limnol Oceanogr 48: 2256–2265.

Buchan, A., LeCleir, G.R., Gulvik, C.A., and González, J.M. (2014) Master recyclers: features and functions of bacteria associated with phytoplankton blooms. Nat Rev Microbiol 12: 686–698.

Bushnell, B. (2016). BBtools

Butler, G., Rasmussen, M.D., Lin, M.F., Santos, M.A.S., Sakthikumar, S., Munro, C.A., Rheinbay, E., Grabherr, M., Forche, A., Reedy, J.L., Agafioti, I., Arnaud, M.B., Bates, S., Brown, A.J.P., Brunke, S., Costanzo, M.C., Fitzpatrick, D.A., de Groot, P.W.J., Harris, D., Hoyer, L.L., Hube, B., Klis, F.M., Kodira, C., Lennard, N., Logue, M.E., Martin, R., Neiman, A.M., Nikolaou, E., Quail, M.A., Quinn, J., Santos, M.C., Schmitzberger, F.F., Sherlock, G., Shah, P., Silverstein, K.A.T., Skrzypek, M.S., Soll, D., Staggs, R., Stansfield, I., Stumpf, M.P.H., Sudbery, P.E., Srikantha, T., Zeng, Q., Berman, J., Berriman, M., Heitman, J., Gow, N.A.R., Lorenz, M.C., Birren, B.W., Kellis, M., and Cuomo, C.A. (2009) Evolution of pathogenicity and sexual reproduction in eight Candida genomes. Nature 459: 657-662. doi:10.1038/nature08064

Carini, P., Campbell, E.O., Morré, J., Sañudo-Wilhelmy, S. a, Thrash, J.C., Bennett, S.E., et al. (2014) Discovery of a SAR11 growth requirement for thiamin's pyrimidine precursor and its distribution in the Sargasso Sea. ISME J 8: 1727–38.

Carini, P., Steindler, L., Beszteri, S., and Giovannoni, S.J. (2012) Nutrient requirements for growth of the extreme oligotroph 'Candidatus Pelagibacter ubique' HTCC1062 on a defined medium. ISME J 7: 592–602.

Chen, G., and Rynearson, T.A. (2016) Genetically distinct populations of a diatom co-exist during the North Atlantic spring bloom. Limnology and Oceanography 61: 2165-2179. doi:10.1002/lno.10361

Cheng, H., Song, S., Xiao, L.X., Soo, H.M., cheng, Z., Xie, D., and Peng, J. (2009) Gibberellin acts through jasmonate to control the expression of MYB21, MYB24, and MYB57 to promote stamen filament growth in Arabidopsis. PLOS Genetics 5doi:10.1371/journal.pgen.1000440

Chepurnov, V.A., Chaerle, P., Roef, L., Van Meirhaeghe, A., and Vanhoutte, K. (2011) Classical breeding in diatoms: Scientific background and practical perspectives. In Diatom Biology: Springer, pp. 167-194.

Chepurnov, V.A., Mann, D.G., Sabbe, K., and Vyverman, W. (2004) Experimental studies on sexual reproduction in diatoms. In A Survey of Cell Biology. Jeon, K.W. (ed). London, UK: Elsevier Academic Press, pp. 91-154.

Chepurnov, V.A., Mann, D.G., Von Dassow, P., Armbrust, E.V., Sabbe, K., Dasseville, R., and Vyverman, W. (2006) Oogamous reproduction, with two-step auxosporulation, in the centric diatom Thalassiosira punctigera (Bacillariophyta). Journal of Phycology 42: 845-858. doi:10.1111/j.1529-8817.2006.00244.x

Chepurnov, V.A., Mann, D.G., von Dassow, P., Vanormelingen, P., Gillard, J., Inze, D., Sabbe, K., and Vyverman, W. (2008) In search of new tractable diatoms for experimental biology. BioEssays 30: 692-702.

Chevenet, F., Brun, C., Bañuls, A.L., Jacq, B., and Christen, R. (2006) TreeDyn: towards dynamic graphics and annotations for analyses of trees. BMC Bioinformatics 7: 439.

Collos, Y., and Harrison, P.J. (2014) Acclimation and toxicity of high ammonium concentrations to unicellular alage. Marine Pollution Bulletin 80: 8-23. doi:10.1016/j.marpolbul.2014.01.006

Colomb, A., Yassaa, N., Williams, J., Peeken, I., and Lochte, K. (2008a) Screening volatile organic compounds (VOCs) emissions from five marine phytoplankton species by head space gas chromatography/mass spectrometry (HS-GC/MS). J Environ Monit 10: 325–330.

Cooper, K.F., Mallory, J.J., Egeland, D.B., Jarnik, M., and Strich, R. (2000) Ama1p is a meiosis-specific regulator of the anaphase promoting complex/cyclosome in yeast. Proceedings of the National Academy of Sciences 97: 14548-14553. doi:10.1073/pnas.250351297

Cotsaris, E., Bruchet, A., Mallevialle, J., and Bursill, D.B. (1995) The identification of odorous metabolites produced from algal monocultures. Water Sci Technol 31: 251–258.

Cullen, J.J. (1990) On models of growth and photosynthesis in phytoplankton. Deep Sea Res Part A Oceanogr Res Pap 37: 667–683.

d'Ippolito, G., Sardo, A., Paris, D., Vella, F.M., Adelfi, M.G., Botte, P., Gallo, C., and Fontana, A. (2015) Potential of lipid metabolism in marine diatoms for biofuel production. Biotechnology for Biofuels 8: 28-38. doi:10.1186/s13068-015-0212-4

Dachs, J., Calleja, M.L., Duarte, C.M., del Vento, S., Turpin, B., Polidori, A., et al. (2005) High atmosphere-ocean exchange of organic carbon in the NE subtropical Atlantic. Geophys Res Lett 32: L21807.

Dani, K.G.S. and Loreto, F. (2017) Trade-Off Between Dimethyl Sulfide and Isoprene Emissions from Marine Phytoplankton. Trends Plant Sci 22: 361–372.

de Gouw, J.A. (2003) Emission sources and ocean uptake of acetonitrile (CH 3 CN) in the atmosphere. J Geophys Res 108: 4329.

Dereeper, A., Guignon, V., Blanc, G., Audic, S., Buffet, S., Chevenet, F., Dufayard, J.F., Guindon, S., Lefort, V., Lescot, M., Claverie, J.M., and Gascuel, O. (2008) Phylogeny.fr: robust phylogenetic analysis for the non-specialist. Nucleic Acids Research 1: W465-W469.

Dixon, J.L., Beale, R., and Nightingale, P.D. (2013) Production of methanol, acetaldehyde, and acetone in the Atlantic Ocean. Geophys Res Lett 40: 4700–4705.

Dixon, J.L., Beale, R., Sargeant, S.L., Tarran, G.A., and Nightingale, P.D. (2014) Microbial acetone oxidation in coastal seawater. Front Microbiol 5: 1–9.

Donoghue, N.A. and Trudgill, P.W. (1975) The Metabolism of Cyclohexanol by Acinetobacter NCIB 9871. Eur J Biochem 60: 1–7.

Drebes (1977) Sexuality. In The Biology of Diatoms. Werner, D. (ed). Oxford: Blackwell Scientific Publications, pp. 250-283.

Dress, A.W., Flamm, C., Fritzsch, G., Grünewald, S., Kruspe, M., Prohaska, S.J., and Stadler, P.F. (2008) Noisy: Identification of problematic columns in multiple sequence alignments. Algorithms Mol Biol 3: 7.

Durham, B.P., Boysen, A.K., Carlson, L.T., Groussman, R.D., Heal, K.R., Cain, K.R., et al. (2019) Sulfonate-based networks between eukaryotic phytoplankton and heterotrophic bacteria in the surface ocean. Nat Microbiol 1.

Durham, B. P., Sharma, S., Luo, H., Smith, C.B., Amin, S.A., Bender, S.J., et al. (2015) Cryptic carbon and sulfur cycling between surface ocean plankton. PNAS 112: 453–457.

Dyhrman, S.T., Jenkins, B.D., Rynearson, T.A., Saito, M.A., Mercier, M.L., Alexander, H., Whitney, L., Drzewianowski, A., Bulygin, V.V., Bertrand, E.M., Wu, Z., Benitez-Nelson, C., and Heithoff, A. (2012) The transcriptome and proteome of the diatom Thalassiosira pseudonana reveal a diverse phosphorus stress response. PLoS One 7: e33768. doi:10.1371/journal.pone.0033768

Edgar, R.C. (2004) MUSCLE: a multiple sequence alignment method with reduced time and space complexity. BMC Bioinformatics 19: 113.

Edlund, M.B., and Stoermer, E.F. (1991) Sexual reproduction in Stephanodiscus niagarae (Bacillariophyta). Journal of Phycology 27: 780-793.

Edlund, M.B., and Stoermer, E.F. (1997) Ecological, evolutionary, and systematic significance of diatom life histories. Journal of Phycology 33: 897-918.

El Khawand, M., Crombie, A.T., Johnston, A., Vavlline, D. V., McAuliffe, J.C., Latone, J.A., et al. (2016) Isolation of isoprene degrading bacteria from soils, development of isoA gene probes and identification of the active isoprene-degrading soil community using DNA-stable isotope probing. Environ Microbiol 18: 2743–2753.

Exton, D.A., Suggett, D.J., McGenity, T.J., and Steinke, M. (2013) Chlorophyll-normalized isoprene production in laboratory cultures of marine microalgae and implications for global models. Limnol Oceanogr 58: 1301–1311.

Ezzati, J., Dolatabadi, N., and de la Guardia, M. (2011) Applications of diatoms and silica nanotechnology in biosensing, drug and gene delivery, and formation of complex metal nanostructures. Trends in Analytical Chemistry 30: 1538-1548.

Facchini, M.C., Rinaldi, M., Decesari, S., Carbone, C., Finessi, E., Mircea, M., et al. (2008) Primary submicron marine aerosol dominated by insoluble organic colloids and aggregates. Geophys Res Lett 35:.

Falkowski, P.G., Fenchel, T., and Delong, E.F. (2008) The microbial engines that drive earth's biogeochemical cycles. Science (80-) 320: 1034–1039.

Fall, R. and Copley, S.D. (2000) Bacterial sources and sinks of isoprene, a reactive atmospheric hydrocarbon. Environ Microbiol 2: 123–130.

Fink, P. (2007) Ecological functions of volatile organic compounds in aquatic systems. Mar Freshw Behav Physiol 40: 155–168.

Fischer, E. V., Jacob, D.J., Millet, D.B., Yantosca, R.M., and Mao, J. (2012) The role of the ocean in the global atmospheric budget of acetone. Geophys Res Lett 39:.

Fisher, N.L. and Halsey, K.H. (2016) Mechanisms that increase the growth efficiency of diatoms in low light. Photosynth Res 129: 183–197.

Folkins, I. and Chatfield, R. (2000) Impact of acetone on ozone production and OH in the upper troposphere at high NOx. J Geophys Res Atmos 105: 11585–11599.

Fouilland, E., Tolosa, I., Bonnet, D., Bouvier, C., Bouvier, T., Bouvy, M., et al. (2014) Bacterial carbon dependence on freshly produced phytoplankton exudates under different nutrient availability and grazing pressure conditions in coastal marine waters. FEMS Microbiol Ecol 87: 757–769.

Frazee, A.C., Pertea, G.M., Jaffe, A.E., Langmead, B., Salzberg, S.L., and Leek, J.T. (2015) Ballgown bridges the gap between transcriptome assembly and expression analysis. Nature Biotechnology 33: 243-246.

French III, F.W., and Hargraves, P.E. (1985) Spore formation in the life cycles of the diatoms Chaetoceros diadema and Leptocylindrus danicus. Journal of Phycology 21: 477-483.

Friedrich, R. and Obermeier, A. (1999) Anthropogenic Emissions of Volatile Organic Compounds. In, Reactive Hydrocarbons in the Atmosphere. Elsevier, pp. 1–39.

Fuhrman, J.A., Cram, J.A., and Needham, D.M. (2015) Marine microbial community dynamics and their ecological interpretation. Nat Publ Gr 13: 133–146.

Gallagher, J.C. (1983) Cell Enlargement in Skeletonema costatum (Bacillariophyceae). Journal of Phycology 19: 539-542.

Geitler, L. (1932) Der Formwechsel der pennaten Diatomeen. Arch Protistenk 78: 1-226.

Gillard, J., Devos, V., Huysman, M.J.J., De Veylder, L., D'Hondt, S., Martens, C., Vanormelingen, P., Vuylsteke, M., and Vyverman, W. (2008) Physiological and transcriptomic evidence for a close coupling between chloroplast ontogeny and cell cycle progression in the pennate diatom Seminavis robusta. Plant Physiology 148: 1394-1411. doi:10.1104/pp.108.122176

Giovannoni, S., Bibbs, L., Cho, J.C., Stapels, M., Desiderio, R., Vergin, K., et al. (2005) Proteorhodopsin in the ubiquitous marine bacterium SAR11. Nature 438: 82–85.

Giovannoni, S., Tripp, J., Givan, S., Podar, M., Vergin, K., Baptista, D., et al. (2005) Genome streamlining in a cosmopolitan oceanic bacterium. Science 309: 1242–1245.

Giovannoni, S.J. (2017) SAR11 Bacteria: The Most Abundant Plankton in the Oceans. Ann Rev Mar Sci 9: 231–255.

Giovannoni, S.J., Halsey, K.H., Saw, J., Muslin, O., Suffridge, C.P., Sun, J., et al. (2019) A Parasitic Arsenic Cycle That Shuttles Energy from Phytoplankton to Heterotrophic Bacterioplankton. MBio 10:.

Giovannoni, S.J., Tripp, H.J., Givan, S., Podar, M., Vergin, K.L., Baptista, D., et al. (2005) Genome streamlining in a cosmopolitan oceanic bacterium. Science 309: 1242–1245.

Godhe, A., Kremp, A., and Montresor, M. (2014) Genetic and microscopic evidence for sexual reproduction in the centric diatom Skeletonema marinoi. Protist 165: 401-416. doi:10.1046/j.protis.2014.04.006

Goecke, F., Thiel, V., Wiese, J., Labes, A., and Imhoff, J.F. (2013) Algae as an important environment for bacteria - phylogenetic relationships among new bacterial species isolated from algae. Phycologia 52: 14–24.

González, J.M. and Moran, M.A. (1997) Numerical dominance of a group of marine bacteria in the α-subclass of the class Proteobacteria in coastal seawater. Appl Environ Microbiol 63: 4237–4242.

Grossart, H.P., Levold, F., Allgaier, M., Simon, M., and Brinkhoff, T. (2005) Marine diatom species harbour distinct bacterial communities. Environ Microbiol 7: 860–873.

Guenther, A., Nicholas, C., Fall, R., Klinger, L., Mckay, W.A., and Scholes, B. (1995) A global model of natural volatile organic compound emissions. J Geophys Res 100: 8873–8892.

Guenther, A.B., Jiang, X., Heald, C.L., Sakulyanontvittaya, T., Duhl, T., Emmons, L.K., and Wang, X. (2012) The model of emissions of gases and aerosols from nature version 2.1 (MEGAN2.1): An extended and updated framework for modeling biogenic emissions. Geosci Model Dev 5: 1471–1492.

Guillard, R.R.L. (1975) Culture of phytoplankton for feeding marine invertebrates. In Culture of Marine Invertebrate Animals. Smith, W.L., and Chanley, M.H. (eds). New York: Plenum Press, pp. 26-60.

Guillard, R.R.L. and Ryther, J.H. (1962) Studies of marine planktonic diatoms. I. Cyclotella nana Hustedt and Detonula confervacea Cleve. Can J Microbiol 8: 229–239.

Guindon, S., Dufayard, J.-F., Lefort, V., Anisimova, M., Hordijk, W., and Gascuel, O. (2010) New Algorithms and Methods to Estimate Maximum-Likelihood Phylogenies: Assessing the Performance of PhyML 3.0. Syst Biol 59: 307–321.

Hackenberg, S.C., Andrews, S.J., Airs, R., Arnold, S.R., Bouman, H.A., Brewin, R.J.W., et al. (2017) Potential controls of isoprene in the surface ocean. Global Biogeochem Cycles 31: 644–662.

Halsey, K.H. and Jones, B.M. (2015) Phytoplankton strategies for photosynthetic energy allocation. Annu Rev Mar Sci 7: 265–297.

Halsey, K.H., Carter, A.E., and Giovannoni, S.J. (2012) Synergistic metabolism of a broad range of C1 compounds in the marine methylotrophic bacterium HTCC2181. Environ Microbiol 14: 630–640.

Halsey, K.H., Giovannoni, S.J., Graus, M., Zhao, Y., Landry, Z., Thrash, J.C., et al. (2017) Biological cycling of volatile organic carbon by phytoplankton and bacterioplankton. Limnol Oceanogr.

Hartmans, S. and de Bont, J.A.M. (1986) Acetol monooxygenase from Mycobacterium Py1 cleaves acetol into acetate and formaldehyde. FEMS Microbiol 36: 155–158.

Hauser, E.J., Dickhut, R.M., Falconer, R., and Wozniak, A.S. (2013) Improved method for quantifying the air-sea flux of volatile and semi-volatile organic carbon. Limnol Oceanogr Methods 11: 287–297.

Hausinger, R.P. (2007) New Insights into Acetone Metabolism. J Bacteriol 189: 671–673.

Hense, I., Stemmler, I., and Sonntag, S. (2017) Ideas and perspectives: Climate-relevant marine biologically driven mechanisms in Earth system models. Biogeosciences 14: 403–413.

Hildebrand, D., Smith, S.R., Traller, J.C., and Abbriano, R.M. (2012) The place of diatoms in the biofuels industry. Biofuels 3: 221-240.

Hildebrand, M., Frigeri, L.G., and Davis, A.K. (2007) Synchronized growth of Thalassiosira pseudonana (Bacillariophyceae) provides novel insights into cell-wall synthesis processes in relation to the cell cycle. Journal of Phycology 43: 730-740.

Hildebrand, M., York, E., Kelz, J.I., Davis, A.K., Frigeri, L.G., Allison, D.P., and Doktycz, M.J. (2006) Nanoscale control of silica morphology and three-dimensional structure during diatom cell wall formation. Journal of Materials Research 21: 2689-2698.

Holtermann, K.E., Bates, S.S., Trainer, V.L., Odell, A., and Armbrust, E.V. (2010) Mass sexual reproduction in the toxigenic diatoms Pseudo-Nitzscia australis and P. pungens (Bacillariophyceaea) on the Washington coast, USA. Journal of Phycology 46: 41-52. doi:10.1111/j.1529-8817.2009.00792.x

Honda, D., Shono, T., Kimura, K., Fujita, S., Iseki, M., Makino, Y., and Murakami, A. (2007) Homologs of the sexually induced gene 1 (sig1) product constitute the Stramenopile mastigonemes. Protist 158: 77-88.

Hoops, H.J., and Floyd, G.L. (1979) Ultrastructure of the centric diatom, Cyclotella meneghiniana: vegetative cell and auxospore development. Phycologia 18: 424-435.

Huysman, M.J.J., Vyverman, W., and De Veylder, L. (2014) Molecular regulation of the diatom cell cycle. Journal of Experimental Botany 65: 2573-2584.

Idei, M., Osada, K., Sato, S., Toyoda, K., Nagumo, T., and Mann, D.G. (2012) Gametogenesis and auxospore development in Actinocyclus (Bacillariophyta). PLoS One 7: e41890.

Idei, M., Sato, S., Nagasato, C., Motomura, T., Toyoda, K., Nagumo, T., and Mann, D.G. (2015) Spermatogenesis and auxospore structure in the multipolar centric diatom Hydrosera. Journal of Phycology 51: 144-158.

Jewson, D.H. (1992) Size reduction, reproductive strategy and the life cycle of a centric diatom. Philosophical Transactions of the Royal Society B-Biological Sciences 336: 191-213.

Johnston, A., Crombie, A.T., El Khawand, M., Sims, L., Whited, G.M., McGenity, T.J., and Colin Murrell, J. (2017) Identification and characterisation of isoprene-degrading bacteria in an estuarine environment. Environ Microbiol 19: 3526–3537.

Jüttner, F. (1984) Dynamics of the volatile organic substances associated with cyanobacteria and algae in a eutrophic shallow lake. Appl Environ Microbiol 47: 814–820.

Jüttner, F., Messina, P., Patalano, C., and Zupo, V. (2010) Odour compounds of the diatom Cocconeis scutellum: Effects on benthic herbivores living on Posidonia oceanic. Mar Ecol Prog Ser 400: 63–73.

Kaczmarska, I., Poulíčková, A., Sato, S., Edlund, M.B., Idei, M., Watanabe, T., and Mann, D.G. (2013) Proposals for a terminology for diatom sexual reproduction, auxospores and resting stages. Journal of Diatom Research 28: 263-294.

Katoh, K. and Standley, D.M. (2013) MAFFT Multiple Sequence Alignment Software Version 7: Improvements in Performance and Usability. Mol Biol Evol 30: 772–780.

Keller, M.D. (1989) Dimethyl Sulfide Production and Marine Phytoplankton: The Importance of Species Composition and Cell Size. Biol Oceanogr 6: 375–382.

Kesselmeier, J. and Staudt, M. (1999) Biogenic Volatile Organic Compounds (VOC): An Overview on Emission, Physiology and Ecology. J Atmos Chem 33: 23–88.

Khalil, M.A.K., Moore, R.M., Harper, D.B., Lobert, J.M., Erickson, D.J., Koropalov, V., et al. (1999) Natural emissions of chlorine-containing gases: Reactive Chlorine Emissions Inventory. J Geophys Res 104: 8333–8346.

Kim, D., Langmead, B., and Salzberg, S.L. (2015) HISAT: a fast spliced aligner with low memory requirements. Nature Methods 12: 357-360.

Koedooder, C., Stock, W., Willems, A., Mangelinckx, S., De Troch, M., Vyverman, W., and Sabbe, K. (2019) Diatom-Bacteria Interactions Modulate the Composition and Productivity of Benthic Diatom Biofilms. Front Microbiol 10: 1255.

Koester, J.A., Brawley, S.H., Karp-Boss, L., and Mann, D.G. (2008) Sexual reproduction in the marine centric diatom Ditylum brightwellii (Bacillariophyta). European Journal of Phycology 42: 351-366.

Kolber, Z.S., Prášil, O., and Falkowski, P.G. (1998) Measurements of variable chlorophyll fluorescence using fast repetition rate techniques: defining methodology and experimental protocols. Biochim Biophys Acta - Bioenerg 1367: 88–106.

Kotani, T., Yurimoto, H., Kato, N., and Sakai, Y. (2007) Novel acetone metabolism in a propane-utilizing bacterium, Gordonia sp. strain TY-5. J Bacteriol 189: 886–893.

Kroth, P. (2007) Molecular biology and the biotechnological potential of diatoms. Advances in Experimental Medicine and Biology 616: 23-33.

Landa, M., Burns, A.S., Roth, S.J., and Moran, M.A. (2017) Bacterial transcriptome remodeling during sequential co-culture with a marine dinoflagellate and diatom. ISME J 1–14.

Lemoine, F., Correia, D., Lefort, V., Doppelt-Azeroual, O., Mareuil, F., Cohen-Boulakia, S., and Gascuel, O. (2019) NGPhylogeny.fr: new generation phylogenetic services for non-specialists. Nucleic Acids Res 47: W260–W265.

Letunic, I. and Bork, P. (2019) Interactive Tree Of Life (iTOL) v4: recent updates and new developments. Nucleic Acids Res 47: W256–W259.

Levine, S. and Krampitz, L.O. (1952) The oxidation of acetone by a soil diphtheroid.

Lewis, A.C., Hopkins, J.R., Carpenter, L.J., Stanton, J., Read, K.A., and Pilling, M.J. (2005) Sources and sinks of acetone, methanol, and acetaldehyde in North Atlantic marine air. Atmos Chem Phys 5: 1963–1974.

Lewis, W.M. (1984) The diatom sex clock and its evolutionary importance. American Naturalist 123: 73-80.

Liakakou, E., Vrekoussis, M., Bonsang, B., Donousis, C., Kanakidou, M., and Mihalopoulos, N. (2007) Isoprene above the Eastern Mediterranean: Seasonal variation and contribution to the oxidation capacity of the atmosphere. Atmos Environ 41: 1002–1010.

Longnecker, K., Kido Soule, M.C., and Kujawinski, E.B. (2015) Dissolved organic matter produced by Thalassiosira pseudonana. Mar Chem 168: 114–123.

Lutzmann, M., Grey, C., Traver, S., Ganier, O., Maya-Mendoza, A., Ranisavljevic, N., Bernex, F., Nishiyama, A., Montel, N., Gavois, E., Forichon, L., de Massy, B., and Méchali, M. (2012) MCM8- and MCM9-deficient mice reveal gametogenesis defects and genome instability due to impaired homologous recombination. Molecular Cell 47: 523-534.

Mann, D.G. (1988) Why didn't Lund see sex in Asterionella? A discussion of the diatom life cycle in nature. In Algae and the Aquatic Environment, (ed). Bristol: Biopress, pp. 384-412.

Mann, D.G. (1999) The species concept in diatoms. Phycologia 38: 437-495.

Marandino, C.A., De Bruyn, W.J., Miller, S.D., Prather, M.J., and Saltzman, E.S. (2005) Oceanic uptake and the global atmospheric acetone budget. Geophys Res Lett 32: 2–5.

Marchetti, A. and Cassar, N. (2009) Diatom elemental and morphological changes in response to iron limitation: A brief review with potential paleoceanographic applications. Geobiology 7: 419–431.

Marra, J. (2002) Approaches to the Measurement of Plankton Production. In, Phytoplankton Productivity. Oxford, UK: Blackwell Science Ltd, pp. 78–108.

Mayali, X. and Doucette, G.J. (2002) Microbial community interactions and population dynamics of an algicidal bacterium active against Karenia brevis (Dinophyceae). Harmful Algae 1: 277–293.

Mazin, A.V., Mazina, O.M., Bugreev, D.V., and Rossi, M.J. (2010) Rad54, the motor of homologous recombination. DNA Repair 9: 286-302.

McGenity, T.J., Crombie, A.T., and Murrell, J.C. (2018) Microbial cycling of isoprene, the most abundantly produced biological volatile organic compound on Earth. ISME J 12: 931–941.

Mckay, W.A., Turner, M.F., Jones, B.M.R., and Halliwell, C.M. (1996) Emissions of hydrocarbons from marine phytoplankton - some results from controlled laboratory experiments. Atmos Environ 30: 2583–2593.

Merchant, S.S., Prochnik, S.E., Vallon, O., Harris, E.H., Karpowicz, S.J., Witman, G.B., Terry, A., Salamov, A., et al. (2007) The Chlamydomonas genome reveals the evolution of key animal and plant functions. Science 318: 245-250. doi:10.1126/science.1143609

Meskhidze, N., Sabolis, A., Reed, R., and Kamykowski, D. (2015) Quantifying environmental stress-induced emissions of algal isoprene and monoterpenes using laboratory measurements. Biogeosciences 12: 637–651.

Mills, K.E., and Kaczmarska, I. (2006) Autogamic reproductive behavior and sex cell structure in Thalassiosira angulata (Bacillariophyta). Botanica Marina 49: 417-430. doi:10.1515/BOT.2006.053

Milovanović, I., Mišan, A., Simeunović, J., Kovač, D., Jambrec, D., and Mandić, A. (2015) Determination of Volatile Organic Compounds in Selected Strains of Cyanobacteria. J Chem 2015: 1–6.

Mitchell, B.G. and Kieper, D.A. (1988) Variability in pigment particulate fluorescence and absorption spectra in the northeastern Pacific Ocean. Deep Res 35: 665–689.

Moeys, S., Frenkel, J., Lembke, C., Gillard, J.T.F., Devos, V., Van den Berge, K., et al. (2016) A sex-inducing pheromone triggers cell cycle arrest and mate attraction in

the diatom Seminavis robusta. Scientific Reports 6: 19252. doi:10.1038/srep19252

Moore, E.R., Davie-Martin, C.L., Giovannoni, S.J., and Halsey, K.H. (2019) Pelagibacter metabolism of diatom-derived volatile organic compounds imposes an energetic tax on photosynthetic carbon fixation. Environ Microbiol 10.1111/14:

Moore, R.M., Webb, M., Tokarczyk, R., and Wever, R. (1996) Bromoperoxidase and iodoperoxidase enzymes and production of halogenated methanes in marine diatom cultures. J Geophys Res 101: 899–919.

Morris, R.M., Frazar, C.D., and Carlson, C.A. (2012) Basin-scale patterns in the abundance of SAR11 subclades, marine Actinobacteria (OM1), members of the Roseobacter clade and OCS116 in the South Atlantic. Environ Microbiol 14: 1133–1144.

Morris, R.M., Rappé, M.S., Connon, S.A., Vergin, K.L., Siebold, W.A., Carlson, C.A., and Giovannoni, S.J. (2002) SAR11 clade dominates ocean surface bacterioplankton communities. Nature 420: 806–810.

Mouget, J.-L., Gastineau, R., Davidovich, O., Gaudin, P., and Davidovich, N.A. (2009) Light is a key factor in triggering sexual reproduction in the pennate diatom Haslea ostrearia. FEMS Microbiology Ecology 69: 194-201.

Mtolera, M.S.P., Collén, J., Pedersén, M., Ekdahl, A., Abrahamsson, K., and Semesi, A.K. (1996) Stress-induced production of volatile halogenated organic compounds in Eucheuma denticulatum (Rhodophyta) caused by elevated pH and high light intensities. Eur J Phycol 31: 89–95.

Müller, J.F. and Brasseur, G. (1999) Sources of upper tropospheric HOx: A three-dimensional study. J Geophys Res Atmos 104: 1705–1715.

Myklestad, S.M. (2000) Dissolved Organic Carbon from Phytoplankton. Handb Environ Chem 5: 111–148.

Nagai, S., Hori, Y., Manabe, T., and Imai, I. (1995) Restoration of cell size by vegetative cell enlargement in Coscinodiscus wailesii (Bacillariophyceae). Phycologia 34: 533-535.

Nan, C., Zhang, H., and Zhao, G. (2004) Allelopathic interactions between the macroalga Ulva pertusa and eight microalgal species. J Sea Res 52: 259–268.

Nelson, D.M., Tréguer, P., Brzezinski, M.A., Leynaert, A., and Quéguiner, B. (1995) Production and dissolution of biogenic silica in the ocean: Revised global estimates, comparison with regional data and relationship to biogenic sedimentation. Biogeochemical Cycles 9: 359-372.

Nemecek-Marshall, M., Wojciechowski, C., Kuzma, J., Silver, G.M., and Fall, R. (1995) Marine Vibrio species produce the volatile organic compound acetone. Appl Environ Microbiol 61: 44–47.

Nguyen, L.T., Schmidt, H.A., Von Haeseler, A., and Minh, B.Q. (2015) IQ-TREE: A fast and effective stochastic algorithm for estimating maximum-likelihood phylogenies. Mol Biol Evol 32: 268–274.

O'Dowd, C.D. and de Leeuw, G. (2007) Marine aerosol production: a review of the current knowledge. Philos Trans R Soc A 365: 1753–1774.

Pacheco, A.R., Moel, M., and Segrè, D. (2019) Costless metabolic secretions as drivers of interspecies interactions in microbial ecosystems. Nat Commun 10: 103.

Palmer, P.I. and Shaw, S.L. (2005) Quantifying global marine isoprene fluxes using MODIS chlorophyll observations. Geophys Res Lett 32:.

Park, J., Long, D.T., Lee, K.Y., Abbas, T., Shibata, E., Negishi, M., Luo, Y., Schimenti, J.C., Gambus, A., Walter, J.C., and Dutta, A. (2013) The MCM8-MCM9 complex promotes RAD51 recruitment at DNA damage sites to facilitate homologous recombination. Molecular and Cellular Biology 33: 1632-1644.

Patel, R.N., Hou, C.T., Laskin, A.I., and Felix, A. (1982) Microbial oxidation of hydrocarbons: Properties of a soluble methane monooxygenase from a facultative methane-utilizing organism, Methylobacterium sp. strain CRL-26. Appl Environ Microbiol 44: 1130–1137.

Patil, S., Moeys, S., Von Dassow, P., Huysman, M.J.J., Mapleson, D., De Veylder, L., Sanges, R., Vyverman, W., Montresor, M., and Immacolata, M. (2015) Identification of the meitic toolkit in diatoms and exploration of meiosis-specific SPO11 and RAD51 homologs in the sexual species Pseudo-nitzchia multistriata and Seminavis robusta. BMC Genomics 2015doi:10.1186/s12864-015-1983-5

Paul, C. and Pohnert, G. (2011) Production and role of volatile halogenated compounds from marine algae. Nat Prod Rep 28: 186–195.

Paul, C., Mausz, M.A., and Pohnert, G. (2012) A co-culturing/metabolomics approach to investigate chemically mediated interactions of planktonic organisms reveals influence of bacteria on diatom metabolism. Metabolomics 9: 349–359.

Pertea, M., Kim, D., Pertea, G.M., Leek, J.T., and Salzberg, S.L. (2016) Transcript-level expression analysis of RNA-seq experiments with HISAT, StringTie and Ballgown. Nature Protocols 11: 1650-1667. doi:10.1038/nprot.2016.095

Pertea, M., Pertea, G.M., Antonescu, C.M., Chang, T.C., Mendell, J.T., and Salzberg, S.L. (2015) StringTie enables improved reconstruction of a transcriptome from RNA-seq reads. Nature Biotechnology 33: 290-295.

Pohnert, G., Lumineau, O., Cueff, A., Adolph, S., Cordevant, C., Lange, M., and Poulet, S. (2002) Are volatile unsaturated aldehydes from diatoms the main line of chemical defence against copepods? Mar Ecol Prog Ser 245: 33–45.

Ponomarova, O. and Patil, K.R. (2015) Metabolic interactions in microbial communities: untangling the Gordian knot. Curr Opin Microbiol 27: 37–44.

Prince, E.K., Myers, T.L., and Kubanek, J. (2008) Effects of harmful algal blooms on competitors: Allelopathic mechanisms of the red tide dinoflagellate Karenia brevis. Limnol Oceanogr 53: 531–541.

Rappé, M.S. and Giovannoni, S.J. (2003) The uncultured microbial majority. Annu Rev Microbiol 57: 369–94.

Read, K.A., Carpenter, L.J., Arnold, S.R., Beale, R., Nightingale, P.D., Hopkins, J.R., et al. (2012) Multiannual Observations of Acetone, Methanol, and Acetaldehyde in Remote Tropical Atlantic Air: Implications for Atmospheric OVOC Budgets and Oxidative Capacity.

Ritchie, R.J. (2006) Consistent sets of spectrophotometric chlorophyll equations for acetone, methanol and ethanol solvents. Photosynth Res 89: 27–41.

Rooney-Varga, J.N., Giewat, M.W., Savin, M.C., Sood, S., Legresley, M., and Martin, J.L. (2005) Links between Phytoplankton and Bacterial Community Dynamics in a Coastal Marine Environment. Microb Ecol 49: 163–175.

Rosenbaum, J.L., and Witman, G.B. (2002) Intraflagellar transport. Nature Reviews Molecular Cell Biology 3: 813-825.

Round, F.E. (1972) The problem of size reduction in diatoms. Nova Hedwigia 23: 291-303.

Ruiz-Halpern, S., Sejr, M.K., Duarte, C.M., Krause-Jensen, D., Dalsgaard, T., Dachs, J., and Rysgaard, S. (2010) Air-water exchange and vertical profiles of organic carbon in a subarctic fjord. Limnol Oceanogr 55: 1733–1740.

Sabbe, K. (2004) Apomixis in Achnanthes (Bacillariophyceae); development of a model system for diatom reproductive biology. European Journal of Phycology 39: 327-341.

Samo, T.J., Kimbrel, J.A., Nilson, D.J., Pett-Ridge, J., Weber, P.K., and Mayali, X. (2018) Attachment between heterotrophic bacteria and microalgae influences symbiotic microscale interactions. Environ Microbiol 20: 4385–4400.

Sander, R. (2015) Compilation of Henry's law constants (version 4.0) for water as solvent. Atmos Chem Phys 15: 4399–4981.

Santos, A.B., Viera, K.R., Nogara, G.P., Wagner, R., Jacob-Lopes, E., and Zepka, L.Q. (2016) Biogeneration of Volatile Organic Compounds by Microalgae: Occurrence, Behavior, Ecological Implications and Industrial Applications. In, Volatile Organic Compounds: Occurrence, Behavior and Ecological Implications., pp. 1–24.

Sañudo-Wilhelmy, S.A., Gómez-Consarnau, L., Suffridge, C., and Webb, E.A. (2014) The Role of B Vitamins in Marine Biogeochemistry. Ann Rev Mar Sci 6: 339–367.

Sargeant, S.L., Murrell, J.C., Nightingale, P.D., and Dixon, J.L. (2018) Basin-scale variability of microbial methanol uptake in the Atlantic Ocean. Biogeosciences 15: 5155–5167.

Sato, S., Beakes, G., Idei, M., Nagumo, T., and Mann, D.G. (2011) Novel Sex Cells and Evidence for Sex Pheromones in Diatoms. PLoS One 6: e26923.

Schmidt, R., Cordovez, V., De Boer, W., Raaijmakers, J., and Garbeva, P. (2015) Volatile affairs in microbial interactions. ISME J 9: 2329–2335.

Segev, E., Wyche, T.P., Kim, K.H., Petersen, J., Ellebrandt, C., Vlamakis, H., et al. (2016) Dynamic metabolic exchange governs a marine algal-bacterial interaction. Elife 5: 1–28.

Sharkey, T.D. and Yeh, S. (2001) Isoprene emission from plants. Annu Rev Plant Physiol Plant Mol Biol 52: 407–436.

Sharkey, T.D., Chen, X., and Yeh, S. (2001) Isoprene Increases Thermotolerance of Fosmidomycin-Fed Leaves 1.

Shaw, S.L., Chisholm, S.W., and Prinn, R.G. (2003) Isoprene production by Prochlorococcus, a marine cyanobacterium, and other phytoplankton. Mar Chem 80: 227–245.

Shirokawa, Y., and Shimada, M. (2013) Sex allocation pattern of the diatom Cyclotella meneghiniana. Proceedings of the Royal Society B: Biological Sciences 280: 20130503.

Simonsen, R. (1979) The diatom system: Ideas on phylogeny. Bacillaria 2: 9-71.

Sindelarova, K., Granier, C., Bouarar, I., Guenther, A., Tilmes, S., Stavrakou, T., et al. (2014) Global data set of biogenic VOC emissions calculated by the MEGAN model over the last 30 years. Atmos Chem Phys 14: 9317–9341.

Singh, H.B., O'Hara, D., Herlth, D., Sachse, W., Blake, D.R., Bradshaw, J.D., et al. (1994) Acetone in the atmosphere: Distribution, sources, and sinks. J Geophys Res 99: 1805.

Sinha, V., Williams, J., Meyerhöfer, M., Riebesell, U., Paulino, A.I., and Larsen, A. (2007) Air-sea fluxes of methanol, acetone, acetaldehyde, isoprene and DMS from a Norwegian fjord following a phytoplankton bloom in a mesocosm experiment. *Atmos. Chem. Phys*. 7, 739-755.

Sorokin, D.Y., van Pett, S., Tourova, T.P., Takaichi, S., and Muyzer, G. (2007) Acetonitrile degradation under haloalkaline conditions by Natronocella acetinitrilica gen. nov., sp. nov. *Microbiology* 153: 1157–1164.

Spracklen, D. V., Arnold, S.R., Sciare, J., Carslaw, K.S., and Pio, C. (2008) Globally significant oceanic source of organic carbon aerosol. Geophys Res Lett 35:.

Srikanta Dani, K.G., Silva Benavides, A.M., Michelozzi, M., Peluso, G., Torzillo, G., and Loreto, F. (2017) Relationship between isoprene emission and photosynthesis in diatoms, and its implications for global marine isoprene estimates. Mar Chem 189: 17–24.

Stamatakis, A. (2006) RAxML-VI-HPC: maximum likelihood-based phylogenetic analyses with thousands of taxa and mixed models. Bioinformatics 22: 2688-2690.

Sterner, R.W., and Elser, J.J. (2002) Ecological stoichiometry: the biology of elements from molecules to the biosphere. Princeton, New Jersey, USA: Princeton University Press.

Stonik, V. and Stonik, I. (2015) Low-Molecular-Weight Metabolites from Diatoms: Structures, Biological Roles and Biosynthesis. Mar Drugs 13: 3672–3709.

Sun, J., Steindler, L., Thrash, J.C., Halsey, K.H., Smith, D.P., Carter, A.E., et al. (2011) One Carbon Metabolism in SAR11 Pelagic Marine Bacteria. PLoS One 6: e23973.

Sun, J., Todd, J.D., Thrash, J.C., Qian, Y., Qian, M.C., Temperton, B., et al. (2016) The abundant marine bacterium Pelagibacter simultaneously catabolizes dimethylsulfoniopropionate to the gases dimethyl sulfide and methanethiol. Nat Microbiol 1: 16065.

Sunda, W.G. and Huntsman, S.A. (2011) Interactive effects of light and temperature on iron limitation in a diatom: Implications for marine productivity and carbon cycling. Limnol Oceanogr 56: 1475–1488.

Tait, V.K. and Moore, R.M. (1995) Methyl chloride (CH3Cl) production in phytoplankton cultures. Limnol Oceanogr 40: 189–195.

Taylor, D.G., Trudgill, P.W., Cripps, R.E., and Harris, P.R. (1980) The Microbial Metabolism of Acetone. J Gen Microbiol 118: 159–170.

Thornton, D.C.O. (2014) Dissolved organic matter (DOM) release by phytoplankton in the contemporary and future ocean. Eur J Phycol 49: 20–46.

Tillmann, U. (2004) Interactions between planktonic microalgae and protozoan grazers. Journal of Eukaryotic Microbiology 51: 156-168.

Tripp, H.J., Kitner, J.B., Schwalbach, M.S., Dacey, J.W.H., Wilhelm, L.J., and Giovannoni, S.J. (2008) SAR11 marine bacteria require exogenous reduced sulphur for growth. Nature 452: 741–4.

Uitz, J., Claustre, H., Gentili, B., and Stramski, D. (2010) Phytoplankton class-specific primary production in the world's oceans: Seasonal and interannual variability from satellite observations. Global Biogeochem Cycles 24

van Hylckama Vlieg, J.E.T., Leemhuis, H., Jeffrey, H., Spelberg, L., and Janssen, D.B. (2000) Characterization of the Gene Cluster Involved in Isoprene Metabolism in Rhodococcus sp . Strain AD45. J Bacteriol 187: 1956–1963.

Van Tol, H.M., Amin, S.A., and Armbrust, V. (2016) Ubiquitous marine bacterium inhibits diatom cell division. ISME J 11: 31–42.

Vaulot, D., and Chisholm, S.W. (1987) A simple model for the growth of phytoplankton populations in light/dark cycles. Journal of Plankton Research 9: 345-366.

Villar, E., Vannier, T., Vernette, C., Lescot, M., Cuenca, M., Alexandre, A., et al. (2018) The Ocean Gene Atlas: Exploring the biogeography of plankton genes online. Nucleic Acids Res 46: W289–W295.

Von Dassow, P., and Montresor, M. (2011) Unveiling the mysteries of phytoplankton life cycles: patterns and opportunities behind complexity. Journal of Plankton Research 33: 3-12.

Webb, A.L., Leedham-Elvidge, E., Hughes, C., Hopkins, F.E., Malin, G., Bach, L.T., et al. (2016) Effect of ocean acidification and elevated f CO2 on trace gas production by a Baltic Sea summer phytoplankton community. Biogeosciences 13: 4595–4613.

Weigert, M. and Kümmerli, R. (2017) The physical boundaries of public goods cooperation between surface-attached bacterial cells. Proc R Soc B 284:.

Westberry, T., Behrenfeld, M.J., Siegel, D.A., and Boss, E. (2008) Carbon-based primary productivity modeling with vertically resolved photoacclimation. Global Biogeochem Cycles 22:.

White, A., Giovannoni, S., Zhao, Y., Vergin, K., and Carlson, C. (2018) Elemental content and stoichiometry of SAR11 chemoheterotrophic marine bacteria. Limnol Oceanogr (In Rev.

Williams, J., Holzinger, R., Gros, V., Xu, X., Atlas, E., and Wallace, D.W.R. (2004) Measurements of organic species in air and seawater from the tropical Atlantic. Geophys Res Lett 31: 1–5.

Wright, S.W., Jeffrey, S.W., Mantoura, R.F.C., Llewellyn, C.A., Bjørnland, T., Repeta, D., and Welschmeyer, N. (1991) Improved HPLC method for the analysis of chlorophylls and carotenoids from marine phytoplankton. Mar Ecol Prog Ser 77: 183–196.

Xu, Q., Yang, L., Yang, W., Bai, Y., Hou, P., Zhao, J., et al. (2017) Volatile organic compounds released from Microcystis flos-aquae under nitrogen sources and their toxic effects on Chlorella vulgaris. Ecotoxicol Environ Saf 135: 191–200.

Yang, J. and Zhang, Y. (2015) Protein Structure and Function Prediction Using I-TASSER. Curr Protoc Bioinforma 52: 5.8.1-5.8.15.

Yang, M., Beale, R., Liss, P., Johnson, M., Blomquist, B., and Nightingale, P. (2014) Air-sea fluxes of oxygenated volatile organic compounds across the Atlantic Ocean. Atmos Chem Phys 14: 7499–7517.

Ye, C., Yang, Y., Xu, Q., Ying, B., Zhang, M., Gao, B., et al. (2018a) Volatile organic compound emissions from Microcystis aeruginosa under different phosphorus sources and concentrations. Phycol Res 66: 15–22.

Yoch, D.C. (2002) Dimethylsulfoniopropionate: Its sources, role in the marine food web, and biological degradation to dimethylsulfide. Appl Environ Microbiol 68: 5804–5815.

Yoshiyama, K., and Sharp, J.H. (2006) Phytoplankton response to nutrient enrichment in an urbanized estuary: Apparent inhibition of primary production by overeutrophication. Limnology and Oceanography 51: 424-434.

Zachariae, W., Shevchenko, A., Andrews, P.D., Ciosk, R., Galova, M., Stark, M.J.R., Mann, M., and Nasmyth, K. (1998) Mass spectrometric analysis of the anaphase-promoting complex from yeast: Identificaiton of a subunit related to cullins. Science 279: 1216-1219.

Zhao, L., Chang, W., Xiao, Y., Liu, H., and Liu, P. (2013) Methylerythritol Phosphate Pathway of Isoprenoid Biosynthesis. Annu Rev Biochem 82: 497–530.

Zuo, Z. (2019) Why Algae Release Volatile Organic Compounds—The Emission and Roles. Front Microbiol 10: 491.